LINKS BETWEEN LONG-LIVED HOT SPOTS, MANTLE PLUMES, D″, AND PLATE TECTONICS

A. Mark Jellinek
Geophysical Laboratories, Department of Physics
University of Toronto
Toronto, Ontario, Canada

Michael Manga
Department of Earth and Planetary Science
University of California
Berkeley, California, USA

Received 31 October 2003; revised 27 April 2004; accepted 10 June 2004; published 14 September 2004.

[1] The existence, spatial distribution, and style of volcanism on terrestrial planets is an expression of their internal dynamics and evolution. On Earth a physical link has been proposed between hot spots, regions with particularly persistent, localized, and high rates of volcanism, and underlying deep mantle plumes. Such mantle plumes are thought to be constructed of large spherical heads and narrow trailing conduits. This plume model has provided a way to interpret observable phenomena including the volcanological, petrological, and geochemical evolution of ocean island volcanoes, the relative motion of plates, continental breakup, global heat flow, and the Earth's magnetic field within the broader framework of the thermal history of our planet. Despite the plume model's utility the underlying dynamics giving rise to hot spots as long-lived stable features have remained elusive. Accordingly, in this review we combine results from new and published observational, analog, theoretical, and numerical studies to address two key questions: (1) Why might mantle plumes in the Earth have a head-tail structure? (2) How can mantle plumes and hot spots persist for large geological times? We show first that the characteristic head-tail structure of mantle plumes, which is a consequence of hot upwellings having a low viscosity, is likely a result of strong cooling of the mantle by large-scale stirring driven by plate tectonics. Second, we show that the head-tail structure of such plumes is a necessary but insufficient condition for their longevity. Third, we synthesize seismological, geodynamic, geomagnetic, and geochemical constraints on the structure and composition of the lowermost mantle to argue that the source regions for most deep mantle plumes contain dense, low-viscosity material within D″ composed of partial melt, outer core material, or a mixture of both (i.e., a "dense layer"). Fourth, using results from laboratory experiments on thermochemical convection and new theoretical scaling analyses, we argue that the longevity of mantle plumes in the Earth is a consequence of the interactions between plate tectonics, core cooling, and dense, low-viscosity material within D″. Conditions leading to Earth-like mantle plumes are highly specific and may thus be unique to our own planet. Furthermore, long-lived hot spots should not a priori be anticipated on other terrestrial planets and moons. Our analysis leads to self-consistent predictions for the longevity of mantle plumes, topography on the dense layer, and composition of ocean island basalts that are consistent with observations. *INDEX TERMS:* 8121 Tectonophysics: Dynamics, convection currents and mantle plumes; 1060 Geochemistry: Planetary geochemistry (5405, 5410, 5704, 5709, 6005, 6008); 8125 Tectonophysics: Evolution of the Earth; 7207 Seismology: Core and mantle; 1522 Geomagnetism and Paleomagnetism: Paleomagnetic secular variation; *KEYWORDS:* hot spots, mantle plumes, thermochemical convection, ocean island basalt geochemistry.

Citation: Jellinek, A. M., and M. Manga (2004), Links between long-lived hot spots, mantle plumes, D″, and plate tectonics, *Rev. Geophys.*, *42*, RG3002, doi:10.1029/2003RG000144.

1. INTRODUCTION AND MOTIVATION

[2] One of the most enduring problems in Earth science is the persistence of hot spot volcanoes over geological time. Indeed, apparently negligible relative motion between individual hot spots motivated early proposals that hot spots are fixed within the mantle [e.g., *Wilson*, 1963] and that hot spots may be linked to mantle plumes [e.g., *Morgan* 1971, 1972, 1981]. Over the last few decades this presumed hot spot–plume connection has provided a basis for using geological, geophysical, and geochemical observations at the Earth's surface to study the Earth's deep interior and evolution. From such a conceptual link, there evolved, for example, bold suggestions of an absolute "hot spot reference frame" for plate motions [e.g., *Morgan*, 1972], estimates of core cooling rate [e.g., *Davies*, 1988; *Sleep*, 1990], explanations for the chemistry and volume of flood basalts and hot spot tracks [e.g., *White and McKenzie*, 1989; *Campbell and Griffiths*, 1990, 1993; *Farnetani and Richards*, 1994, 1995; *Cordery et al.*, 1997], and mid-ocean ridge basalts [e.g., *Schilling et al.*, 1983; *Allegre et al.*, 1984; *Schilling*, 1986; *Langmuir et al.*, 1992; *Jellinek et al.*, 2003]. Mantle plumes have been proposed to contribute strongly to the anomalously high elevation of southern Africa [e.g., *Lithgow-Bertelloni and Silver*, 1998] and the central Pacific basin [e.g.,

8755-1209/04/2003RG000144$15.00
Paper number 2003RG000144

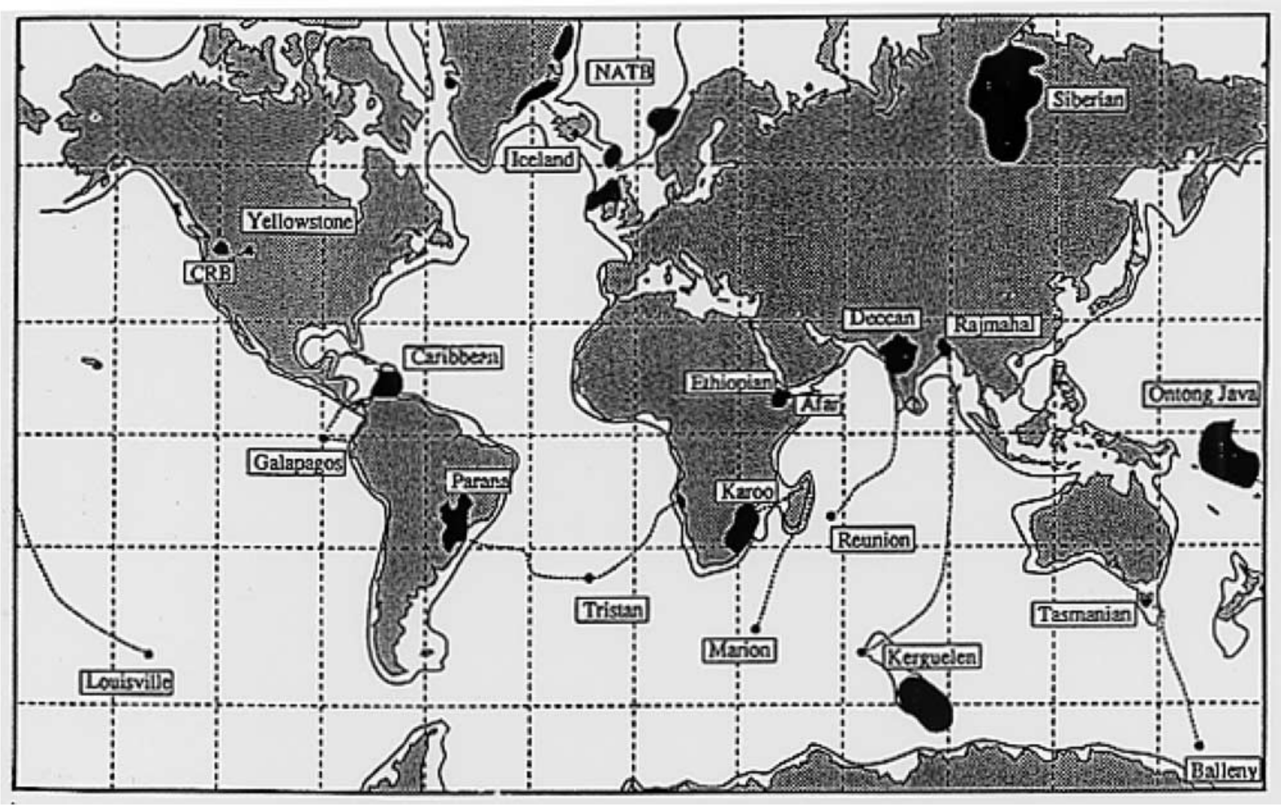

Figure 1. A map of hot spots that have both well-defined hot spot tracks and flood basalts at their origins [from *Duncan and Richards*, 1991].

McNutt, 1998], to the topography and geometry of the global mid-ocean ridge system [*Morgan et al.*, 1987; *Parmentier and Morgan*, 1990; *Small*, 1995; *Abelson and Agnon*, 2001; *Ito et al.*, 2003] and to cause lithospheric instabilities leading to continental breakup [e.g., *Morgan*, 1974; *White and McKenzie*, 1989; *Arndt and Christensen*, 1992]. Viewing mantle plumes as an intrinsic part of how the Earth cools led also to efforts toward self-consistent models for the thermal and compositional evolution of the planet as a whole [e.g., *Christensen*, 1984a; *Zindler and Hart*, 1986; *Turcotte and Kellogg*, 1986; *Kellogg and Wasserburg*, 1990; *Davies and Richards*, 1992; *Davies*, 1990, 1993; *Campbell and Griffiths*, 1992, 1993; *Christensen and Hofmann*, 1994; *O'Nions and Tolstikhin*, 1996; *Albarede*, 1998; *Tackley*, 1998a, 1998b; *Coltice and Ricard*, 2002; *van Keken and Ballentine*, 1999; *Coltice et al.*, 2000; *Tackley and Xie*, 2002; *Korenaga*, 2003; *Samuel and Farnetani*, 2003]. The plume–hot spot model is also useful for comparative planetology. Basic differences in the nature of volcanism on the Earth, where most volcanism occurs at plate boundaries, compared with Venus and Mars, both of which have hot spot–like features but no plate tectonics, likely reflect fundamental differences in the way these terrestrial planets have evolved thermally and compositionally.

[3] Perhaps because of the riveting appearance of hot spot tracks on the Earth's surface (Figure 1), the apparent fixity of hot spots relative to moving plates has historically captured the greatest attention and been often considered a defining characteristic of such features. In recent years, however, an improved resolution of hot spot motion has challenged, or at least redefined, the notion of hot spot fixity. For example, a number of paleomagnetic studies have shown that hot spots may be divided into at least two global families that move relative to each other at a rate currently less than about 1 cm yr^{-1}: the Pacific family and the Indo-Atlantic family, which may or may not include Iceland [e.g., *Raymond et al.*, 2000; *Norton*, 2000; *Courtillot et al.*, 2003]. Within each group, however, there is negligible relative motion between individual hot spots [e.g., *Burke et al.*, 1973; *Molnar and Atwater*, 1973]. Furthermore, building on earlier work by *Gordon and Cape* [1981] and *Morgan* [1981], *Tarduno et al.* [2003] find that the paleolatitude of the Hawaiian hot spot is not fixed. Consequently, these authors argue that the well-known bend in the Hawaiian-Emperor seamount chain, and possibly that in the Louisville hot spot track, may be dominated by motion of the underlying plumes relative to the Pacific plate rather than the reverse, which is the conventional explanation. The movement of the hot spots is thus interpreted to reflect the influence of lower mantle flow on the plume source at the base of the mantle [e.g., *Steinberger*, 2000; *Steinberger and O'Connell*, 1998, 2000; *Steinberger et al.* 2004]. Although it is a contentious study [*Gordon et al.*, 2004], the conclusion of *Tarduno et al.* [2003] that hot spots move relative to overlying plates is not surprising. Mantle convection and stirring is expected to be time-dependent, and plumes that originate at the base of the mantle should drift

in response to transient variations in the lower mantle velocity field. Moreover, changes in hot spot position can also occur if the plume buoyancy flux or conduit rise velocity varies in time [e.g., *Richards and Griffiths*, 1988; *Griffiths and Campbell*, 1991]. Several studies have shown that the eruption rate at Hawaii has likely increased over the last 40 Myr [e.g., *Davies*, 1992], reflecting such transient behavior [*Vidal and Bonneville*, 2004].

[4] Regardless of the reality of hot spot fixity, the longevity of hot spots remains undisputed. Thus the connection of hot spots to underlying mantle plumes is probably a vital component of the Earth's thermal evolution. The origin of long-lived hot spots within the context of plate tectonics and mantle stirring, however, remains elusive. Our current understanding of the dynamics of surface plates and their role in Earth's evolution is significantly advanced over our knowledge of processes governing the style of convection due to core cooling [e.g., *Richards et al.*, 2000]. In large part, this imbalance in knowledge is due to the fact that we can observe the top boundary of the planet much more readily than the core-mantle boundary (hereinafter abbreviated CMB). Over mostly the last 10 years, however, improved observational and modeling constraints on the composition, structure, and physical properties of the CMB region, and particularly D″, together with dynamic models of mantle convection, have yielded new insight into the dynamics of mantle plumes. In this review we synthesize, develop, and extend these results with two goals in mind. First, we show that the dynamical conditions leading to mantle plumes in the Earth are unusual and likely unique to this planet. Second, we argue that the origin and longevity of Earth-like mantle plumes are a result of the interaction between plate tectonics, mantle stirring, core cooling, and a dense, low-viscosity chemical boundary layer within D″.

[5] Our review is organized in the following way. In section 2 we summarize the observational and modeling constraints on the structure and dynamics of mantle plumes rising from the CMB. The mechanics of plumes are discussed within the context of theoretical studies, laboratory experiments, and numerical simulations of convection in fluids with strongly temperature-dependent viscosities. A key result of all of these studies is that the inferred head and tail structure of mantle plumes in the Earth requires large viscosity variations in the thermal boundary in the source region of plumes. We show that the presence of such viscosity variations is unusual and likely a particular consequence of plate tectonics. Although buoyant low-viscosity upwellings will have the requisite head-tail structure, this does not guarantee their longevity or persistence over timescales that are large in comparison to their risetime. In section 3 we summarize the observational constraints for the structure and composition of D″ and review evidence that the source region for deep mantle plumes is composed partly of dense, low-viscosity material. In sections 4 and 5 the quantitative influence of such a dense layer on convection from the base of the mantle is considered in detail with a combination of laboratory experiments and new theoretical scaling analyses. We show that the entrainment of dense, low-viscosity material from the base of the mantle enhances the head and tail structure of mantle plumes and will likely influence the geochemistry of magmas erupted from hot spot volcanoes. Moreover, we find that deformation of this dense layer by flow into plumes can stabilize the positions of plumes for hundreds of millions of years or longer. We thus argue that ultimately the existence and longevity of hot spots and mantle plumes in the Earth are a consequence of interactions among plate tectonics, core cooling, and D″.

2. THERMAL BOUNDARY LAYER THEORY AND THE UNCERTAIN ORIGIN OF MANTLE PLUMES

2.1. Hot Spots Associated With Deep Mantle Plumes

[6] A spatial link between flood basalts and hot spot tracks on the Earth (Figure 1) is most commonly attributed to the ascent and melting of mantle plumes constructed of large heads and long-lived, narrow underlying conduits (Figure 2a) [*Richards et al.*, 1989]: Whereas melts from the voluminous head lead to flood basalt volcanism and large igneous provinces, melts from the tail result in features such as hot spot island chains. Although alternative models for large igneous provinces have been proposed [e.g., *King and Anderson*, 1995; *King and Ritsema*, 2000], to many geoscientists this hypothesis is assumed to be as well established at the theory of plate tectonics [*DePaolo and Manga*, 2003], and the plume model is featured in many introductory textbooks [e.g., *Hamblin and Christiansen*, 1998; *Tarbuck and Lutgens*, 1999; *Plummer et al.*, 1999; *Skinner and Porter*, 2000]. Nevertheless, the mantle plume origin of hot spots remains controversial and a topic of very active research [e.g., *Anderson*, 1998; *Foulger and Pearson*, 2001; *Foulger and Natlund*, 2003].

[7] Over the years since the inception of the mantle plume hypothesis the catalog of possible hot spots has grown to be very large. Consequently, in recent years, there has been an effort to define those hot spots explicitly related to mantle plumes ascending from the core-mantle boundary (i.e., deep mantle plumes). *Campbell and Griffiths* [1992] define such hot spots as being associated with particularly high MgO contents (i.e., picrites), indicative of high melting temperatures and large extents of melting. The identification of picrites necessarily depends on the available exposure in the field and is thus not a rigorous guideline. Nevertheless, these authors identify a small number including Hawaii, Reunion, Kerguelen, and Tristan deCunha. More recently, *Courtillot et al.* [2003] develop a set of new criteria for a hot spot related to a deep mantle plume that reduces a popular tally of $\geq$49 [e.g., *Richards et al.*, 1988; *Duncan and Richards*, 1991] to perhaps 7–15, including those recognized by *Campbell and Griffiths* [1992]. Following *Courtillot et al.* [2003], hot spots related to deep mantle plumes are expected to exhibit at least three of five defining characteristics:

[8] 1. Hot spots are associated with an island chain with a monotonic age progression [e.g., *Morgan*, 1972, 1981]. The age progression implies that there is relative motion between the plate on which the hot spot is found and an

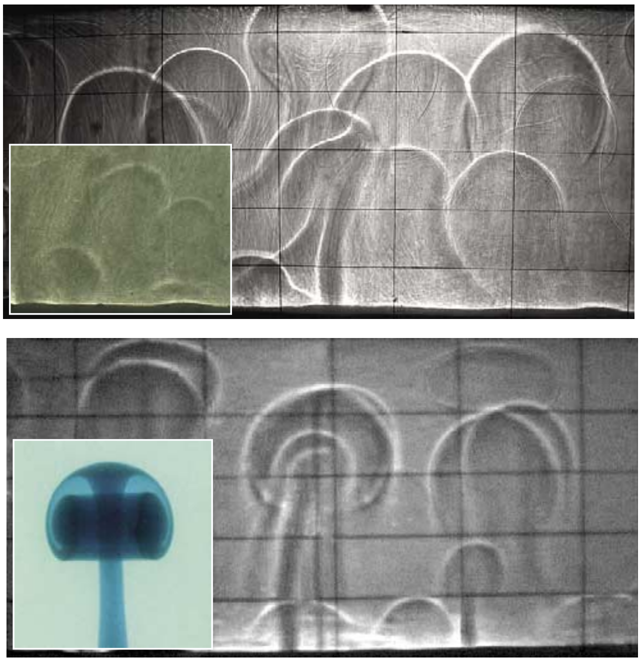

Figure 2. Shadowgraphs illustrating convection from planar heated boundaries in fluids with strongly temperature-dependent viscosities in the form of (top) thermals and (bottom) plumes. Discrete thermals (inset, top) are faint because variations in refractive index, which correspond to the small temperature differences carried by these upwellings, are small. $Ra > 10^6$; $Pr > 10^4$. The photograph of a single blue plume (inset, bottom), showing a classical head-tail form, is generated from a point source of hot fluid (image courtesy of R. W. Griffiths).

underlying plume [*Morgan*, 1972; *Molnar and Stock*, 1987; *Muller et al.*, 1993; *Courtillot et al.*, 1999; *Raymond et al.*, 2000]. The longevity of plumes implied by the length of hot spot tracks implies that hot spots are long-lived relative to the time it takes for a plume to rise through the mantle.

[9] 2. Flood basalts mark the start of island chains [e.g., *Richards et al.*, 1989]. *Clouard and Bonneville* [2001] and *Courtillot et al.* [2003] note, however, that the flood basalts that would have been associated with several Pacific hot spots such as Hawaii and Louisville would probably have been subducted.

[10] 3. Hot spots should have a strong buoyancy flux in excess of 10^3 kg s^{-1}. Smaller buoyancy fluxes may be insufficient for mantle plumes to remain robust or intact over the depth of the mantle [*Griffiths and Campbell*, 1991; *Olson et al.*, 1993]. The buoyancy flux, which is a weight deficiency per unit time, reflects the strength of upwelling flow in a plume and is determined from dynamic models for the associated topographic swells [e.g., *Davies*, 1988; *Sleep*, 1990] as well as by addressing the magma production rate in terms of upwelling velocities in the mantle [e.g., *Ribe and Christensen*, 1999]. At Hawaii, for example, the high magma production rate in a small area implies an upwelling velocity of around 50 cm yr^{-1}, which is about 5 times faster than the average spreading rate of the Pacific plate. In general, hot spot volcanism related to deep mantle plumes should reflect melt production rates that are so large that they cannot be explained by any other origin.

[11] 4. Hot spots are associated with high ^{3}He/^{4}He relative to mid-ocean ridge basalt (MORB). Data from *Kurz et al.* [1982], *Craig* [1990], and *Farley and Neroda* [1998] show that whereas mid-ocean ridge basalts carry uniform ^{3}He/^{4}He ratios in the range 7–9 R_a (R_a denotes ratio in air), individual ocean island basalt (OIB) volcanoes are characterized by ratios either exclusively greater than or equal to MORB or less than or equal to MORB. Strong hot spots, most notably Hawaii and Iceland, are generally characterized by maximum ^{3}He/^{4}He ratios that are far in excess of MORB [e.g., *Kurz et al.*, 1983]. Noble gases are highly incompatible and volatile and are thus expected to enter melt and be outgassed during eruption [e.g., *Farley et al.*, 1992; *Porcelli and Wasserburg*, 1993]. Thus a conventional explanation for elevated ^{3}He/^{4}He ratios is that the plume source is enriched in ^{3}He, undegassed, and therefore "primitive." However, variations in ^{3}He/^{4}He should be reflected also by changes in ^{3}He/U because U decays to produce ^{4}He. That is, elevated ^{3}He/^{4}He ratios can arise from either lots of ^{3}He or little ^{4}He. A number of recent studies show, for example, that elevated ^{3}He/^{4}He ratios can be explained if the plume source contains an eclogite component that is depleted in U and Th and segregated from subducted lithosphere. A depletion of U and Th in eclogite appears counterintuitive because both elements are incompatible and expected to be concentrated in mid-ocean ridge basalts forming the oceanic crust from which eclogite is derived. However, experiments show that U and Th are highly mobile in the aqueous fluids released by dehydration reactions occurring as subducting slabs descend to, and cross, the transition zone [*Tatsumi and Eggins*, 1995]. Indeed, this mechanism has been used to explain U and Th enrichments in arc basalts derived from subduction-related processes [e.g., *Tatsumi et al.*, 1986; *Gill and Williams*, 1990; *McCulloch and Gamble*, 1991; *Brenan et al.*, 1995]. An additional consequence critical to this discussion is that apparently high ^{3}He/^{4}He can be preserved if the dense eclogite is stored for a substantial period of time while the rest of the mantle outgasses ^{3}He [*Anderson*, 1993; *Albarede*, 1998; *Coltice and Ricard*, 1998; *Coltice et al.*, 2000; *Ferrachat and Ricard*, 2001]. This model may be supported by models of melting in mantle plumes in which an eclogite component is required in order to produce melting rates consistent with the formation of flood basalts for reasonable (i.e., ~200°C) plume-mantle temperature differences [e.g., *Cordery et al.*, 1997].

[12] 5. Hot spots are characterized by a significant reduction in shear wave velocity associated with underlying hot mantle. To date, limitations in the global distribution of seismic stations have generally limited the lateral resolution of global tomographic models of the lower mantle to spatial scales of the order of 10^3 km, which is likely a factor of 10 or more greater than plausible conduit diameters [*Loper and Stacey*, 1983; *Griffiths and Campbell*, 1991; *Olson et al.* 1993]. Consequently, although thermal anomalies appear to be present beneath most strong hot spots in the upper mantle

to a depth of a few hundred kilometers, the seismic evidence for plumes in the lower mantle remains equivocal [e.g., *Allen et al.*, 2002; *Ritsema and Allen*, 2003]. Continued refinements in seismic data reduction and modeling [e.g., *Montelli et al.*, 2004], however, have produced *P* wave velocity maps of a low-velocity structure beneath Hawaii, Louisville, and several other plumes to near the CMB. One caveat to accepting this result as proof of any kind is that a natural bias toward "seeing is believing" makes this result deceptively convincing [e.g., *Kerr*, 2003]. That is, although low–seismic velocity material exists, whether such a structure reflects a plume conduit remains to be proved.

2.2. Dynamical Requirements for Deep Mantle Plumes From Observations and Models

[13] Analyses of hot spot swells [*Morgan*, 1972; *Davies*, 1988; *Sleep*, 1990], the geochemistry of associated basalts [e.g., *Schilling et al.*, 1991], and numerical studies of plume formation [*Farnetani*, 1997] indicate that temperature differences between plumes and ambient mantle are a few hundred degrees, implying that the there may be more than a factor of 100 reduction in viscosity across the hot thermal boundary layer in the plume source. Laboratory [*Whitehead and Luther*, 1975; *Olson and Singer*, 1985; *Griffiths and Campbell*, 1990; *Kincaid et al.*, 1996; *Jellinek et al.*, 1999, 2003] and numerical [e.g., *Sleep et al.*, 1988; *Olson et al.*, 1993; *Kellogg and King*, 1997; *van Keken*, 1997] studies show that under such conditions plumes will be constructed of large spherical heads, which preferentially draw the hottest fluid at the base of the thermal boundary layer, followed by narrow conduits with approximately Gaussian internal temperature distributions (Figure 2) [*Yuen and Schubert*, 1976; *Loper and Stacey*, 1983; *Morris and Canright*, 1984; *Loper*, 1984; *Sleep et al.*, 1988; *Olson et al.*, 1993]. The large head reflects the dynamical requirements for a plume to form and ascend from a thermal boundary layer into a higher-viscosity environment [e.g., *Selig*, 1965; *Whitehead and Luther*, 1975; *Lister and Kerr*, 1989]. A narrow trailing conduit is formed ultimately because the low-viscosity fluid within this structure rises faster than the plume head itself. That is, a smaller diameter is required in order to conserve mass. For a given buoyancy flux the relative difference in diameter between the head and trailing conduit is thus governed mostly by the ratio of the viscosity of the ambient mantle to the viscosity of the fluid within the conduit [e.g., *Griffiths and Campbell*, 1990].

[14] Although large viscosity variations are necessary for a head and tail structure, and are likely a prerequisite for long-lived plumes [*Jellinek et al.*, 2002], such conditions at the hot boundary are not sufficient to guarantee the longevity of plume conduits and hot spot volcanism. In particular, weak plumes may be sufficiently deflected by large-scale mantle flow driven by subduction and plate tectonics that they break up into diapirs [e.g., *Skilbeck and Whitehead*, 1978; *Olson and Singer*, 1985; *Richards and Griffiths*, 1988]. One important criterion for a long-lived plume conduit is that it maintains its structure over the full depth of the mantle. Because plumes are hotter than their surroundings, heat transfer and entrainment of surrounding mantle, which is enhanced by any inclination produced by mantle shear flow, can cause ascending conduit fluid to cool and become more viscous [*Griffiths and Campbell*, 1991; *Olson et al.*, 1993]. Assuming that the buoyancy flux is fixed, cooling and entrainment has two effects. First, as we have already alluded, significant decreases in the conduit-mantle temperature anomaly can reduce the buoyancy of the conduit itself such that it becomes prone to the large deflections by mantle flow that, in turn, can result in its breakup into diapirs [e.g., *Ihinger*, 1995]. Second, an increase in viscosity leads to a reduction in conduit flow velocity, resulting in a broadening of the structure. Indeed, a number of studies have shown that the conduit radius is proportional to $\mu_h^{1/4}$, where μ_h is the viscosity of the hot thermal boundary layer [*Loper and Stacey*, 1983; *Griffiths and Campbell*, 1990; *Olson et al.*, 1993].

[15] One condition identified by *Olson et al.* [1993] for establishing robust narrow conduits is that rise velocities are sufficiently high that radial conductive cooling in the conduit has a negligible effect on the temperature, and thus viscosity variations within the conduit over the full mantle depth. Consequently, velocity gradients, which are confined a narrow region at the edge of the conduit [cf. *Morris*, 1982; *Loper and Stacey*, 1983; *Morris and Canright*, 1984], remain largely unperturbed over the depth of the mantle. Thus equating the characteristic timescale for radial conduction, r^2/κ, to the characteristic timescale for the vertical advection of buoyant fluid within the conduit, H/w, gives a scale for maximum height to which a vertical conduit may extend. Here r and w are relevant length and velocity scales for radial conduction and vertical velocity within the conduit, H_m is the mantle depth, and κ is the thermal diffusivity. However, as conduits can be deflected into a parabolic shape by ambient mantle motions [*Richards and Griffiths*, 1988; *Griffiths and Campbell*, 1991], a more appropriate criterion is that the influence of conductive cooling be negligible over several mantle depths. Following *Olson et al.* [1993], the maximum height of a stable narrow conduit is

$$Z_{\max} = r\Lambda Ra_L^{1/3}/4 \gg H_m. \tag{1}$$

In addition, the corresponding conduit diameter is

$$\delta_w = (2/\Lambda\phi)^{1/2}\delta_t, \tag{2}$$

where the temperature drop at $Z_{\max}$ is

$$\phi = \exp\left(-4Z_{\max}Ra_L^{1/3}/\Lambda\right) \tag{3}$$

and the thickness of the thermal halo surrounding the conduit is

$$\delta_t = r\Lambda^{1/2}(\exp(\Lambda\phi/4))Ra_L^{-1/6}. \tag{4}$$

Here $\Lambda = \ln(\mu_i/\mu_h)$, where the subscripts "$h$" and "$i$" refer to the hot thermal boundary layer fluid and interior mantle, respectively. Here r is taken to be approximately one half the lateral spacing between adjacent plume conduits, and Ra_r is a Rayleigh number based on this length scale. This parameter is discussed in more detail below. It should be noted that whereas this picture is accurate for vertical conduits [see also *Loper and Stacey*, 1983], *Griffiths and Campbell* [1991] find that buoyancy-driven azimuthal stirring around the margins of inclined conduits can lead to significantly thinner halos. Thus this scale for δ_t is likely an upper bound.

[16] A major constraint on the strength of plumes is the buoyancy flux or heat flow obtained from studies of hot spot swells. Accordingly, applying their results to the Earth's mantle, *Olson et al.* [1993] find that the total heat flow from a given conduit must exceed about 30–40 GW in order for the plume conduit to remain narrow over the depth of the mantle, which is comparable to the ~10 GW estimates by *Griffiths and Campbell* [1991] for inclined conduits. Thus, whereas the Hawaiian plume is expected to remain narrow for many mantle depths, much weaker hot spots are unlikely to be associated with deep mantle plumes, which is in accord with the criteria for identifying plume-related hot spots proposed by *Courtillot et al.* [2003]. An additional useful result obtained by *Olson et al.* [1993] that is of particular interest to seismologists is that the ratio of the width of the thermal halo to the conduit diameter for the Hawaiian plume, δ_t/δ_w, is expected to be around 2.3.

[17] The predicted head and tail structure is consistent with the observation that hot spot tracks associated with deep mantle plumes have flood basalts at their initiation [e.g., *Richards et al.*, 1989]. In addition, mantle plume models in which melting is considered have led to predictions for the geochemistry of flood basalts and hot spots that are in accord with geochemical observations [e.g., *Campbell and Griffiths*, 1992; *Farnetani et al.*, 1996; *Cordery et al.*, 1997; *Samuel and Farnetani*, 2003]. However, although the structure of low-viscosity plumes ascending through the mantle appears to explain many of the qualitative characteristics of hot spot volcanism on the Earth, for reasons we will outline in section 2.3, the presence of the requisite large viscosity variations is unusual and may reflect conditions unique to our planet.

2.3. A Simple Model for Planetary Mantle Convection: Benard Convection in a Fluid With a Temperature-Dependent Viscosity

[18] A key feature of most models of mantle plumes is that large viscosity variations in the thermal boundary layer at the CMB are required to form axisymmetric plumes with large heads and narrow trailing conduits. In this section we review some of the major results from studies of thermal convection in fluids with strongly temperature-dependent viscosities. A central aim here is to show that the large viscosity variations required to form Earth-like mantle plumes are not expected and require special circumstances. In this and subsequent sections we will show that either plate tectonics or the entrainment of dense, low-viscosity material from D″ is probably required.

[19] For the forthcoming discussion it is useful to distinguish "plumes" from "thermals" (Figure 2). We use "plume" to describe buoyant upwellings that are constructed of large spherical heads and narrow underlying tails (conduits) [e.g., *Richards et al.*, 1989]. Plume conduits remain connected to the hot boundary layer for timescales that are long in comparison to the time for an upwelling to ascend from a hot boundary through the full depth of an overlying fluid layer (i.e., one plume risetime). In very viscous (Stokes) flows this regime occurs only if the viscosity variations in the hot boundary layer are $>10^2$ [e.g., *Whitehead and Luther*, 1975; *Griffiths and Campbell*, 1990; *Olson and Singer*, 1985; *Jellinek et al.*, 1999; *Lithgow-Bertelloni et al.*, 2001; *Jellinek et al.*, 2003]. In contrast, "thermal" [*Sparrow et al.*, 1970; *Griffiths*, 1986] is used to indicate a discrete buoyant upwelling or an upwelling with a transient trailing tail that persists for less than about one plume risetime. In order for this regime to occur, vertical viscosity variations in the hot boundary layer must be about order 1.

[20] Estimates of the temperature of the CMB are typically in the range of 3000–4500 K [e.g., *Williams*, 1998; *Boehler*, 2000; *Anderson*, 2003]. The conduction of heat from the core to the base of the mantle and from the mantle to the atmosphere and ocean drives natural thermal convection. At thermal equilibrium (heat in equals heat out), and in the absence of plate tectonics, the simplest approximation for such a flow is Benard convection, in which a plane layer of incompressible fluid of height H is bounded above and below by cold and hot isothermal boundaries. Because the Prandtl number, $Pr = \mu/\kappa\rho$, for planetary mantles is effectively infinite, the viscous response to motions is instantaneous, and flow is driven by a balance between buoyancy and viscous forces. In this limit the pattern and heat transfer characteristics of mantle convection are characterized with a Rayleigh number based on the depth of the mantle

$$Ra_i = \rho g \alpha \Delta T H^3/\mu_i \kappa, \tag{5}$$

where ρ is the average density of the fluid, g is gravity, α is the coefficient of thermal expansion, ΔT is the temperature difference across the layer, H is the layer depth, μ is the viscosity, and κ is the thermal diffusivity. The subscript i again indicates properties evaluated at the interior temperature of the convecting fluid. Ra_i is essentially a ratio of the driving buoyancy force, modulated by thermal diffusion, to the retarding viscous force arising from the diffusion of momentum. In the diffusion creep limit, a reasonable approximation for the viscosity law is

$$\mu = \mu_c \exp(-\gamma T). \tag{6}$$

Differentiating with respect to T thus gives a rheological temperature scale $\gamma = -(d\ln \mu/dT)$, which is a constant determined from laboratory measurements on the relevant materials. Thus an additional dimensionless parameter that characterizes the temperature dependence of the viscosity is

$$P = \gamma \Delta T, \tag{7}$$

where ΔT is the full temperature difference between the hot and cold boundaries. It will be useful to introduce a

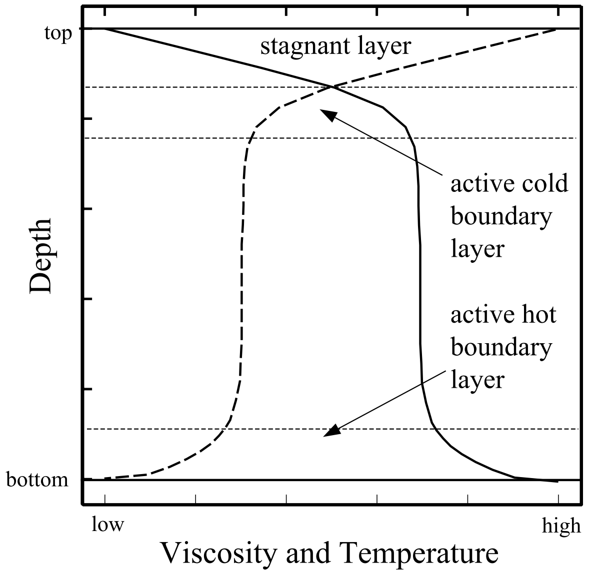

Figure 3. A schematic illustration of the horizontally averaged variation of temperature (solid line) and viscosity (bold dashed line) with depth during an experiment. Also shown are the active thermal boundary layers (thin dashed lines) at the top and bottom of the fluid layer. The high viscosity of the coldest region makes the upper part of the cold thermal boundary layer stagnant. Resultant weak cooling keeps the actively convecting region nearly isothermal and, in turn, the viscosity ratio across the hot thermal boundary layer small.

dimensionless internal temperature, $\theta = (T_i - T_c)/(T_h - T_c)$, the ratio of the viscosity at the cold boundary to that at the hot boundary, $\lambda_t = \mu_c/\mu_h$, and the ratio of the viscosity in the interior fluid to the viscosity at the hot boundary, $\lambda = \mu_i/\mu_h$. In the high-*Pr* limit, as *Ra* increases from 10^3, which is the critical *Ra* required for convection to begin, to $>10^6$, which is typical for planetary mantles, the flow evolves from steady two-dimensional overturning motions to unsteady three-dimensional flow and ultimately to a regime dominated by the intermittent formation and rise and fall of thermals from the hot and cold boundaries, respectively [*Krishnamurti*, 1970a, 1970b; *Weeraratne and Manga*, 1998].

[21] An important characteristic of flows for which $Ra > 10^6$ is that the flow can be divided into three regions (Figure 3): a well-mixed interior in which the horizontally averaged temperature T_i is approximately constant and two thin thermal boundary layers with thickness δ_c and δ_h. In this regime the formation of thermals is governed only by the internal dynamics of each boundary layer, and thus heat transfer across the layer is to a first approximation independent of the layer depth. Said differently, convective heat transport is more important than conductive heat transport over most of the depth of the fluid by a factor $wH/\kappa \gg 1$, where w and κ/H are convective and conductive velocity scales. Conductive heat transfer is, however, a critical component to any convecting system because the conduction of heat across thin thermal boundary layers at the hot and cold boundaries governs the heat flux that must ultimately be carried by the fluid motions in the interior. At high *Ra* in a Newtonian isoviscous fluid with no-slip boundaries, symmetry requires that T_i be the mean of the hot and cold boundaries and also that $\delta_c = \delta_h \sim HRa^{-1/3}$. In a fluid with a viscosity that varies strongly with temperature, however, this is no longer the case. Figure 3 shows that convection from the cold upper boundary occurs beneath a thick stagnant lid of relatively viscous fluid and involves only a fraction of the temperature drop across the cold thermal boundary layer [*Booker*, 1976; *Weinstein and Christiansen*, 1991; *Stengel et al.*, 1982; *Richter et al.*, 1983; *Christensen*, 1984a; *Ogawa et al.*, 1991; *Davaille and Jaupart*, 1993; *Giannandrea and Christensen*, 1993; *Solomatov*, 1995; *Moresi and Solomatov*, 1995, 1998; *Solomatov and Moresi*, 1996, 2000; *Trompert and Hansen*, 1998]. Moreover, viscosity varies by at most a factor of 5–10 across the active or convecting part of the cold thermal boundary layer [e.g., *Richter et al.*, 1983; *Davaille and Jaupart*, 1993; *Deschamps and Sotin*, 2000; *Korenaga and Jordan*, 2003]. Using a scaling analysis that is in broad agreement with the results of experiments and numerical simulations, *Solomatov* [1995] finds that for $P \gg 1$, the scale δ_c/P characterizes the thickness of both the hot and cold thermal boundary layers and that $\delta_h \sim \delta_c/P$.

[22] The presence of a stagnant lid has significant implications for convective heat flow. Consequently, the relationship between the dimensionless global convective heat flux or Nusselt number *Nu* and *Ra* is a focus of many studies of thermal convection in variable viscosity fluids [e.g., *Booker*, 1976; *Richter et al.*, 1983; *Christensen*, 1984a; *Manga and Weeraratne*, 1999] and of the thermal evolution of planets [e.g., *Giannandrea and Christensen*, 1993] because it relates global heat transfer characteristics to the physical properties and boundary conditions of a convecting system. For our purpose, a quantitative understanding of the heat transfer properties of thermal convection in the stagnant lid regime is important because this characteristic governs the temperature and viscosity structure in the hot thermal boundary layer which, in turn, determines the structure of ascending plumes.

[23] The most general *Nu-Ra* relationship is

$$Nu = aRa_\gamma^\beta. \tag{8}$$

In the stagnant lid regime the temperature difference driving convection scales with $1/\gamma$ and is much less than the full temperature drop ΔT. Thus a Rayleigh number based on the temperature difference across the active part of the convecting system is $Ra_\gamma = \rho g\alpha d^3/\mu_i\kappa\gamma$, where the constant a depends mostly on boundary conditions and β is a generalized power law exponent determined on theoretical grounds or from empirical fits to experimental measurements or results from numerical simulations.

[24] A heuristic theoretical model developed by *Howard* [1964] suggests that at high Ra_γ, conductive thermal boundary layers are inherently unsteady with cold or hot material breaking away intermittently with a frequency that is proportional to $Ra_\gamma^{2/3}$. Consequently, the mean thickness δ of a thermal boundary layer is such that the Rayleigh

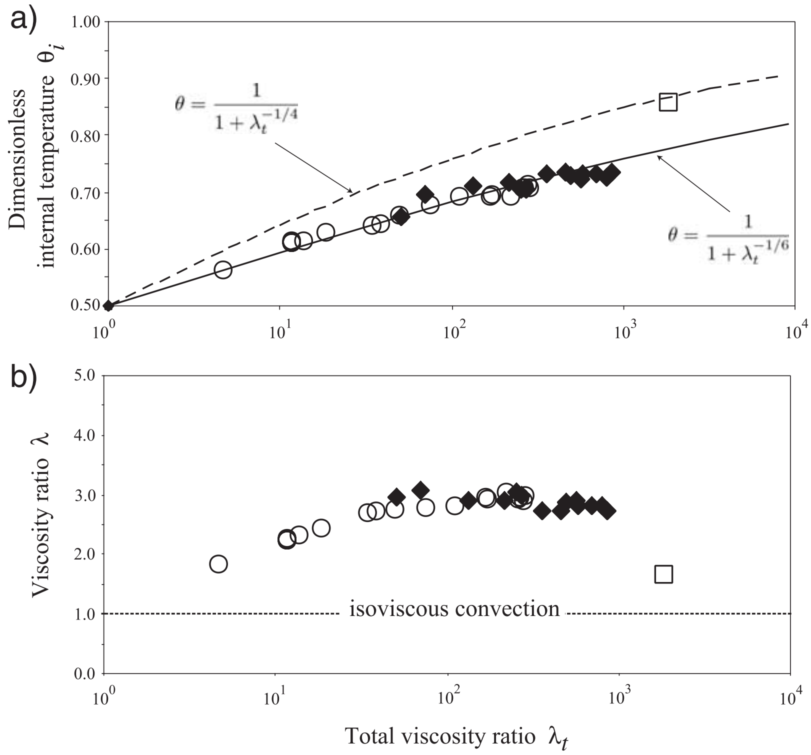

Figure 4. The variation of the (a) dimensionless internal temperature θ_i and (b) the viscosity ratio λ, as a function of the total viscosity ratio λ_t. Circles are data from *Schaeffer and Manga* [2001]; diamonds are data from no-slip experiments. The square is datum from a free-slip experiment. Solid and dashed curves in Figure 4a are theoretical predictions for θ_i assuming steady flow and a no-slip and free-slip lower boundary condition, respectively [*Morris and Canright*, 1984; *Solomatov*, 1995; *Manga and Weeraratne*, 1999].

number based on the boundary layer thickness δ, Ra_δ, is always close to critical or of the order of 10^3. In this regime, heat transport is governed by processes local to the thermal boundary layers and is independent of the layer depth (see review by *Turner* [1973]). Thus, on dimensional grounds, it is expected that $\beta = 1/3$ and

$$Nu = H/\delta \approx \left(Ra_\gamma/Ra_\delta\right)^{1/3} \approx 0.1 Ra_\gamma^{1/3}, \tag{9}$$

where δ is the thickness of either the hot thermal boundary layer or the active part of the cold thermal boundary layer, respectively. Several experimental studies of convection at high Ra_γ in variable viscosity fluids validate this model. In particular, *Schaeffer and Manga* [2001] show that the frequency of thermal formation at the hot or cold boundary is approximately proportional to $Ra^{2/3}$, which verifies that processes responsible for the formation of thermals are local to the boundary layers [cf. *Howard*, 1964]. However, although the 1/3 exponent apparently captures the basic heat transfer characteristics of these unsteady flows, experimental measurements and numerical simulations for high Ra flows in the high- or infinite-Pr limit find that β can be slightly smaller, depending mostly on the upper and lower mechanical boundary conditions [e.g., *Christensen*, 1984a; *Giannandrea and Christensen*, 1993; *Solomatov*, 1995; *Moresi and Solomatov*, 1998; *Niemela et al.*, 2000].

[25] Figure 4 shows that the internal temperature and viscosity ratio across the hot thermal boundary layer approaches a factor of 3–4 (no-slip experiments) or about 1.5 (free-slip experiments) as the total viscosity ratio λ_t becomes large [*Manga et al.*, 2001; *Jellinek et al.*, 2002], which is consistent with theoretical predictions [*Morris and Canright*, 1984] as well as experimental studies [*Manga et al.*, 2001]. One key implication of all of the experiments and numerical results is that the dynamics associated with large viscosity variations in the cold thermal boundary layer lead to weak convective cooling that, in turn, limit the viscosity ratio in the hot boundary layer λ_h to order 1. A second and more important result with regard to this discussion is that Earth-like mantle plumes cannot form in the stagnant lid limit.

[26] *Nataf* [1991] was among the first to speculate that one way to increase the cooling of the interior fluid, and hence increase the temperature and viscosity variations in the hot thermal boundary layer, is to stir in the stagnant lid itself. On Earth this is thermally equivalent to subduction. Indeed, from results of an early series of two-dimensional numerical calculations, *Lenardic and Kaula* [1994, p. 15,697] argue that the "introduction of (mobile) plate-like behavior in a convecting temperature-dependent medium can increase the temperature drop across the lower boundary layer." These authors go on to speculate that (1) the resultant increase in viscosity variations therein causes a change in the morphology of buoyant upwellings and (2) the nature of mantle convection in one-plate planets will thus be different than that in planets with active plate tectonics (which will be addressed next).

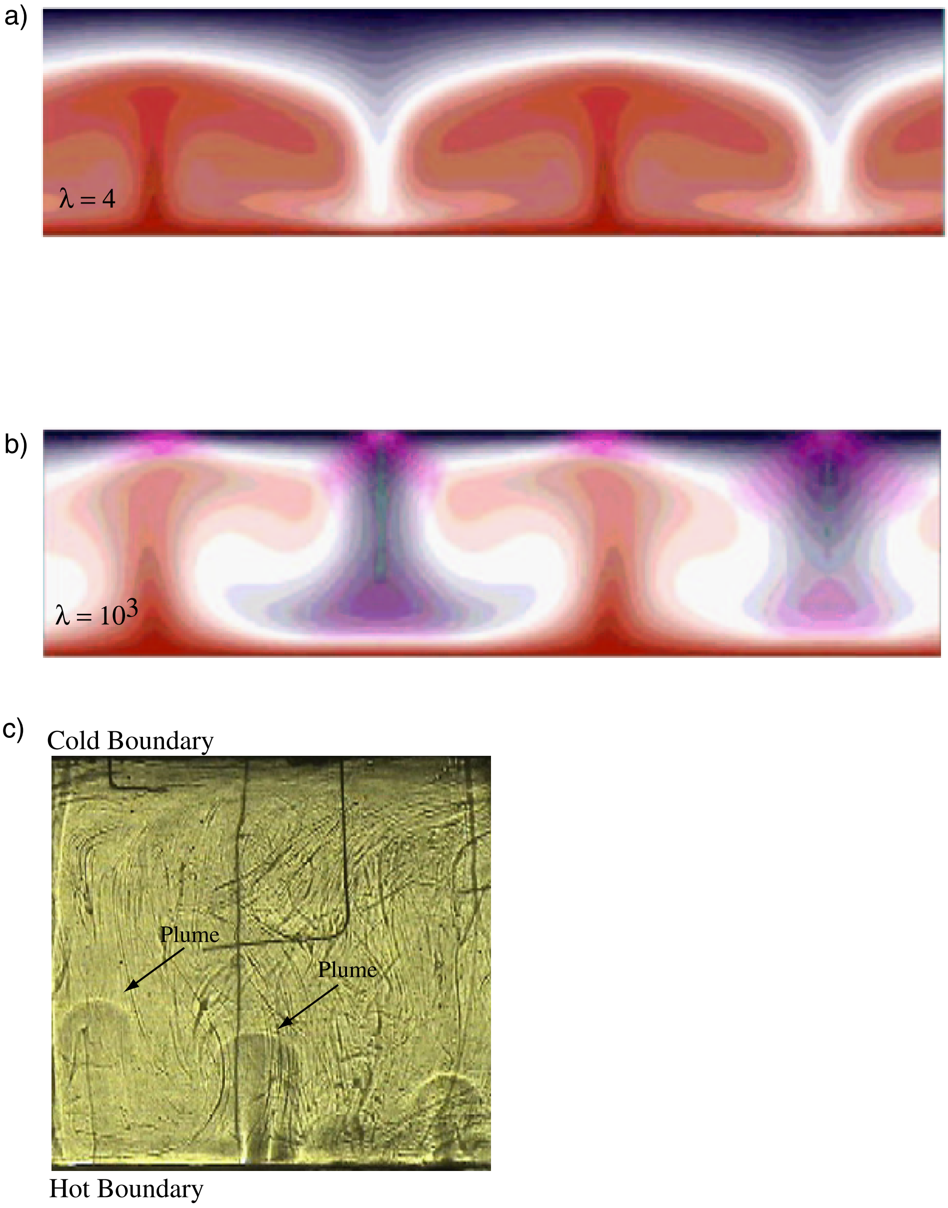

Figure 5. Two-dimensional numerical simulations of convection under statistically steady state conditions in the (a) stagnant lid and (b) active lid regimes (A. Lenardic, personal communication, 2003). $Ra = 10^6$; $\lambda_t = 10^6$. In the stagnant lid limit, weak cooling leads to a small temperature difference between the mantle and underlying core and, in turn, to a hot boundary layer viscosity ratio, $\lambda = 4$. In contrast, strong cooling due to subduction and stirring of the cold lithosphere into the underlying mantle produce large temperature variations in the hot thermal boundary layer and to a viscosity ratio $\lambda = 10^3$. (c) Shadowgraphs of plumes with large heads and narrow trailing conduit from (three-dimensional) laboratory experiments in which the stagnant lid is stirred into an underlying convecting layer using a conveyor belt under thermally steady state conditions. $Ra = 10^6$; $\lambda \approx 10^2$.

[27] Figure 5 shows the potentially fundamental importance of subduction and mantle stirring to producing large viscosity variations within the thermal boundary layer at the CMB (A. Lenardic, personal communication, 2003). In these simulations the mantle has a viscoplastic rheology [*Moresi and Solomatov*, 1998], which can self-consistently allow for an active lid mode of convection for the oceanic lithosphere (i.e., subduction) and for an internal mantle viscosity consistent with the diffusion creep limit (see equation (6)). If convective stresses within the cold thermal boundary layer remain below a critical yield stress, the flow remains in a stagnant lid regime. Alternatively, larger than critical convective stresses lead to shear localization, weak plate margins, and subduction of the cold boundary layer. Comparison of the results for the stagnant lid and active lid cases shows that in the absence of subduction (Figure 5a) the viscosity ratio at the base is of the order of 1 and quantitatively identical to the experimental results presented by *Manga et al.* [2001]. In contrast, the strong cooling following the subduction and stirring of the stagnant lid (Figure 5b) leads to large viscosity variations in the hot thermal boundary layer that are approximately the square root of the total variation in viscosity

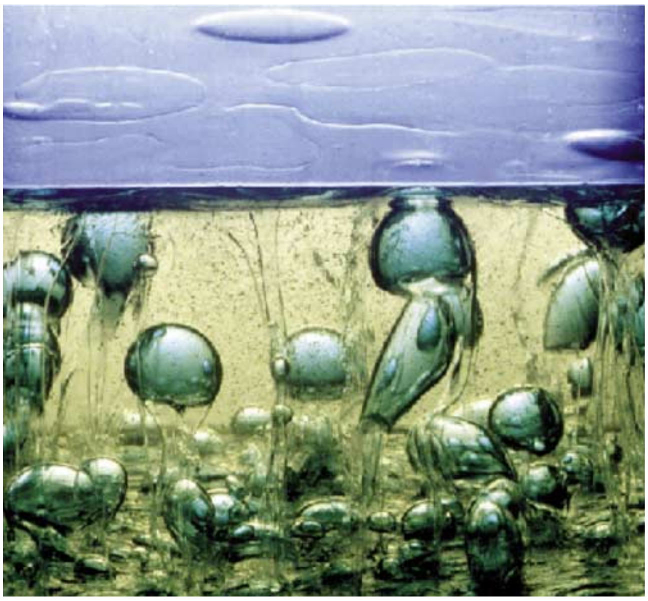

Figure 6. A laboratory experiment with compositional convection in which low-viscosity water (blue) is injected through a permeable plate into high-viscosity glucose syrup. In a way that is dynamically similar to thermal convection, water collects in a gravitationally unstable compositional boundary layer at the base of the syrup and then drains intermittently as plumes with large heads and narrow underlying conduits. Despite the presence of robust low-viscosity conduits, complicated interactions among rising plumes prevent their becoming long-lived stable features.

across the convecting system. Two-dimensional calculations cannot accurately capture the axisymmetric head-tail structure of Earth-like mantle plumes. Figure 5c is a shadowgraph image from a laboratory experiment on convection in a temperature-dependent fluid in which the cold stagnant lid is mechanically stirred into the underlying layer using a conveyor belt. The resulting strong cooling of the interior leads to axisymmetric plumes with large heads and narrow trailing conduits.

3. COMPOSITION, STRUCTURE, AND PHYSICAL PROPERTIES OF THE PLUME SOURCE WITHIN D″

[28] The results from a number of laboratory studies of transient high *Ra* convection indicate that even when the flow is composed of low-viscosity upwellings with head-tail structures, complicated and destructive interactions between such plumes lead to their being spatially and temporally unstable and short-lived (Figure 6) [e.g., *Jellinek et al.*, 1999; *Lithgow-Bertelloni et al.*, 2001; *Jellinek et al.*, 2003]. That is, the presence of large viscosity variations is a necessary but insufficient condition for long-lived Earth-like mantle plumes. We have argued that large viscosity variations arise from plate tectonics and thus that these conditions are a consequence of the upper boundary condition for mantle convection in the Earth. An additional natural question to consider is whether plume stability is a consequence of the physical state of the plume source region, that is, the lower boundary condition for mantle convection.

[29] Over the last 5 decades, explanations for D″, which constitutes the lowermost 200 km of the mantle, have evolved in complexity in response to a growing number of inferred constraints derived from seismological, geodynamic, geomagnetic, and geochemical studies. The original conceptual picture of D″ as essentially a global phase boundary [cf. *Bullen*, 1949, 1950] has expanded to variously include (Figure 7) a thermal boundary layer [cf. *Stacey and Loper*, 1983] locally modulated by subduction [e.g., *Houard and Nataf*, 1993; *Nataf and Houard*, 1993; *Sidorin and Gurnis*, 1998], chemical components left over from the formation and early differentiation of the planet (e.g., see discussions by *Ringwood* [1975] and *Anderson* [1989]), a “slab graveyard” [e.g., *Dickinson and Luth*, 1971; *Chase*, 1981; *Hofmann and White*, 1982; *Ringwood*, 1982; *Davies and Gurnis*, 1986], chemical “dregs” segregated from subducted lithosphere [e.g., *Chase*, 1981; *Hofmann and White*, 1982; *Zindler et al.*, 1982; *Christensen and Hofmann*, 1994; *Marcantonio et al.*, 1995], partial melt [e.g., *Williams and Garnero*, 1996], and metals from the outer core [e.g., *Knittle*

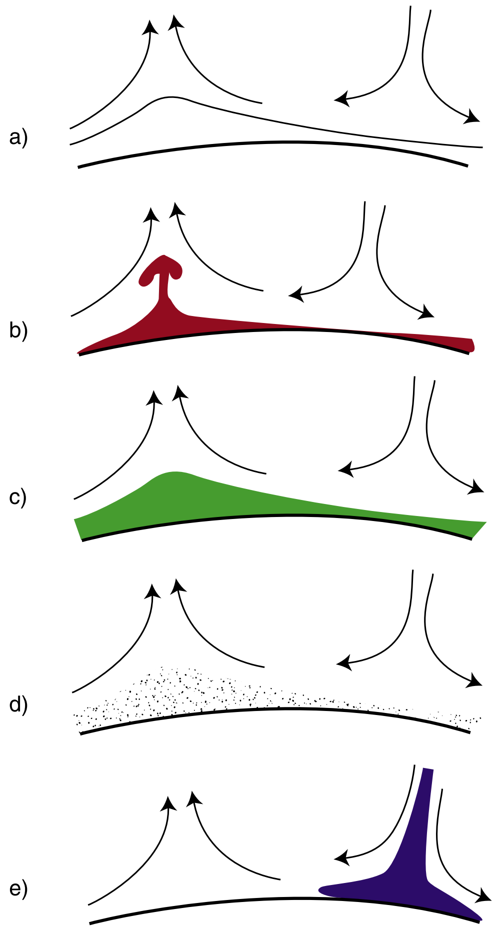

Figure 7. Schematic illustration of several models for D″. Within the context of plate tectonics, D″ has been explained variously as (a) a phase change, (b) a thermal boundary layer, (c) a compositional boundary layer, (d) ponded chemical dregs from subducted lithosphere, and (e) a slab graveyard.

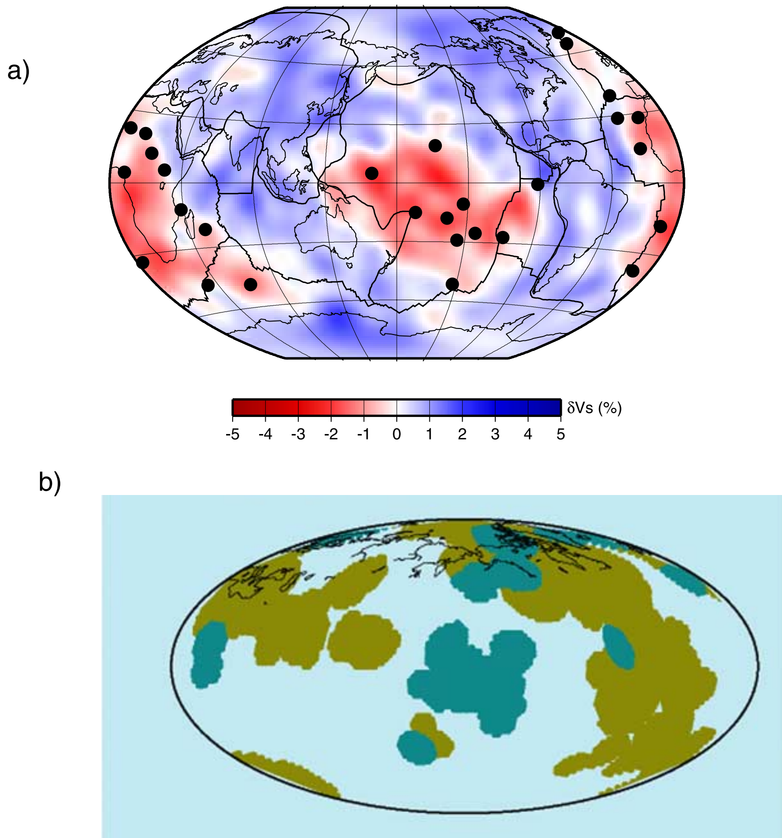

Figure 8. Seismological models showing that the base of the mantle is laterally heterogeneous. (a) Map of shear wave velocity along with the surface position of hot spots (circles) [cf. *Garnero et al.*, 1998; *Ritsema et al.*, 1999]. (b) Sightings (blue) and nonsightings (tan) of ultralow-velocity-zone material as reported by *Castle et al.* [2000].

and Jeanloz, 1989, 1991] to the general picture today of simply "a region of unusual structural complexity" [*Buffett et al.*, 2000, p. 1338] (Figure 7).

[30] Significant advances in our understanding of the nature of D″ have been summarized in a number of thorough papers and reviews [e.g., *Loper*, 1984; *Young and Lay*, 1987; *Campbell and Griffiths*, 1992; *Hart et al.*, 1992; *Loper and Lay*, 1995; *Hofmann*, 1997; *Farley and Neroda*, 1998; *Gurnis et al.*, 1998; *Lay et al.*, 1998a; *Silver et al.*, 1998; *Garnero*, 2000; *Garnero and Wysession*, 2000; *Buffett et al.*, 2002; *Lay et al.*, 2004]. In line with current thinking we review the main controls on the composition, structure, and physical properties of this region. In particular, we identify those features that are presently well accepted and those that remain topics for speculation. Our goal is to establish a picture of the structure, composition, and physical properties of D″ and particularly the plume source region in order that we may address the dynamics of this layer and their influence on convection from the CMB in section 4.

3.1. Seismological Observations

[31] The most numerous constraints on the structure and composition of D″ come from seismological studies of the lower mantle. A now well-established result is that lateral variations within D″ and vertical variations across the D″ discontinuity are much stronger than those found in the mid-mantle. Moreover, whereas velocity anomalies in the mantle overlying D″ can be explained reasonably as being dominated by temperature effects [e.g., *Lay et al.*, 2004], several features of the D″ region require a combination of thermal and compositional variations.

[32] D″ is laterally heterogeneous over a wide range of length scales (Figure 8a). At the largest spatial scales (thousands of kilometers) most models of shear and compressional wave velocity indicate high velocities beneath the circum-Pacific rim and low velocities beneath the central Pacific and Africa [e.g., *Dziewonski*, 1984; *Dziewonski and Woodhouse*, 1987; *Young and Lay*, 1987; *Inoue et al.*, 1990; *Tanimoto*, 1990; *Su and Dziewonski*, 1991; *Garnero and Helmberger*, 1993; *Grand*, 1994; *Su et al.*, 1994; *Wysession*, 1996; *Garnero and Helmberger*, 1996; *Vasco and Johnson*, 1998; *Ritsema et al.*, 1999; *Masters et al.*, 2000; *Kuo et al.*, 2000; *Megnin and Romanowicz*, 2000; *Castle et al.*, 2000; *Romanowicz*, 2001; *Zhao*, 2001]. In addition, whereas high-velocity regions appear to correspond to the positions of subduction zones [e.g., *Richards and Engebretsen*, 1992; *Grand et al.*, 1997; *van der Hilst et al.*, 1997; *van der Hilst and Karason*, 1999; *Fukao et al.*, 2001; *Grand*, 2002], low-velocity regions correlate to the surface position of hot spots [*Weinstein and Olson*, 1989; *Williams et al.*, 1998] as well as to the positions of inferred buoyant deep mantle upwellings [e.g., *Forte and Mitrovica*, 2001; *Forte et al.*,

2002; *Romanowicz and Gung*, 2002] and superswells [e.g., *McNutt*, 1998] in the mid-Atlantic and central Pacific. The slow regions are also marked by "sharp-sided" [*Ritsema et al.*, 1999; *Ni et al.*, 2002] long-wavelength topographic relief with maximum amplitudes likely around 300–450 km above the CMB [e.g., *Wysession et al.*, 1998; *Wen et al.*, 2001; *Ni and Helmberger*, 2001a; *Lay et al.*, 2004], although heights as large as 1000 km above the CMB have been suggested beneath the Pacific and Africa [e.g., *Ritsema et al.*, 1999; *Breger and Romanowicz*, 1998]. Studies of the scattering characteristics of short-wavelength seismic waves [e.g., *Bataille et al.*, 1990; *Bataille and Lund*, 1996; *Earle and Schearer*, 1997; *Schearer et al.*, 1998; *Thomas et al.*, 1999] as well as variations in shear wave velocity [e.g., *Vidale and Benz*, 1993; *Lay et al.*, 1997; *Wysession et al.*, 1998] show that smaller-wavelength (<10^2 km) structures are superimposed on these broad swells and may also occur within D$''$ and on the CMB itself [e.g., *Doornbos*, 1978, 1988; *Menke*, 1986; *Buffet et al.*, 2000; *Garnero and Jeanloz*, 2000; *Rost and Revenaugh*, 2001].

[33] In addition to spatial and topographic variability the heterogeneity along the D$''$ discontinuity and within the layer is complex. The D$''$ discontinuity is characterized by approximately stepwise vertical and (where there is topographic relief) lateral changes in seismic velocity [e.g., *Loper and Lay*, 1995; *Lay et al.*, 2004]. In high-velocity regions, *S* wave velocity V_s and *P* wave velocity V_p increase by about 1.5–3% and 0.5–3%, respectively, over a vertical distance of only 0–30 km. Within D$''$, similarly extreme vertical and lateral variations in V_s, V_p, and the bulk sound speed V_ϕ occur and are accompanied by widespread but locally intense anisotropy, which is generally characterized by horizontally polarized shear wave components traveling faster than vertically polarized shear wave components [e.g., *Lay et al.*, 1998b; *Kendall and Silver*, 1998; *Russell et al.*, 1998; *Kendall*, 2000; *Fouch et al.*, 2001; *Lay et al.*, 2004; *Panning and Romanowicz*, 2004]. Beneath the Pacific and Africa, however, anisotropy can be complex and characterized by local patches in which the vertical shear wave components travel faster than the horizontal shear wave components [*Panning and Romanowicz*, 2004]. Systematic variations in V_s and V_p also occur between regions that have undergone subduction in the last 120 Myr and those that have not. Moreover, V_s and V_ϕ are anticorrelated in the lowermost mantle [*Saltzer et al.*, 2001]. In addition, at the bases of the slow regions beneath Africa and the central Pacific, there are 5–40 km thick ultralow-velocity zones (ULVZ) (Figure 8b) marked by sharp 5–10% and 10–30% reductions in V_p and V_s, respectively [e.g., *Mori and Helmberger*, 1995; *Garnero and Helmberger*, 1993; *Sylvander and Souriau*, 1996; *Revenaugh and Meyer*, 1997; *Garnero et al.*, 1998; *Wen and Helmberger*, 1998; *Vidale and Hedlin*, 1998; *Ni and Helmberger*, 2001b], and a monotonic increase in Poisson's ratio with depth [*Lay et al.*, 2004].

[34] This complex suite of observations has several important implications. First, the presence of both positive and negative anomalies in V_s and V_p within D$''$ is inconsistent with the layer being simply a global phase change [e.g., *Bullen*, 1949]. The occurrence of acute lateral and vertical velocity gradients, anisotropy, and ULVZ within D$''$, along with steep velocity gradients across the D$''$ discontinuity, preclude D$''$ as a simple thermal boundary layer due to the conduction of heat from the core [cf. *Stacey and Loper*, 1983; *Loper and Stacey*, 1983]. Rather, that strong lateral variations in V_s and V_p correspond to regions where subduction has occurred suggests lateral chemical heterogeneity related to this process, a conclusion which is supported further by the associated anticorrelation in V_s and V_ϕ. Because both V_s and V_ϕ are proportional to $1/\sqrt{\rho}$, where ρ is the mantle density, an anticorrelation of V_s and V_ϕ is inconsistent with temperature variations alone and can be explained by changes in constitution and mineralogy.

[35] *Ishii and Tromp* [1999] use a combination of normal mode and free-air gravity constraints to argue that well-defined low-velocity structures beneath Africa and the Pacific are underlain by dense, compositionally distinct material near the CMB. Although the resolution of such high-density material remains controversial [e.g., *Kuo and Romanowicz*, 2002], the proposed "buoyant top, dense bottom" structure for these upwelling structures is supported by *Ni et al.* [2002], who infer the presence of compositionally dense material at the base of a buoyant upwelling beneath Africa using variations in V_s. Finally, ultralow but nonzero shear wave velocities combined with a monotonic increase in Poisson's ratio with depth in ULVZ are consistent with the average physical properties being due to a mixture of a solid and a fluid phase. Currently, the preferred explanation is that the fluid phase is silicate melt [*Williams and Garnero*, 1996; *Revenaugh and Meyer*, 1997; *Wen and Helmberger*, 1998; *Vidale and Hedlin*, 1998; *Simmons and Grand*, 2002], although the data do not demand this interpretation. Other possible fluid phases include an iron-rich fluid leaked from the outer core [e.g., *Knittle and Jeanloz*, 1989, 1991; *Goarant et al.*, 1992; *Poirier*, 1993; *Jeanloz*, 1993; *Song and Ahrens*, 1994; *Dubrovinsky et al.*, 2001], although the viability of such a process remains a matter for debate [e.g., *Poirier et al.*, 1998], or a mixture of partial melt and outer core fluid [*Garnero and Jeanloz*, 2000].

[36] One reason for the current popularity for partial melt models is their inherent simplicity. *Lay et al.* [2004] show that most of the observational database can be explained in a simple and self-consistent way if D$''$ is a dense, partially molten, thermochemical boundary layer. Partial melting may occur within D$''$ if the solidus temperature, T_s, is between the temperature at the CMB, T_{cmb}, and the temperature of the interior mantle, T_m. Assuming that the Earth's liquid outer core is well mixed (i.e., adiabatic) and that the boundary with the solid inner core is approximately at thermal equilibrium, T_{cmb} can be estimated using the phase diagram for the outer core, which remains uncertain in detail owing to unknown concentrations of O, S, and other light elements [e.g., *Anderson*, 2003]. However, an upper bound for T_{cmb} can be obtained from the freezing temperature for pure iron at the inner core–outer core boundary and projection of this temperature along an

adiabat. Combined experimental and theoretical studies [e.g., *Birch*, 1972; *Williams*, 1998; *Boehler*, 1996, 2000; *Anderson*, 2003] have constrained this value to be close to 4850 K. An addition of 20 mol % S, which is probably too large [*Anderson*, 2003], gives what we will assume to be lower bound of around 3300 K (see review by *Williams et al.* [1998]). T_s depends on the choice of bulk composition, which remains contentious. However, one simple analog that satisfies seismic observations, and that is broadly consistent with experimental studies [e.g., *Kesson et al.*, 1998], is a (Mg,Fe)SiO_3-perovskite–(Mg,Fe)O-magnesiowustite (i.e., pyrolite) binary system. *Lay et al.* [2004] argue that whereas T_s for the end-member compositions is greater than T_{cmb}, for many plausible mixtures of these components the resulting freezing point depression should lead to $T_s < T_{\mathrm{cmb}}$. On extrapolating the pyrolite solidus of *Zerr et al.* [1998] to CMB conditions Lay et al. find that $T_s \approx 4300$ K, significantly below possible CMB temperatures. It should be noted that the pyrolite composition of Zerr et al. is an approximation of the actual thermodynamic system. Additional components, especially volatiles, will likely lead to greater freezing point depression and thus a lower T_s and more extensive melting.

[37] One implication of the partial melt model is that if D$''$ has a uniform composition, then the partially molten layer must be global because the temperature at the core-mantle boundary is the same everywhere. If the ULVZ does represent a partially molten region, because the ULVZ is discontinuous or at least not detectable in many regions (Figure 8b), it implies a chemically heterogeneous D$''$. Moreover, areas with a ULVZ have a composition with a lower melting temperature than regions without a ULVZ.

[38] Incorporating additional topographic observations of the D$''$ discontinuity, the following conceptual picture of D$''$ emerges [cf. *Lay et al.*, 2004]: It is a piecewise continuous global feature characterized by lateral variations in thickness and composition due to interaction with mantle flow. Thickening beneath Africa and the central Pacific and thinning around the Pacific rim is due to a combination of material being pushed aside into piles by downgoing slabs and that which is entrained into upwelling plumes and mantle return flows beneath the central Pacific and Africa [e.g., *Tackley*, 1998b, 2000; *Zhong et al.*, 2000; *Jellinek et al.*, 2003; *Gonnermann et al.*, 2004]. Thus sharp boundaries between slow and fast regions in D$''$ reflect the transition from ponded slab material to partially molten regions. A conceptual model in which subduction and convection from the CMB interact with a partially molten thermochemical boundary layer satisfies the majority of the observable constraints for ULVZ outlined above, at least in a qualitative way. In particular, an increase in the extent of the partial melt fraction with temperature is consistent with the observed monotonic increase in Poisson's ratio. Moreover, the ratio of 3–3.5:1 shear to compressional wave velocity reduction can be reconciled with >6 vol % partial melt, where the estimate of melt fraction depends on the geometry of the melt itself [*Williams et al.*, 1998].

[39] A further observation that will be useful for analysis of the dynamics of D$''$ is that $V_s \neq 0$ in ULVZ on spatial scales comparable to or greater than the wavelengths of the seismic waves. Thus, over these length scales the viscosity and density can be interpreted in an average sense in terms of homogeneous mixtures of melt and solid matrix. Qualitatively, the presence of even very small amounts of melt can substantially lower the viscosity of mantle rocks deforming by diffusion creep [e.g., *Hirth and Kohlstedt*, 1995], and thus we can conclude that partially molten material in D$''$ will be significantly less viscous than overlying mantle. Quantitatively, the absolute reduction of viscosity depends on the phase assemblage, the grain size within the solid phase, and the geometry of the melt inclusions, for which there are no constraints. Constraints on the density of such a partially molten layer are indirect. Comparison of the results from a wide range of experiments on silicate liquids at very high pressures has shown that whether melts are dense, neutrally buoyant, or even buoyant under lower mantle–CMB conditions depends critically on the detailed chemistry and physical properties of the liquid phase and possibly the solid phase with which it equilibrates [e.g., *Brown et al.*, 1987; *Rigden et al.*, 1984, 1989; *Knittle*, 1998; *Ohtani and Maeda*, 2001; *Moore et al.*, 2004; *Akins et al.*, 2004]. Given this uncertainty, the main constraint on the density of the partially molten material is the probable longevity of the layer over geological time, which is governed ultimately by the rate at which it is eroded by either large-scale mantle motions or by flow into plumes. A buoyant or neutrally buoyant layer is unlikely to persist. We return to this issue in section 3.4.

3.2. Geodynamic and Geomagnetic Constraints Derived From Observations

[40] Geodynamic and geomagnetic studies present additional constraints on the nature of D$''$ as well as the CMB and may provide the most stringent requirements for the composition of ULVZ. One heuristic constraint is that core cooling is required to drive the geodynamo and produce the magnetic field observed at the surface of the Earth [e.g., *Verhoogen*, 1961; *Gubbins*, 1977; *Stevenson*, 1981; *Loper*, 1989; *Buffett et al.*, 1996; *Stevenson et al.*, 1983; *Buffett*, 2002; *Stevenson*, 2003]. Thus D$''$ must include a thermal boundary layer across which heat is conducted to the mantle [e.g., *Stacey and Loper*, 1983; *Loper and Stacey*, 1983; *Stacey and Loper*, 1984]. In addition, a joint analysis of current uplift rates and the dynamic topography of southern Africa by *Gurnis et al.* [2000] shows that the underlying mantle upwelling flow may be both buoyant and constructed of anomalously dense material near the base of the mantle, a result that is consistent with the findings of *Ishii and Tromp* [1999] discussed in section 3.1. That the underlying mantle is buoyant and not simply a passive return flow is supported also by a number of studies [e.g., *Forte and Mitrovica*, 2001]. Notably, the ellipticity of the CMB, as determined from observational and theoretical studies of the origin of the Earth's retrograde free-core nutation, can be explained as a result of viscous stresses

generated by mantle upwellings beneath the central Pacific and Africa [e.g., *Forte et al.*, 1994].

[41] The results of increasingly detailed studies of the influence of electromagnetic coupling between the outer core and lower mantle on gravitationally forced periodic variations in the orientation of the Earth (i.e., nutations) [*Mathews and Shapiro*, 1992; *Buffett*, 1992, 1993; *Buffett et al.*, 2000; *Mathews et al.*, 2002; *Buffett et al.*, 2002] and of the Earth's rate of rotation (i.e., the length of day) [e.g., *Holme*, 1998] require a thin, immobile (relative to fluid in the outer core) layer of high conductance (electrical conductivity multiplied by layer thickness) at the base of the mantle in order to reconcile very long baseline interferometry observations with inferred, well-constrained magnetic field intensities at the CMB [cf. *Langel and Estes*, 1982]. Such a layer may be on either side of the CMB and $\sim$200 m thick if constructed of pure Fe.

[42] This layer must have a conductance $>10^8$ S rather than of the order of 10^3-10^5 S expected for a comparably thick layer of silicate rocks or melt. *Buffett et al.* [2002] show that in the absence of a high-conductivity layer the low conductivity of solid or even partially molten mantle demands magnetic field intensities at the CMB that are probably more than a factor of 10 too large. Nutation data are also well explained if ULVZ is composed partly or completely of a mush of silicate sediments, precipitated within the outer core on inner core growth, and interstitial outer core fluid. Such a mush is expected to collect and compact on the core side, within radially displaced segments of the CMB or basins [*Buffett et al.*, 2000], the presence of which is supported by the observational and theoretical constraints on CMB ellipticity mentioned above [e.g., *Forte et al.*, 1994]. *Buffett et al.* [2002] estimate that the sharp lateral reduction in V_s from the lower mantle to the compacted sediment is about a factor of 2 larger than the reduction in V_p, which, given uncertainties, is comparable to the factor of 3 reduction obtained from seismological studies.

[43] Although a layer with high electrical conductance may be required at the CMB, the analysis of the Earth's nutations is insensitive to the spatial connectivity of such material because the net exchange of angular momentum between the outer core and the lower mantle depends only on its total surface area. Potential support for the high electrical conductivity of observed ULVZ patches, however, may come from studies of the positions of the pole for the dipole component of the magnetic field (i.e., virtual geomagnetic pole (VGP)) during polarity reversals. A number of studies have shown that VGP reversal paths are confined to longitudes through the Americas and Asia over the last few million years [e.g., *Clement*, 1991; *Laj et al.*, 1991; *Constable*, 1992; *Gubbins and Coe*, 1993; *Love*, 1998, 2000; *Constable*, 2003]. As the dipole field decays during a magnetic reversal, currents are generated in the highly conductive patches of ULVZ, resulting in a secondary magnetic field in addition to that due to the geodynamo. *Runcorn* [1992] suggests and *Aurnou et al.* [1996] argue that the confinement of VGP paths can be explained by resulting electromagnetic torques acting at the CMB to rotate the core such that the net torque at the CMB is zero. *Brito et al.* [1999] have subsequently argued that such a mechanism is unrealistic because such torques are insufficiently large to influence core rotation. In a recent study, however, *Costin and Buffett* [2004] show that the geometry of the secondary field, which is superposed onto the transitional field because of the geodynamo, can, indeed, govern VGP paths during reversals. Moreover, the observed longitudinal confinement of VGP paths during reversals can be explained by the mapped spatial distribution of highly conductive ULVZ beneath the central Pacific and Africa.

[44] Analyses of the secular variation of the geomagnetic field suggest that this property is also influenced by lateral heterogeneity at the CMB, although rigorous constraints on CMB structure are at an early stage and remain speculative. A number of studies of the historic and paleomagnetic fields [e.g., *Bloxham et al.*, 1989; *Gubbins and Kelly*, 1993; *Johnson and Constable*, 1997; *Gubbins*, 1998] identify persistent hemispheric asymmetries in the average value and secular variation of the field over the last 5 Myr. Specifically, these studies find low secular variation in the Pacific hemisphere and anomalously low radial magnetic field centered on Hawaii [e.g., *Johnson and Constable*, 1998]. That these anomalous features persist for timescales much longer than the timescale for outer core overturn suggests that they are related to the details of core-mantle coupling [e.g., *Gubbins*, 2003] rather than to the style of flow in the outer core. In addition, this structure corresponds spatially with the location of ULVZ beneath the Pacific, and consequently, the longevity of the field structure in the Pacific has been variously explained as being due to "screening" by a thin, high-conductivity shell [e.g., *Runcorn*, 1992], the influence of a variable temperature [e.g., *Bloxham et al.*, 1989], and variable heat flux [e.g., *Olson and Glatzmaier*, 1996; *Gibbons and Gubbins*, 2000] condition at the CMB. The extent to which any of these effects is uniquely responsible for the structure of the observed field has not yet been established, but this avenue of research remains promising.

3.3. Geodynamic Constraints Derived From Dynamic Models

[45] Another approach to developing constraints on the composition and structure of D$''$ is to investigate the geodynamical consequences of inferred properties for this layer in models of mantle convection and the Earth's thermal and compositional evolution (see reviews by *Tackley* [2002] and *Tackley and Xie* [2002]). In particular, the results of such studies yield bounds on the density and viscosity structure of D$''$. Numerical, experimental, and theoretical studies of the dynamics of D$''$ generally assume that this layer has existed over the bulk or all of the history of the Earth in spite of erosion by mantle flow. Thus a goal of such work is to identify conditions in which D$''$ may persist for geological time. Layered mantle convection models can generally be divided into two groups. In one group of models, D$''$ is a compositionally distinct layer that predates the onset of mantle convection, and so its composition, thickness, and

physical properties are specified as initial conditions. In this case the results of numerical simulations [e.g., *Christensen*, 1984b; *Davies and Gurnis*, 1986; *Hansen and Yuen*, 1988, 1989, 2000; *Tackley*, 1998b; *Sidorin and Gurnis*, 1998; *Farnetani*, 1997; *Montague et al.*, 1998; *Kellogg et al.*, 1999; *Montague and Kellogg*, 2000; *Tackley*, 2000; *Tackley and Xie*, 2002; *Solomatov and Moresi*, 2002; *Samuel and Farnetani*, 2003; *McNamara and Zhong*, 2004a, 2004b], analog experiments [*Olson and Kincaid*, 1991; *Davaille*, 1999a, 1999b; *Gonnermann et al.*, 2002; *Davaille et al.*, 2002; *Namiki*, 2003], and analytical studies [e.g., *Sleep*, 1988] show that for plausible thicknesses a layer must be around 2–6% denser than overlying mantle if it is to persist over timescales comparable to the age of the Earth. Furthermore, models in which these density differences are applied show that D″ will be thin or nonexistent beneath subducting slabs [e.g., *Sidorin and Gurnis*, 1998; *Tan et al.*, 2002], which push the dense material and thermal boundary layer fluid aside and into "piles" beneath upwelling mantle return flow [e.g., *Tackley*, 1998b; *Jellinek et al.*, 2003; *Gonnermann et al.*, 2004], and plumes [e.g., *Manga and Jeanloz*, 1996; *Davaille*, 1999a; *Gonnermann et al.*, 2002; *Jellinek and Manga*, 2002].

[46] In alternative models, D″ is generated continuously through the ponding of dense material from subducting slabs or the infiltration of outer core fluid. Analog [*Olson and Kincaid*, 1991] and numerical simulations [e.g., *Kellogg and King*, 1993; *Christensen and Hofmann*, 1994; *Kellogg*, 1997; *Coltice and Ricard*, 1998] show that dense, low-viscosity eclogite components from slabs are likely to pond at the CMB. Moreover, *Christensen and Hofmann* [1994] and *Coltice and Ricard* [1998] show that such a process can be reconciled with Nd, Pb, and He isotopic characteristics of OIBs. In contrast, *Kellogg and King* [1993] investigate the upward percolation from the CMB of outer core fluid and find that an appropriate stabilizing density difference is possibly larger. We note that a viable mechanism by which core fluid leaks into the lower mantle to form a significant thickness (>1 km) of dense material remains controversial [e.g., *Poirier*, 1993; *Poirier et al.*, 1998]. However, this model cannot be discarded because explanation for both the Earth's gravitationally forced nutations and VGP reversal paths (see section 3.2.) apparently require high-conductivity material at the base of the mantle. Moreover, Os isotopic characteristics and platinum group element geochemistry of lavas related to a number of plumes may suggest entrainment of core material into the silicate source material for plumes. This is discussed in section 3.4.

3.4. Geochemical Constraints on the Source Region for Deep Mantle Plumes

[47] Geochemical studies of ocean island basalts (OIBs) can provide additional, albeit indirect, information on the thermal state and composition of the plume source region within D″. In order to appeal to geochemical observations to provide such insight, however, two assumptions must first be made. The first is that hot spots related to deep mantle plumes sample the base of the Earth's mantle. The second is that the bulk composition of plume material is not significantly influenced by entrainment from the mantle during ascent such that the signature of the plume source is preserved [e.g., *Farnetani and Richards*, 1995]. Bearing in mind these caveats, in addition to the He isotope systematics discussed in section 2, lavas from hot spot volcanoes generally have major element concentrations that reflect large (200°C) temperature differences [e.g., *Schilling*, 1991], are enriched in light rare earth elements and the radiogenic isotopes of Sr, U, and Pb, and are depleted in radiogenic isotopes of Nd [e.g., *Schilling*, 1973; *Schilling et al.*, 1983; *Schilling*, 1986; *Langmuir et al.*, 1992; *Campbell and Griffiths*, 1992; *Hofmann*, 1997; *Jellinek et al.*, 2002].

[48] A number of distinct mantle components have been identified and systematized within a geological context in a number of thoughtful reviews to explain the isotopic composition of hot spot lavas [e.g., *Zindler and Hart*, 1986; *Hart et al.*, 1992; *Hofmann*, 1997; *Farley and Neroda*, 1998]:

[49] 1. Depleted MORB mantle, characterized by low $^{206}Pb/^{204}Pb$, low $^{87}Sr/^{86}Sr$, and high $^{143}Nd/^{144}Nd$, is chondritic mantle from which the material forming continents has been removed.

[50] 2. Three "enriched" mantle sources include HIMU (i.e., high $^{238}U/^{234}U$, high $^{206}Pb/^{204}Pb$, high $^{143}Nd/^{144}Nd$, and low $^{87}Sr/^{86}Sr$); enriched mantle 1 (EM1) (i.e., low $^{87}Sr/^{86}Sr$ and $^{143}Nd/^{144}Nd$, high $^{207}Pb/^{204}Pb$, and high $^{208}Pb/^{204}Pb$ for a given $^{206}Pb/^{204}Pb$); and enriched mantle 2 (EM2) (i.e., EM2, which is EM1 with high $^{87}Sr/^{86}Sr$). Explanations for these compositions include recycled lower continental crust, recycled oceanic crust and sediment, and metasomatized mantle.

[51] 3. "Focus Zone," or FOZO, is marked by EM and high $^{3}He/^{4}He$ mantle (see section 2).

[52] Understanding the origin, dynamics, and evolution of the various geochemical reservoirs remains an active area of research. Explanations usually permit multiple interpretations, and thus many of the conclusions are controversial. Consequently, we focus specifically on geochemical characteristics potentially diagnostic of the source region within D″ alone and, particularly, of the compositionally dense (ULVZ) material inferred to exist beneath African and the central Pacific hot spots. We adopt this approach because, as will be discussed in section 4, entrainment from this dense material into rising plumes is expected to influence the bulk and trace element composition of associated lavas.

[53] From the discussion in section 2.1, characteristic high $^{3}He/^{4}He$ values for hot spots are thought to be indicative of the silicate lower mantle part of the plume source. Geomagnetic and geodynamic studies (section 3.2) also require an additional electrically conductive outer core component in the lowermost mantle. Thus the main aim of this section is to complement the He isotopic systematics in hot spot lavas outlined in section 2.1 and to identify possible evidence of core-mantle interaction in these regions. In addition, characterization of outer core components in the source will help constrain whether the unusual properties of ULVZ material are related to partial melt, outer core material, or a mixture of both. We review arguments

for core-mantle interaction based on recent and ongoing studies of highly siderophile elements concentrated in the Earth's core [*Shirey and Walker*, 1998]. In particular, we consider whether such evidence is consistent with the dense ULVZ material being a reasonable mixture of outer core fluid and solid (or partially molten) lower mantle. The physical properties of such a mixture are briefly explored along with the extent to which their behavior is coupled to variations in ^{3}He/^{4}He values.

[54] Although contentious [e.g., *Schersten et al.*, 2004], currently, the most compelling case for core-mantle interaction in regions where ULVZ material occurs, as well as the entrainment of outer core material into ascending mantle plumes, is based on studies of the Os isotope systematics of Gorgona Island komatiites, which are related to the Caribbean flood basalts and possibly the Galapagos plume [*Brandon et al.*, 2003], and Hawaiian picrites [*Brandon et al.*, 1998]. Similar characteristics occur also in ores from intrusive rocks associated with Siberian flood basalt lavas [e.g., *Walker et al.*, 1995], although the source region for these lavas is unclear. Notably, lavas from Iceland contain no evidence of core material [*Brandon*, 2002], and this hot spot is apparently not underlain by ULVZ material at the CMB. The presence of core material in the Hawaiian plume source is further supported by new high-precision measurements of Fe/Mn ratios. Initial results indicate that this ratio is uniform in MORB and elevated in Hawaiian picrites, consistent with the presence of outer core material [*Humayun*, 2003, also unpublished data, 2004]. Variations in platinum group element geochemistry of Ontong Java plateau lavas [*Ely and Neal*, 2003] and in unradiogenic W in southern African kimberlites [*Collerson et al.*, 2002] also suggest core-mantle exchange in source regions containing ULVZ material.

[55] Two key observations are at the heart of arguments based on Os isotopic studies for outer core material being in the plume source but absent from the mantle sampled at mid-ocean ridges. First, samples from these locations have coupled suprachondritic ^{187}Os/^{188}Os and ^{186}Os/^{188}Os values (i.e., "excesses"). Second, the Pt-Re-Os systematics for Hawaiian, Gorgonan, and Siberian samples are identical [*Brandon et al.*, 2003], implying that the Os isotopic reservoir is homogeneously distributed over large spatial scales.

[56] The outer core readily satisfies the requirement of a spatially extensive reservoir. The main issue is, then, whether it is reasonable to expect the observed Os isotopic excesses to occur in the outer core. Rhenium 187 decays to ^{187}Os with a half-life of around 45 Gyr and ^{190}Pt decays to ^{186}Os with a half-life of about 500 Gyr. Thus the observed ^{187}Os and ^{186}Os anomalies require long-term (>1 Gyr) radiogenic Os growth in a reservoir that is moderately enriched in Re relative to Os and strongly enriched in Pt relative to Os. Qualitatively, Pt/Os must be much larger than Re/Os because ^{190}Pt is composed of only around 0.01% of all isotopes of Pt and decays to ^{186}Os with a very long half-life. Quantitatively, the coupled excesses in the Hawaiian data demand Pt/Re $\approx$ 88–100 [*Brandon et al.*, 1999]. *Walker et al.* [1995] propose that one way such large Pt/Re values can be produced in the outer core is if Os is concentrated more strongly into the solid inner core than Re and much more strongly than Pt during inner core growth. The magnitudes of the resulting ^{187}Os and ^{186}Os anomalies thus depend on the bulk composition of the core, the timing and rate of inner core growth, and the extent to which the absolute and relative partitioning of behaviors of Pt, Re, and Os are known under core conditions. All models ascribing coupled Os excesses to the outer core ultimately rely on three conditions:

[57] 1. The Earth has a chondritic bulk composition, and $\approx$99.9% of all Re, Os, and Pt are concentrated into the core during its formation.

[58] 2. The inner core began to grow by about 3.5 Ga [e.g., *Brandon et al.*, 2003].

[59] 3. Os is concentrated relative to Re and Pt in the inner core, consistent with the partition coefficients, $D_{Os} > D_{Re} \gg D_{Pt}$. This partitioning behavior is derived from analytical and experimental studies of Fe-meteorites [e.g., *Pernicka and Wasson*, 1987; *Morgan et al.*, 1995; *Smoliar et al.*, 1996; *Shirey and Walker*, 1998] as well as pure liquid iron conducted at low (i.e., atmospheric to upper mantle) pressures (e.g., see discussions by *Walker et al.* [1995, 1997] and *Walker* [2000]).

[60] The first condition is widely accepted and the second is reasonable on geochemical grounds [e.g., *Walker et al.*, 1995; *Brandon et al.*, 2003], although geodynamical constraints on the timing and rate of inner core growth are model-dependent [e.g., *Labrosse et al.*, 2001; *Labrosse*, 2002]. The most significant unknown is the partitioning behavior of Pt, Re, and Os at core pressures in pure iron or appropriate iron alloys and in the presence of light elements such as S or O (see discussion by *Walker* [2000]). Despite this uncertainty, however, *Walker* [2000, p. 2908] notes in his review that

> "the group II meteorites remain the best guide to the expected fractionations [and that] this guide leads us to expect that the fractionations of Pt, Re and Os required to explain the Os-isotopic anomalies can occur in the Earth's core as proposed by *Walker et al.* [1995] and *Brandon et al.* [1998]."

[61] Two other results of the work by Brandon and colleagues support the existence, and constrain physical and chemical properties of, a mixture of solid or partially molten silicate with outer core material in the Hawaiian plume source. First, in order to explain the Os isotope geochemistry of erupted picrites, ~0.8–1.2 wt % outer core material must be added, depending on the rate at which the inner core grows [*Brandon et al.*, 1999]. Assuming that this material is homogeneously distributed, this additional core material plausibly increases the density of ambient lower mantle by 2–3%. This stabilizing density increase is consistent with this dense material persisting for the age of the Earth (see section 3.3), which is, in turn, compatible with possible evidence of core material in plume-related Archaean komatiites and Proterozoic picrites [*Shirey and Walker*, 1998; *Puchtel et al.*, 1999; *Puchtel and Humayun*, 2000; *Walker et al.*, 1997]. A second result suggesting an iron-silicate mixture in the Hawaiian plume source is indicated in Figure 9. Figure 9a shows that variations in ^{3}He/^{4}He and ^{186}Os/^{188}Os are linearly correlated. This behavior is expected

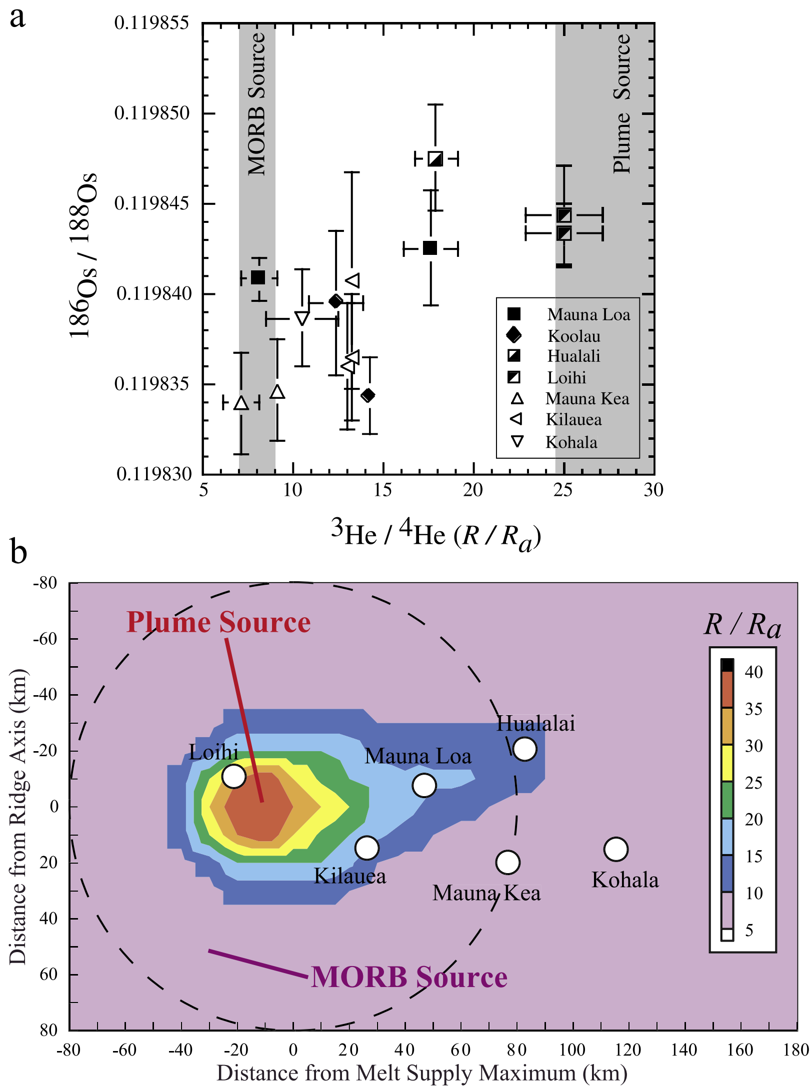

Figure 9. (a) Plot showing an approximately linear correlation between $^3He/^4He$ and $^{186}Os/^{188}Os$ in Hawaiian lavas based on the study of *Brandon et al.* [1999]. (b) Map of the variation of $^3He/^4He$ among Hawaiian volcanoes superimposed on a model for the Hawaiian plume adapted from *DePaolo et al.* [2001]. The center of the plume conduit is inferred to lie beneath the Loihi seamount, where $^3He/^4He$ values are highest. The dashed line is a mantle isotherm corresponding to a potential temperature of 1400°C.

from linear mixture theory, assuming variations in both components reflect differing contributions of plume source and upper mantle (MORB source) material to erupted lavas. Whereas the highest $^3He/^4He$ and $^{186}Os/^{188}Os$ values correspond to a maximum concentration of plume source material, $^3He/^4He \approx 7-9$ is indicative of upper mantle MORB source. Figure 9b, based on results of *Depaolo et al.* [2001], shows an additional spatial correlation between the $^3He/^4He$ and distance from the inferred center of the Hawaiian plume that supports this proposed mixing. The largest $^3He/^4He$ values and the highest $^{186}Os/^{188}Os$ values occur in lavas from Lohi, which is inferred to nearly overlie the highest-temperature central part of the plume. As the central part of a plume conduit is expected to be composed of the lowest-viscosity material from near the bottom of the thermal boundary layer at the base of the mantle (see section 2.2), Loihi lavas are probably derived from melting of predominantly plume source material that is enriched in both ^3He and ^{186}Os. In contrast, MORB-like $^3He/^4He$ and the lowest $^{186}Os/^{188}Os$ values are recorded in young lavas from Mauna Kea and likely reflect melting of ambient upper mantle material. Intermediate $^3He/^4He$ and $^{186}Os/^{188}Os$ values are due to varying contributions of plume source and MORB source mantle.

[62] The core-mantle interaction hypothesis derived from Os isotopic studies is appealing ultimately for its simplicity and because it is consistent with a number of geophysical constraints outlined in section 3.3. Assuming Pt-Re-Os partitioning behavior is compatible with studies of Fe-meteorites, the model requires only that the inner core begin growing early in Earth's history and that the outer core is well mixed. The data, however, require only that the coupled $^{186}Os/^{188}Os$ and $^{187}O/^{188}Os$ excesses be matched and that Pt-Re-Os isotope systematics be similar in the sources for plumes and thus permit alternative interpretations. One such explanation that continues to receive

significant attention is a "crustal recycling" model [e.g., *Lassiter and Hauri*, 1998; *Schersten et al.*, 2004], analogous to the "chemical dregs" models discussed in section 3. In this scenario, developed originally to explain Re/Os characteristics of OIBs, basaltic crust or sediment is segregated into the plume source from subducting lithosphere, resulting in an elevated Re/Os composition. If this segregated material can be stored for the order of 1 Gyr, it is well established that the decay of ^{187}Re to ^{187}Os can produce observed ^{187}Os excesses in OIBs [*Pegram and Allegre*, 1992; *Hauri and Hart*, 1993; *Roy-Barman and Allegre*, 1995; *Marcantonio et al.*, 1995; *Hauri et al.*, 1996; *Widom et al.*, 1997; *Shirey and Walker*, 1998; *Schaefer et al.* 2002].

[63] Reconciling the addition of basaltic crust with the observed coupled excess of ^{186}Os remains, however, problematic for two reasons [cf. *Brandon et al.*, 1999, 2003]. First, whereas Pt/Os excesses can be large in basaltic crust, owing to Pt being concentrated relative to Os in mantle melts, the concentration of Pt is usually chondritic, implying that Os is depleted relative to the lower mantle. Thus, in order to match the ^{186}Os excess, >70% of the source would have to be basaltic crust, which is inconsistent with the bulk chemistry and petrology of the erupted lavas [*Norman and Garcia*, 1999]. Second, in the event that the source could contain this volume of crustal material, the Re/Os ratio of such material is sufficiently high that the linear correlation between ^{186}Os/^{188}Os and ^{187}Os/^{188}Os has a slope that is generally too flat to explain the Hawaiian and Siberian data, regardless of the age of the crust [*Brandon et al.*, 1999, Figure 4]. That is, whereas for basaltic crust that is 1–3 Gyr, Pt/Re $\approx$0.1–33, the Hawaiian data demand Pt/Re $\approx$88–100 [*Brandon et al.*, 1999].

[64] A number of studies suggest that the subduction of sporadically occurring Mn-rich sediments formed as a result of hydrothermal alteration may account for the coupled Os excesses. In some cases, Pt/Re ratios are >600 and characterized by high Pt/Os and sometimes by low Re/Os. *Ravizza et al.* [2001] thus propose that the incorporation of such sediment into the plume source may be a plausible alternative to core-mantle interaction, a suggestion also advocated by *Schersten et al.* [2004]. *Brandon et al.* [2003] test this proposition and find that >30% of the source would have to be composed of a metalliferous sediment component to match the coupled Os excesses in Hawaiian, Siberian, and Gorgonan lavas. This large concentration is, however, incompatible with both the petrology and the Fe/Mn ratios measured in Hawaiian picrites [*Humayun*, 2003; Humayun, unpublished data, 2004]. An additional practical issue is that Mn-rich sediments represent only a small fraction of the surface area of the oceanic crust. Consequently, it is difficult to envision how this compositionally diverse material could form such a large component of the source and also why the resulting Os-Pt-Re isotope systematics in Siberian, Gorgonan, and Hawaiian rocks should be similar.

[65] Crustal recycling has received potential indirect support from a recent study by *Schersten et al.* [2004] of the ^{182}Hf–^{182}W systematics in the same Hawaiian picrites investigated by *Brandon et al.* [2003]. Hafnium 182 decays to ^{182}W with a half-life of only about 9 Myr. As a result, assuming again that the Earth has a chondritic bulk composition, all radiogenic ^{182}W was produced in the first 60 Myr of Earth history. If the core is formed within the first 30 Myr of Earth history [e.g., *Yin et al.*, 2002], *Schersten et al.* [2004] argue that the mantle will be slightly enriched in ^{182}W relative to the core because Hf is concentrated there and would continue to decay, producing ^{182}W for an additional 30 Myr (i.e., $\epsilon W_{\mathrm{mantle}} \approx 0$ and $\epsilon W_{\mathrm{core}} \approx -2$). Thus entrainment of core material into mantle plumes should result in a negative ϵW, whereas $\epsilon W \approx 0$ in Hawaiian picrites. These authors conclude that the absence of such a signature may be evidence for the role of crustal recycling. However, *Hauri* [2004] points out that this interpretation is very sensitive to the age of the Earth's core. In particular, if the core formed earlier, in the first 5 Myr of Earth history, say, then the mantle would be more strongly enriched in ^{182}W (i.e., $\epsilon W_{\mathrm{mantle}} > 30$), and thus an $\epsilon W \approx 0$ is actually consistent with core-mantle mixing. *Halliday* [2004] shows that in addition to being sensitive to the age of the core, $\epsilon W_{\mathrm{core}}$ is influenced strongly by the process of core formation itself. In particular, $\epsilon W_{\mathrm{core}}$ will depend on the extent of Hf-W isotopic disequilibrium because of the mechanics of core formation as well as related variations in Hf-W fractionation between the core and mantle arising from changing redox conditions. Clearly, uncertainties in W behavior and evolution must be resolved before it can be reliably used to test plume models.

[66] In summary, explanation of the Os isotopic systematics and Fe/Mn compositions of lavas from a number of hot spots and flood basalts inferred to overlie patches of ULVZ probably requires outer core fluid to be incorporated into the plume source, consistent with geomagnetic constraints outlined above, although the data do not presently demand this interpretation. However, the diffusion rate of outer core material into solid mantle (as well as the propagation of associated chemical reactions) is too small for any significant transport from the core to the mantle by this mechanism over the age of the Earth. This leaves an intriguing possibility, namely, that because diffusion through liquids is much faster than solids, the presence of partial melt may be required in order to satisfy the geochemical requirement of 1% core material in the plume source as well as the linear correlation between ^{186}Os/^{190}Os and ^{3}He/^{4}He in Hawaiian picrites. An absence of core material in Icelandic lavas correlates with an inferred absence of ULVZ material in the source. If partial melt is required for a significant flux of core material into the lower mantle, this result may indicate an absence of partial melt beneath Iceland.

3.5. An Emerging Picture of D″ in the Source Region for Plumes

[67] With the notable exception of Iceland the foregoing discussion indicates that most hot spots attributed to deep mantle plumes are correlated spatially with buoyant, deep mantle upwellings beneath Africa and the central Pacific that are underlain by patches of ULVZ material. ULVZ material is compositionally different from ambient lower

mantle, and thus mantle convection driven by core cooling involves superposed thermal and compositional boundary layers. Moreover, the combination of seismological, geodynamic, geomagnetic, and geochemical constraints outlined above probably requires that ULVZ material be composed of solid or partially molten silicate lower mantle, as well as material from the outer core. Whether the compositionally distinct component is partial melt, metals, or a mixture of both, such a layer is likely to be denser and significantly less viscous than overlying mantle. A new question thus arises: Does dynamic coupling between convection driven by core cooling and a dense, low-viscosity chemical boundary layer govern the long-term stability of mantle plumes and hot spots?

4. DYNAMICS OF A DENSE, LOW-VISCOSITY CHEMICAL BOUNDARY LAYER AND THE LONGEVITY OF MANTLE PLUMES

[68] In addition to pushing low-viscosity compositionally dense material (referred to as "dense layer" hereinafter) and buoyant thermal boundary layer fluid into piles, consistent with the view developed in section 3, large-scale mantle stirring is expected to confine rising mantle plumes to upwelling regions beneath Africa and the central Pacific [e.g., *Zhong et al.*, 2000; *Tan et al.*, 2002; *Schubert et al.*, 2004; *Jellinek et al.*, 2003; *Gonnermann et al.*, 2004]. Consequently, mantle motions due to subduction govern both the location of convective instabilities and the geometry and distribution of the thermal buoyancy flux from the core-mantle boundary [*Gonnermann et al.*, 2004]. However, as alluded to at the start of section 3, such a control on the location of sources for mantle plumes does not guarantee the longevity of individual hot spots and mantle plumes. In this section we address whether temporal stability is the result of interaction between the dense layer and ascending mantle plumes. We present new and published experimental results that are understood, in turn, with new theoretical scaling analyses. In particular, our scaling theory has the following aims: (1) to identify a general dynamical criterion for the long-term spatial stability of mantle plumes; (2) to constrain the height of topography on dense ULVZ material resulting from flow into mantle plumes (an analysis of particular interest to seismologists in search of evidence for mantle plumes because this topography may be more easily imaged than narrow plume conduits); (3) to quantify entrainment from the dense layer such that the bulk and trace element composition of hot spot lavas may be understood in terms of the dynamics governing plume formation; and (4) to determine whether the spacing of mantle plumes at the CMB can be explained in a straightforward way. Constraints on the spacing of plumes combined with underlying topography on a dense layer can be applied to guide seismological investigations of the structure of the plume source and existence of deep mantle plumes.

[69] It is instructive to discuss why laboratory experiments are used to study thermochemical convection given the significant advances in both computational speed and algorithm development that have occurred over the past decade. Convective motions driven by core cooling have a structure that is three-dimensional and time-dependent. Consequently, the dynamics of the interaction between this flow and an underlying dense layer are complex. Because of the computational challenge of resolving small (kilometer) length scales while tracking continuous viscosity and density interfaces [e.g., *van Keken et al.*, 1997; *Tackley and King*, 2003], numerical simulations for conditions appropriate to mantle convection are typically limited to two dimensions [e.g., *Christensen*, 1984b; *Montague and Kellogg*, 2000; *Farnetani*, 1997; *McNamara and Zhong*, 2004a], though three-dimensional simulations are currently being performed [e.g., *Tackley*, 2002; *Tackley and Xie*, 2002; *McNamara and Zhong*, 2004b]. Consequently, laboratory experiments remain an important tool in the study of thermochemical convection and can lead to new discoveries as well as provide parametric constraints for numerical investigations.

4.1. Dynamic Coupling: Results From Laboratory Experiments

[70] Following *Jellinek and Manga* [2002] (referred to as JM2002 hereinafter) we extend previous laboratory investigations of thermochemical convection [e.g., *Olson and Kincaid*, 1991; *Davaille*, 1999a, 1999b; *Davaille et al.*, 2002; *Gonnermann et al.*, 2002; *Davaille et al.*, 2003; *Wenzel et al.*, 2004] to the situation in which a dense layer is thin and has a low viscosity. In particular, JM2002 investigate the hypothesis that the deformation of an underlying dense layer can stabilize mantle plumes such that they persist for large geological times. Here we investigate this hypothesis more deeply by analyzing the results of JM2002 as well as new and published data in greater detail.

[71] In order to scale tank experiments to understand the influence of a dense layer on convection from the CMB of the Earth it is useful to define several additional dimensionless parameters. The ratio of the initial height of the dense layer to the height of the system, $\zeta = 0.03$, is consistent with constraints on the thickness of D$''$ outlined in section 3. The stabilizing buoyancy effect of the dense layer is expressed through the ratio of the intrinsic compositional density difference to the destabilizing thermal density difference in the overlying thermal boundary layer

$$B = \Delta\rho_c/\rho\alpha\Delta T_\ell. \tag{10}$$

ΔT_ℓ is the temperature difference across the thermal boundary layer, and B in the experiments is in the range 0.7–4.3. The dense layer will be gravitationally stable for B greater than ~0.5. The viscous stresses that govern the mechanical coupling between the dense layer, thermal boundary layer, and interior fluid, respectively, are expressed through two viscosity ratios: the ratio of the viscosity of the dense fluid to the viscosity of the thermal boundary layer,

$$\lambda_d = \mu_d/\mu_h, \tag{11}$$

TABLE 1. Experimental Results[a]

Experiment	Form	BC	Ra	B	λ_d	λ_h	h/δ	Tendril Thickness l/δ	One-Half Spacing $L/2H$
1	steady	FS	6.8×10^4	0.73 ± 0.07	0.00023	4.8	1.1 ± 0.2	-	0.63
2	steady	FS	7.1×10^4	0.71 ± 0.07	0.00026	7.9	1.2 ± 0.2	-	0.62
3	steady	FS	3.4×10^5	4.1 ± 0.4	0.0058	7.0	0.64 ± 0.32	-	0.47
4	steady	FS	1.3×10^6	1.9 ± 0.4	0.0074	5.1	1.2 ± 0.4	0.044 ± 0.013	0.22
5	steady	FS	2.1×10^6	1.8 ± 0.2	0.0058	4.2	0.79 ± 0.16	-	0.26
6	steady	FS	2.4×10^6	2.1 ± 0.5	0.014	3.8	1.5 ± 0.2	-	0.22
7	unsteady	FS	4.4×10^6	2.2 ± 0.3	0.022	1.6	0.46	-	-
8	steady	NS	1.8×10^4	4.3 ± 0.4	0.00052	3.2	0.53 ± 0.27	0.026 ± 0.003	0.32
9	steady	NS	1.2×10^5	1.36 ± 0.14	0.00069	5.6	0.94 ± 0.21	-	0.54
10	steady	NS	3.2×10^5	1.30 ± 0.13	0.0014	6.0	1.34 ± 0.27	-	0.39
11	steady	NS	3.6×10^5	1.21 ± 0.12	0.0013	3.7	1.1 ± 0.2	0.045 ± 0.015	0.32
12	unsteady	NS	1.6×10^6	3.0 ± 0.6	0.34	3.1	1.2	-	-
13	unsteady	NS	1.9×10^6	2.9 ± 0.4	0.34	3.0	1.2	-	-
14	unsteady	NS	2.4×10^6	1.5 ± 0.2	0.0063	1.9	0.20	-	-
15	steady	NS	3.6×10^7	1.88 ± 0.19	0.0090	2.7	1.1 ± 0.2	0.12 ± 0.04	0.26

[a]BC, boundary condition; FS, free slip; and NS, no slip.

and the ratio of viscosity of the cold interior fluid to the viscosity of the thermal boundary layer,

$$\lambda = \mu_c/\mu_h. \tag{12}$$

Here μ is viscosity and the subscripts d, h, and c refer to the dense layer, hot thermal boundary layer, and cold interior fluid, respectively.

[72] Experiments with a dense layer are performed by introducing dense fluid into the base of a layer convecting at

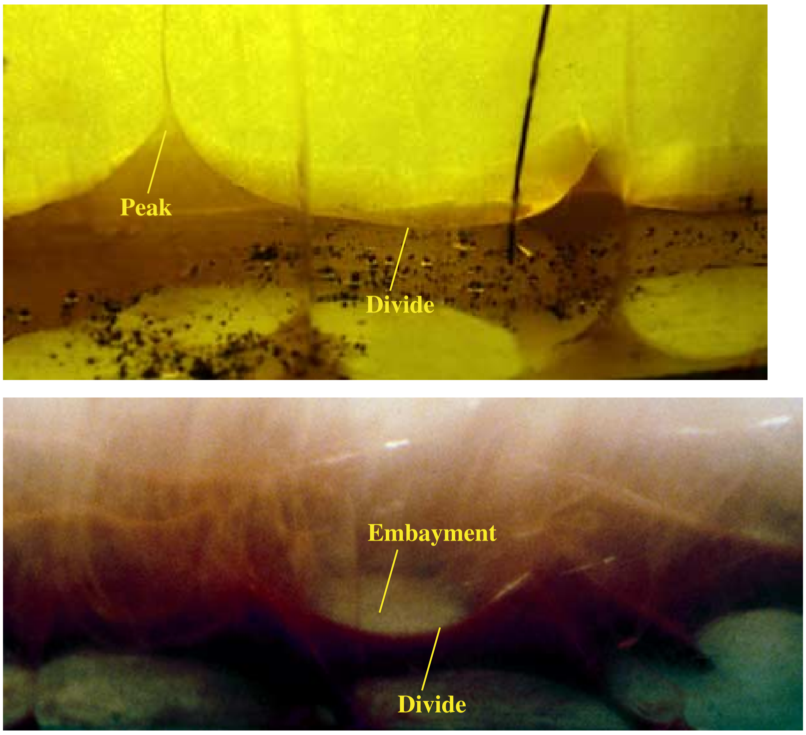

Figure 10. Photographs showing oblique views of the topography formed on a dense low-viscosity layer emplaced at the base of a vigorously convecting layer with (top) free-slip and (bottom) no-slip basal mechanical boundary conditions. In both experiments, entrainment from the dense layer by flow into ascending thermals produces circular embayments, divides, and peaks. Horizontal temperature differences between hot thermal boundary layer fluid and interior fluid drive flow from the tank floor up the sides of embayments to peaks on the divides, where upwellings become approximately fixed. Upwellings persist for the duration of an experiment (hundreds to thousands of plume risetimes) or until the dense layer is sufficiently eroded that the topography becomes small in comparison to the thermal boundary layer thickness. In the top photograph $Ra = 2.1 \times 10^6$, $B = 1.84$, $\lambda_d = 0.02$, and $\lambda = 4.2$. In the bottom photograph $Ra = 3.6 \times 10^7$, $B = 1.88$, $\lambda_d = 0.02$, and $\lambda = 2.7$. The heavy, dark vertical line in the top photograph is a thermocouple.

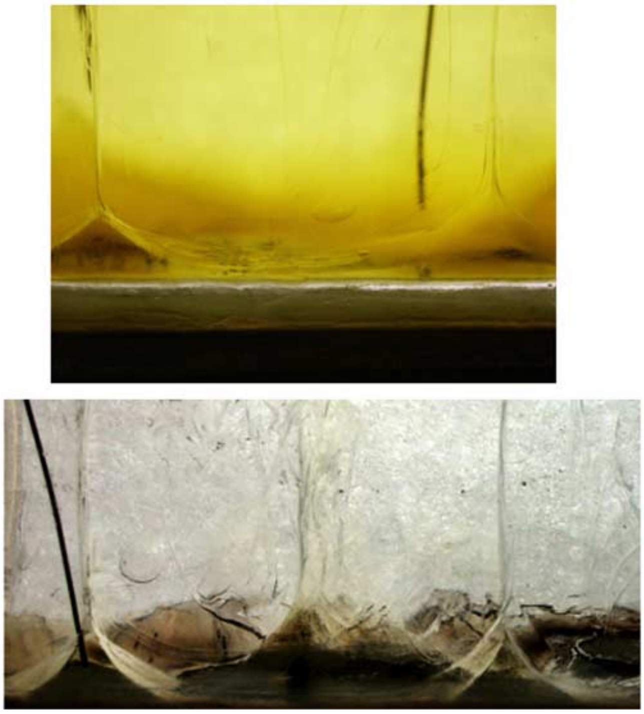

Figure 11. Photographs illustrating persistent, axisymmetric, low-viscosity conduits on top of topographic peaks on the dense layer in experiments with (top) free-slip and (bottom) no-slip basal mechanical boundary conditions. Once formed, conduits govern the flow of buoyant fluid from the hot boundary and persist until the dense layer is eroded such that the height of the topography becomes small in comparison to the thermal boundary layer thickness. The conduits are thus regarded as stable, long-lived structures. The heavy, dark vertical lines in the photographs are thermocouples.

high Ra (see section 2). Quantitative results from both JM2002 and new experiments are given in Table 1 and will be analyzed in detail in section 4.2. Qualitatively, regimes in which long-lived plumes occur are characterized by the following observations:

[73] 1. Flow into rising thermals deforms the dense layer, resulting in topographic features such as circular embayments, sharp "divides," and peaks formed beneath upwelling flows (Figure 10).

[74] 2. Upwellings become situated on topographic peaks on divides, where, once formed, they can remain for hundreds of plume risetimes (Figure 11).

[75] 3. Finite deformation of the dense layer is needed to stabilize plume locations because a flat boundary permits only thermals to form.

[76] 4. Once established, the spacing between the centers of embayments remains approximately constant over the course of a given experiment. This spacing is apparently governed by the wavelength of the first Rayleigh-Taylor instability of the thermal boundary layer (discussed in more detail in section 4.2.3).

[77] 5. Entrainment of dense, low-viscosity material establishes narrow, cylindrical, low-viscosity conduits beneath ascending thermals. Consequently, there is a transition from an unsteady flow composed of intermittent upwelling thermals to a steady flow from the hot boundary layer into axisymmetric plume conduits. We now develop a quantitative understanding of this coupling and its influence on the spatial stability, spacing, and composition of these upwellings.

[78] From these observations, JM2002 conclude that the dynamic coupling between topography and motions driven by lateral temperature variations stabilizes the pattern of flow for large times.

4.2. Theory for Effects of Dynamic Coupling

4.2.1. Dense Layer Topography and Long-Lived Plumes

[79] Figure 11 shows that long-lived plumes are located on top of topographic peaks on the dense layer. In order for a plume conduit to become fixed on top of such a feature it is clear that thermal boundary layer fluid must flow along the interface with the dense layer faster than it can rise vertically into the interior as a new thermal. Said differently, the timescale for thermal boundary layer fluid to flow laterally from the center of an embayment to a peak must be less than the timescale for a new convective instability to grow. The problem is outlined in Figure 12. Lateral flow in the thermal boundary layer is driven by buoyancy forces caused by horizontal temperature variations between the thermal boundary layer fluid and interior fluid. Assuming that the thermal boundary layer is very thin relative to the spacing between adjacent plumes, L, the dominant retarding force is the viscous stress arising from the vertical velocity gradients within the thermal boundary layer.

[80] Following the lubrication theory analysis used to study similar flows [e.g., *Koch and Koch*, 1995], we write

$$u(z) = U + u'(z), \tag{13}$$

where U is the velocity at the boundary between the interior and thermal boundary layer fluid, and $u'(z)$ describes the variations in velocity within the boundary layer. Consequently, the x component of the momentum equation is

$$\partial p/\partial x = \mu\partial^2 u'\partial z^2, \tag{14}$$

where p is dynamic pressure, implying that

$$u' \sim \Delta\rho g h\delta^2/\mu L, \tag{15}$$

where $\partial p/\partial x \approx \Delta\rho gh/L$. Continuity of viscous stresses at the interface between the cold interior fluid and the thermal boundary layer demands that $\mu_c U/L \sim \mu u'/\delta$ and thus that

$$U \sim \Delta\rho g h\delta/\mu_c. \tag{16}$$

The criterion for stable plumes is that the velocity U must be greater than the speed at which a thermal can rise through the mantle, $U_{\mathrm{th}} \sim \Delta\rho g\delta^2/\mu_c$. This condition leads to the requirement that

$$h/\delta > \text{constant}. \tag{17}$$

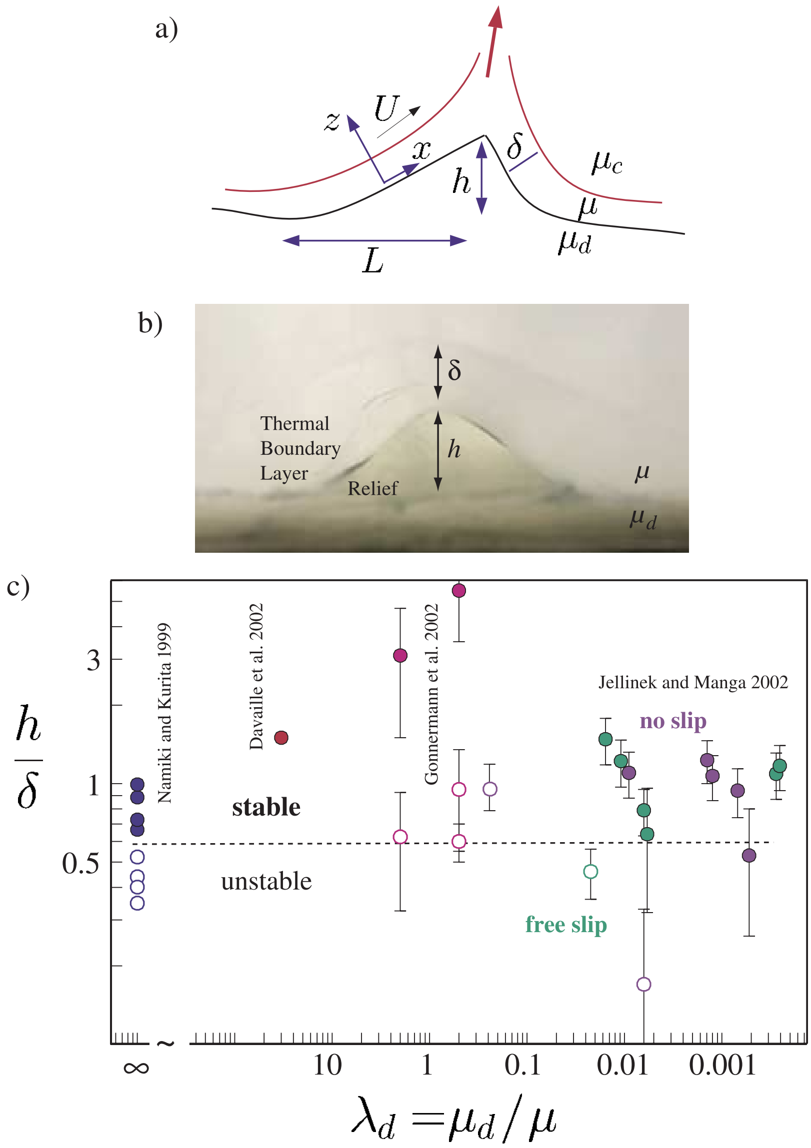

Figure 12. (a) Schematic cross section of the deformed dense layer defining variables and the geometry of the problem addressed in section 4.2.1. (b) Photograph of the dense layer deformed by flow into a nascent plume instability showing the different regions of the flow. (c) Compilation of experimental results identifying regimes in which stable long-lived plumes occur (solid circles) and regimes are dominated by transient plumes or thermals (open circles). Also shown is the theoretical prediction (dashed line) that $h/\delta \sim$ *constant*, where the constant is found to be $\approx$0.6. The experiments shown in purple and green (no-slip and free-slip bottom boundary condition, respectively) are from *Jellinek and Manga* [2002]. Experiments shown in fuschia, red, and blue are from *Gonnermann et al.* [2002], *Davaille et al.* [2002], and *Namiki and Kurita* [1999], respectively. All experiments, except those shown with green circles, have a no-slip bottom boundary condition.

[81] Figure 12c augments results reported by JM2002 with new experiments and data from *Namiki and Kurita* [1999] and *Davaille et al.* [2002] and identifies conditions leading to long-term plume stability. JM2002 define a dashed contour in their Figure 3 separating "fixed plumes" from "no fixed plumes," suggesting a strong dependence on the viscosity of the dense layer. A fixed plume in JM2002 is equivalent to a long-lived stable plume in this study. Improved topographic measurements from the experimental data of JM2002, as well as new data, show that the regime boundary drawn arbitrarily in JM2002 is not correct and that plume stability is, in fact, relatively insensitive to the viscosity of the dense layer. In addition, these experimental results indicate that despite the simplicity of our analysis, equation (17) captures the essential physics governing plume stability. From the experimental results and analysis we thus conclude that the major criterion for stable long-lived plumes is that the minimum height of topography on the dense layer be comparable to about one half the thickness of the thermal boundary layer.

4.2.2. Height of Topography

[82] Knowing the height of the topography on the dense layer is critical for determining the stability of

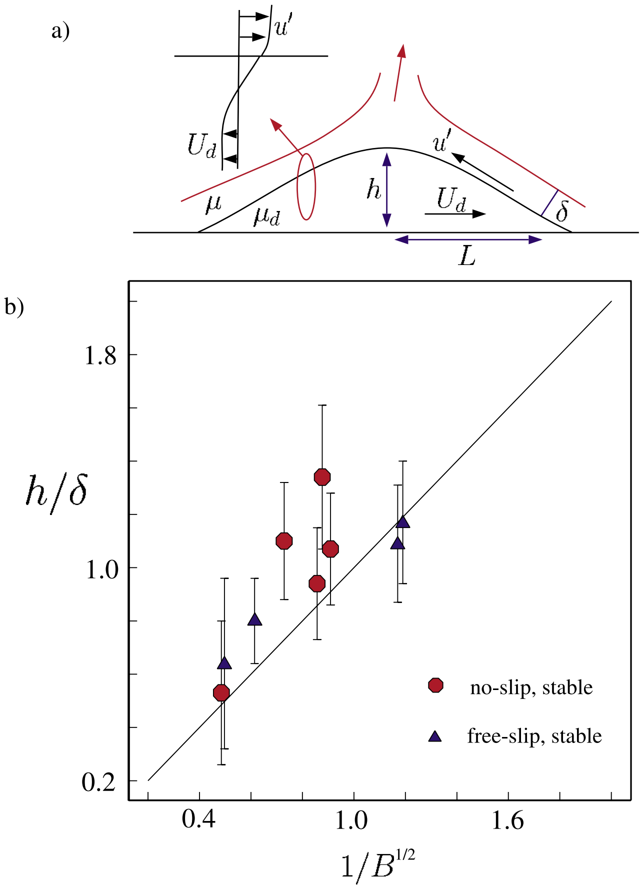

Figure 13. (a) Schematic cross section of the deformed dense layer defining variables and the geometry of the problem addressed in section 4.2.2. In order for topography to be stable $U_d \sim u'$. (b) Relationship between measured topography, normalized by the thermal boundary thickness, and $B^{1/2}$. The solid line shows that the data are consistent with the theoretical prediction that $h/\delta \propto B^{1/2}$. The large error bars reflect variability in h within each experiment as well as intrinsic difficulties with obtaining measurements of absolute topography.

plumes. The topography on the dense layer beneath long-lived upwellings is supported by flow into plumes and declines in amplitude with progressive erosion of the layer over the course of an experiment. In view of the large number of seismological investigations of D″ topography a scale constraining the absolute height of such features is also useful.

[83] One dynamical requirement for stable topography is that the lateral flow of boundary layer fluid must be balanced by the opposing flow of dense layer material (Figure 13). This condition implies that $U_d \sim u'$, where $U_d \sim \Delta\rho_c g h \delta^2 / L\mu$ and thus that

$$h/\delta \sim (\Delta\rho/\Delta\rho_c)^{1/2} \sim (1/B)^{1/2}. \quad (18)$$

[84] Absolute topographic heights are difficult to obtain in laboratory experiments and are spatially variable, and thus uncertainties can be large. Figure 13b shows that available measurements of topography for free-slip and no-slip bottom boundary conditions are consistent with the scaling in equation (18).

4.2.3. Plume Spacing at the Hot Boundary

[85] JM2002 hypothesize that the spacing of persistent low-viscosity upwellings is governed by topography formed as a result of flow due to the first Rayleigh-Taylor instability of thermal boundary layer fluid following the introduction of the dense material to an experiment. For a critically unstable thermal boundary layer of thickness $\sim 10HRa^{-1/3}$ embedded between an underlying low-viscosity dense layer and overlying more viscous fluid, linear stability theory [e.g., *Lister and Kerr*, 1989] predicts the most unstable wavelength to be

$$L = C(\lambda/Ra)^{1/3}, \quad (19)$$

where the scaling factor $C = C(B, \lambda, \lambda_d)$. Figure 14 shows that measured spacings are consistent with the theoretical scaling $L \propto (\lambda/Ra)^{1/3}$. Because the lateral spacing between plumes can now be written in terms of externally controlled parameters, the stability of plumes as well as the topography on the dense layer can be expressed in terms of externally controlled and known parameters. In addition, substituting

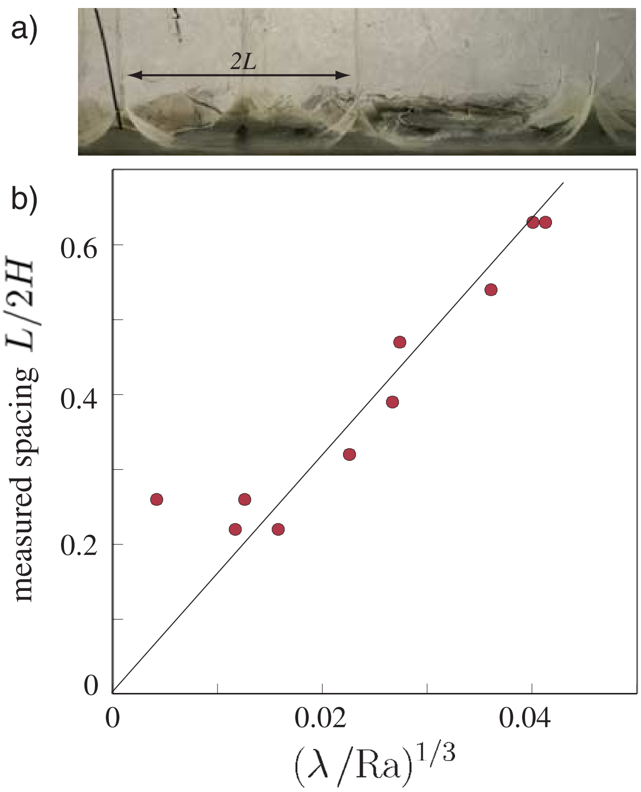

Figure 14. (a) Photograph showing the spacing between stable upwellings. (b) Relationship between plume spacing, ($L/2$), normalized by the layer depth H, and $(\lambda/Ra)^{1/3}$. The data are from bottom-heated experiments and are consistent with predictions from the linear stability analysis for a gravitationally unstable layer in which $L/H \propto (\lambda/Ra)^{1/3}$. See section 4.2.3 for discussion.

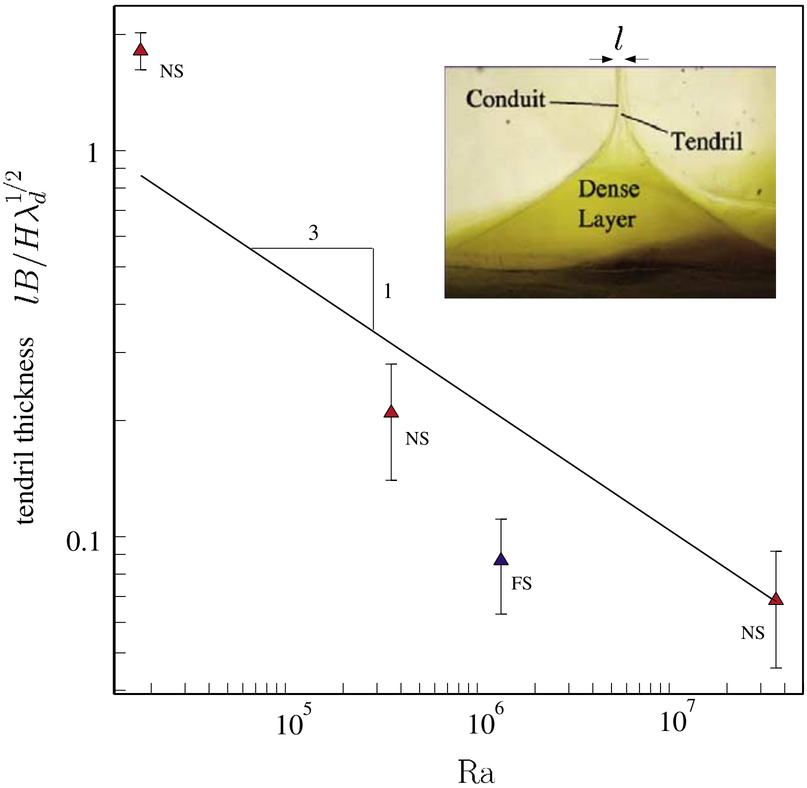

Figure 15. Relationship between tendril thickness l and Ra. The number of experiments with measurements is limited by the small size of the entrained tendrils (which requires both good clarity in the fluid and high resolution in our digital images for measurement). Nevertheless, the limited data are modestly consistent with equation (22), which predicts that $l\ B/H\lambda_d^{1/2} \propto Ra^{1/3}$.

L for H in equation (5) and applying this result to equations (1)–(4) leads to self-consistent scales for the maximum height to which a vertical conduit may extend in the mantle, the conduit diameter as a function of height, the temperature anomaly driving flow up a plume conduit, and the average thermal boundary layer thickness between adjacent plumes.

4.2.4. Entrainment of Dense Material

[86] Boundary layer fluid is coupled viscously to the underlying dense layer. The flow of buoyant fluid into established conduits thus produces velocity gradients within the dense layer that, in turn, result in the entrainment or "dragging" of tendrils of dense material into rising plumes (Figure 15). At the base of the conduit the steady state thickness of an entrained tendril depends on the vertical extent of velocity gradients within the dense material, arising from viscous stresses produced by lateral flow in the thermal boundary layer, compared with the stabilizing buoyancy stresses. Balancing viscous and buoyancy stresses the momentum equation becomes

$$\partial p/\partial z = \mu_d \partial^2 u_d/\partial z^2, \tag{20}$$

where continuity of viscous stresses requires $\Delta\rho_c g \sim \mu_d U/\ell^2$, which leads to a scale for the tendril thickness

$$\ell \sim (\mu_d U/g\Delta\rho_c)^{1/2} \sim \delta/\left(B\lambda_d^{1/2}\right). \tag{21}$$

Equation (21) is similar in form to that derived by *Sleep* [1988]. It differs, however, from the theoretical models of *Davaille* [1999a, 1999b] and *Jellinek and Manga* [2002]. It also differs from the isoviscous numerical results of *Zhong and Hager* [2003].

[87] Recalling that at high Ra, $\delta \sim HRa^{-1/3}$, equation (21) can be rewritten as

$$\ell \sim H\lambda_d^{1/2}/\left(Ra^{1/3}B\right). \tag{22}$$

Accurate measurements of tendril thickness are inherently difficult to obtain because of the small length scales involved. Nevertheless, Figure 15 shows that equation (22) is not inconsistent with the data for the small number of experiments in which we could obtain measurements.

4.3. Comments on Some Assumptions and Limitations

[88] In developing the foregoing theory a number of simplifying assumptions are made that require discussion. First, because we assume λ_d to be very small, the viscosity ratios λ_d and λ do not enter the scaling analysis, but they will affect u' and U_{th} by factors of up to 2 (e.g., Hadamard-Rybczynski effects). Consequently, the "constant" in equation (17) is expected to be constant to within a factor of about 4 over the full range of λ_d and λ. In particular, increased drag due to a higher-viscosity

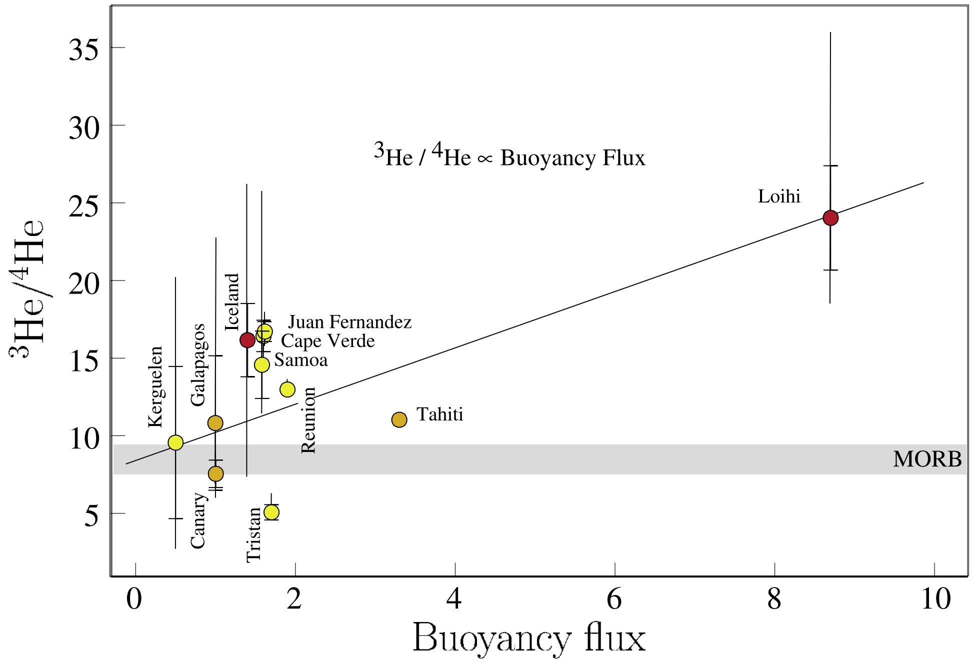

Figure 16. Plot showing average ^{3}He/^{4}He values obtained from ocean island basalt samples as a function of plume buoyancy flux [cf. *Sleep*, 1990] Q for hot spots associated with deep mantle plumes. The red circles indicate well-constrained estimates for the buoyancy flux. Orange and yellow circles indicate buoyancy fluxes that are moderately and poorly constrained, respectively. Variation in the data is compatible with the theoretical prediction that ^{3}He/^{4}He $\propto Q$, and thus the geochemistry of these lavas may be understood in terms of processes governing the formation of mantle plumes. Data are from the Petrological Database of the Ocean Floor, Lamont Doherty Earth Observatory, Columbia University (http://petdb.ldeo.columbia.edu/petdb/), the Geochemistry of Rocks of the Oceans and Continents database, Max-Planck-Institut für Chemie (http://georoc.mpch-mainz.gwdg.de/georoc/), and *Farley and Neroda* [1998].

dense layer will reduce lateral velocities within the thermal boundary layer, and slightly higher topography will be required to stabilize plumes. A second assumption is that to first order, convection within the dense layer itself [e.g., *Namiki*, 2003] is dynamically unimportant to the mechanics governing topography on and entrainment from the dense layer. As noted by JM2002, convection does occur within the dense layer in the experiments reported here and is found to influence heat transfer across the interface between the dense layer and the thermal boundary layer [see also *Namiki and Kurita*, 2003]. The reasonable agreement between the data presented here and our theory, however, lends support to our simple model. Clearly, additional studies of the importance of convection within the lower layer are warranted in future investigations. Last, we ignore the influence of large-scale mantle flow on the dynamics of the dense layer, an effect not considered in our experiments. Relative to the mantle, the outer core is inviscid and presents an approximately stress-free or free-slip mechanical boundary condition. Consequently, in addition to causing dense material and thermal boundary layer fluid to pile up beneath upwellings (see section 3.4), we expect patches of dense material to drift according to the lower mantle flow (see section 1) [see also *Davaille et al.*, 2002]. The additional influence of large-scale mantle stirring on the spacing of upwellings and the size and shape of topography formed on ULVZ is unknown.

5. APPLICATIONS TO LONG-LIVED MANTLE PLUMES AND THE GEOCHEMISTRY OF HOT SPOTS

[89] If long-lived hot spots are connected to plumes ascending from the base of the Earth's mantle, then the results of geochemical studies of erupted lavas provide insight into the CMB region. If robust, such a link to volcanism is particularly powerful because geodynamic, seismological, geomagnetic, mineral physics, and geochemical observations and models of hot spots and mantle plumes can be related directly to the composition, structure, and dynamics of D″.

[90] With constraints on Ra, B, λ, and λ_d, and consideration of the limitations indicated in section 4.3, our experimental results and scaling analyses can be applied to understand the longevity of mantle plumes, the seismologically observed height of topography of structures in the lowermost mantle, and the composition of ocean island basalts in a self-consistent way. We take Ra for the component of mantle convection driven by core cooling to be in the range 10^6–10^8. Geodynamic models (see section 3.4)

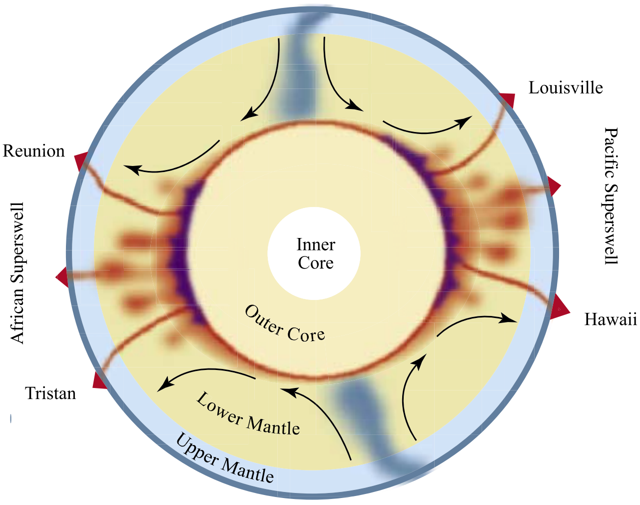

Figure 17. A cartoon modified from *Gonnermann et al.* [2004] showing our proposed interaction between plate tectonics, core cooling, and D″. That such an interaction may be required for long-lived mantle plumes and hot spots to occur suggests that these features are unusual and probably unique to our planet. Reprinted with permission from Elsevier.

show that in order to ensure the longevity of dense low-viscosity material within D″, while still allowing for entrainment by mantle flow, B is plausibly in the range 1–2, where 2 is extreme. In addition, we take $\lambda = 10^2$ (see section 2) and assume $\lambda_d \ll 1$. Applying these constraints to equations (17) and (18), we find that $h/\delta > 0.7$ and is larger than the critical value of about 0.5 identified in Figure 12. Thus mantle plumes in the Earth are in a regime in which longevity and spatial stability are expected. Taking $h \sim 0.7\ HRa^{-1/3}$, this result implies that topography on the dense layer due to flow into mantle plumes is of the order of 40–200 km high. This is comparable to 5–100 km topography inferred to occur on ULVZ patches.

[91] Our analysis shows that the thickness of entrained tendrils of dense material depends on the upwelling velocity within a plume conduit. Because this velocity is proportional to plume buoyancy flux, $Q \sim \rho\alpha\Delta TV\delta_w^2$, where V is velocity, an implication of our results is that the radius of entrained tendrils of dense material within the source region for ocean island basalts will vary, depending on the strength of underlying mantle plumes [cf. *Davies*, 1988; *Sleep*, 1990]. From equation (21) we then expect that $\ell \propto Q^{1/2}$ for $\ell \ll \delta_w$. If the radial extent of the region from where melt is extracted is approximately constant, then the increase in the concentration of any chemical component that is diagnostic of the dense layer in the plume source at the base of the mantle will be proportional to ℓ^2 and hence Q.

[92] Following the discussions in sections 2 and 3, we choose $^3He/^4He$ as an appropriate tracer for the silicate component of the dense layer. Figure 16 shows the variation of $^3He/^4He$ with buoyancy flux as determined by *Sleep* [1990]. Following *Courtillot et al.* [2003], data are taken only from hot spot volcanoes likely related to deep mantle plumes. Data points are the average of the full data set obtained from each location, which assumes that sample collection and analysis are spatially random. Also included are qualitative estimates of the reliability of calculated buoyancy fluxes [cf. *Sleep*, 1990] and the standard deviation from the means and maximum and minimum $^3He/^4He$ ratios in each data set. Despite significant uncertainties in buoyancy fluxes, whose estimates can, in principle, be improved [*Zhong and Watts*, 2002], as well as likely inhomogeneous sampling of ocean island lavas, the data are consistent with the theoretical prediction that the increase in $^3He/^4He$ is $\propto Q$.

6. SUMMARY AND DIRECTIONS FOR FUTURE STUDY

[93] Seismological, geochemical, geomagnetic, and geodynamical investigations conducted over the last few decades constrain the composition, structure, and dynamics of mantle plumes and the D″ region and hence the origin of hot spots. We have attempted to integrate results from these diverse studies in order to provide a self-consistent explanation for the structure and longevity of hot spots and mantle plumes on Earth. Figure 17 is a cartoon based on constraints developed in sections 3 and 4 that summarizes our proposed interplay between plate tectonics, convection driven by core cooling, and D″ that has given rise to conditions in which Earth-like mantle plumes may occur. Subduction and mantle stirring driven by plate tectonics leads to strong cooling, to large viscosity variations in the hot thermal boundary layer, and to the piling up of thermal boundary layer fluid (red) and dense layer (blue) at upwelling return flows beneath Africa and the central Pacific. Upwellings due to large-scale mantle flow draw in plumes, causing them to cluster within these regions [*Zhong et al.*, 2000; *Jellinek et al.*, 2003], resulting in the current distribution of hot spots [*Courtillot et al.*, 2003] and possibly the African and Pacific superswells [*McNutt*, 1998; *Schubert et al.*, 2004]. Large viscosity variations, which are enhanced by the entrainment of low-viscosity material, cause plumes ascending from the base of the mantle to have a head-tail structure. The interaction between flow into such plumes and underlying dense layer produces of the order of 10–10^2 km high topography on the dense layer, which, in turn, stabilizes the location of these upwellings for large geological times.

[94] A general conclusion is that both subduction and a dense chemical boundary layer in the plume source are required in order for long-lived, low-viscosity plumes, with large heads and narrow trailing conduits, to occur. Earth-like mantle plumes are thus the product of highly specific physical conditions that may be unique to our planet. Our review supports several additional specific conclusions. First, the model for plume dynamics and entrainment rate allows us to make two quantitative and ultimately testable predictions: There is a relationship

between buoyancy flux and plume geochemistry and a relationship between structure at the base of the mantle and the location of plumes. Second, with the exception of Iceland, most hot spots related to deep mantle plumes are spatially correlated with inferred patches of dense layer (i.e., ULVZ material indicated in Figure 8b). Third, geochemical, geomagnetic, seismological, and geodynamic studies are consistent with the dense layer being composed of solid or partially molten lower mantle silicate and outer core material.

[95] Our synthesis and analysis suggest a number of directions for future research. The most obvious target areas are related to establishing further quantitative constraints on the geometry, structure, composition, physical properties, spatial distribution, origin, and evolution of the dense layer. There are a number of outstanding issues critical to testing our proposed picture:

[96] 1. Is there a direct relationship between patches of dense layer and the temporal and spatial structure of the geomagnetic field observed in the central Pacific and possibly Africa? In particular, can the structure and secular variation of the time-averaged field constrain the geometry and physical properties of such patches as well as their influence on core cooling and the geodynamo?

[97] 2. Can the height, shape, and possibly three-dimensional seismic anisotropy potentially characteristic of topography on ULVZ due to flow into plumes must be resolved? Along with locating plume conduits our analysis suggests that careful resolution of these features could be an important additional test of the mantle plume hypothesis.

[98] 3. What are the density, physical properties, and constitution of a partially molten layer in the plume source? In particular, how much melt is expected to be generated within the thermal boundary layer? How will this melt be distributed across the implied temperature gradient? How will the geometric distribution of this melt be influenced by mantle flow into rising plumes?

[99] 4. What are the physical state and transport properties of plausible mixtures of solid or partially molten lower mantle silicate with outer core material? Is the presence of a melt phase required in order for core material to penetrate into the lower mantle over kilometer-length scales on plate tectonic timescales? How might such a melt–core fluid mixture be interconnected? Is the resulting average electrical conductivity consistent with geomagnetic and geodynamic constraints on core-mantle coupling? What siderophile element tracer(s) is(are) the most diagnostic of outer core infiltration into the lower mantle? What are appropriate chemical diffusivities for these elements in mantle melts at CMB pressures?

[100] 5. What is the quantitative influence of large-scale mantle flow on the positions of patches of dense layer and the resulting implications for plume stability? How is plume stability influenced by large changes in the geometry of mantle flow resulting from changing plate configurations (i.e., Wilson cycles)?

[101] 6. Can geochemical and geodynamic studies be integrated to infer the structure of flow in plume conduits? Integrating geochemical measurements with dynamical models may be particularly useful here.

[102] **ACKNOWLEDGMENTS.** This work and review was supported by NSF, NSERC, and the Canadian Institute for Advanced Research (CIAR). Many people provided reviews, comments, and suggestions, though their views do not necessarily agree with those presented here: B. A. Buffett, A. Lenardic, E. Garnero, C. Johnson, C. Constable, K. Farley, H. M. Gonnermann, M. Panning, M. Feineman, A. Brandon, M. Humayun, and E. Hauri. We thank Catherine Robin and Vid Thayalan from the University of Toronto for performing the experiment reported in Figure 5c. R. Griffiths, A. Lenardic, E. Garnero, D. DePaolo, A. Brandon, and H. Gonnermann provided us with material that was used to construct Figures 2, 5a, 5b, 8a, 9a, and 17, respectively.

[103] Louise Kellogg was the Editor responsible for this paper. She thanks two technical reviewers and one cross-disciplinary reviewer.

REFERENCES

Abelson, M., and A. Agnon (2001), Hotspot activity and plume pulses recorded by geometry of spreading axes, *Earth Planet. Sci. Lett.*, *189*, 31–47.

Akins, J. A., S.-N. Luo, P. D. Asimow, and T. J. Ahrens (2004), Shock-induced melting of $MgSiO_3$ perovskite and implications for melts in the Earth's lowermost mantle, *Geophys. Res. Lett.*, *31*, L14612, doi:10.1029/2004GL020237.

Albarede, F. (1998), Time-dependent models of U-Th-He and K-Ar evolution and the layering of mantle convection, *Chem. Geol.*, *145*, 413–429.

Allegre, C. J., B. Hamelin, and B. Dupre (1984), Statistical-analysis of isotopic-ratios in MORB: The mantle blob cluster model and the convective regime of the mantle, *Earth Planet. Sci. Lett.*, *71*, 71–84.

Allen, R. M., et al. (2002), Imaging the mantle beneath Iceland using integrated seismological techniques, *J. Geophys. Res.*, *107*(B12), 2325, doi:10.1029/2001JB000595.

Anderson, D. L. (1989), *Theory of the Earth*, Blackwell Sci., Malden, Mass.

Anderson, D. L. (1993), Helium-3 from the mantle primordial signal or cosmic space dust?, *Science*, *261*, 170–176.

Anderson, D. L. (1998), The scales of mantle convection, *Tectonophysics*, *284*, 1–17.

Anderson, O. (2003), The three-dimensional phase diagram of iron, in *Earth's Core: Dynamics*, *Structure, Rotation*, *Geodyn. Ser.*, vol. 31, edited by V. Dehant et al., pp. 83–104, AGU, Washington, D. C.

Arndt, N. T., and U. Christensen (1992), The role of lithospheric mantle in continental flood basalt volcanism: Thermal and geochemical constraints, *J. Geophys. Res.*, *97*, 10,967–10,981.

Aurnou, J. M., J. L. Buttles, G. A. Neumann, and P. Olson (1996), Electromagnetic core-mantle coupling and paleomagnetic reversal paths, *Geophys. Res. Lett.*, *23*, 2705–2708.

Bataille, K., and F. Lund (1996), Strong scattering of short-period seismic waves by the core-mantle boundary and the *P*-diffracted wave, *Geophys. Res. Lett.*, *23*, 2413–2416.

Bataille, K., R. S. Wu, and S. M. Flatte (1990), Inhomogeneities near the core-mantle boundary region evidenced from scattered waves: A review, *Pure Appl. Geophys.*, *132*, 151–174.

Birch, F. (1972), Melting relations of iron, and temperatures in Earth's core, *Geophys. J. R. Astron. Soc.*, *29*, 373–387.

Bloxham, J., D. Gubbins, and A. Jackson (1989), Geomagnetic secular variation, *Philos. Trans. R. Soc. London, Ser. A*, *329*, 415–502.

Boehler, R. (1996), Melting of mantle and core materials at very high pressures, *Philos. Trans. R. Soc. London*, *Ser. A*, *354*, 1265–1278.

Boehler, R. (2000), High-pressure experiments and the phase diagram of lower mantle and core materials, *Rev. Geophys.*, *38*, 221–245.

Booker, J. R. (1976), Thermal convection with strongly temperature-dependent viscosity, *J. Fluid Mech.*, *76*, 741–754.

Brandon, A. D. (2002), ^{186}Os-^{187}Os systematics of Gorgona komatiites and Iceland picrites (abstract), *Geochim. Cosmochim. Acta*, *66*, 100.

Brandon, A. D., R. J. Walker, J. W. Morgan, M. D. Norman, and H. M. Prichard (1998), Coupled ^{186}Os and ^{187}Os evidence for core-mantle interaction, *Science*, *280*, 1570–1573.

Brandon, A. D., M. D. Norman, R. J. Walker, and J. W. Morgan (1999), ^{186}Os-^{187}Os systematics of Hawaiian picrites, *Earth Planet. Sci. Lett.*, *174*, 25–42.

Brandon, A. D., R. J. Walker, I. S. Puchtel, H. Becker, M. Humayun, and S. Revillon (2003), ^{186}Os-^{187}Os systematics of Gorgona Island komatiites: Implications for early growth of the inner core, *Earth Planet. Sci. Lett.*, *206*, 411–426.

Breger, L., and B. Romanowicz (1998), Three-dimensional structure at the base of the mantle beneath the central Pacific, *Science*, *282*, 718–720.

Brenan, J. M., H. F. Shaw, F. J. Ryerson, and D. L. Phinney (1995), Mineral-aqueous fluid partitioning of trace elements at 900°C and 2.0 GPA: Constraints on the trace element chemistry of mantle and deep-crustal fluids, *Geochim. Cosmochim. Acta*, *16*, 3331–3350.

Brito, D., J. Aurnou, and P. Olson (1999), Can heterogeneous core-mantle electromagnetic coupling control geomagnetic reversals?, *Phys. Earth Planet. Inter.*, *112*, 159–170.

Brown, J. M., M. D. Furnish, and R. G. McQueen (1987), Thermodynamics for (Mg, Fe)$_2$SiO$_4$ from the Hugoniot, in *High-Pressure Research in Mineral Physics*, *Geophys. Monogr. Ser.*, vol. 39, edited by M. H. Manghnani and Y. Syono, pp. 373–384, AGU, Washington, D. C.

Buffett, B. A. (1992), Constraints on magnetic energy and mantle conductivity from forced nutations of Earth, *J. Geophys. Res.*, *97*, 19,581–19,597.

Buffett, B. A. (1993), Influence of a toroidal magnetic field on the nutations of Earth, *J. Geophys. Res.*, *98*, 2105–2117.

Buffett, B. A. (2002), Estimates of heat flow in the deep mantle based on the power requirements for the geodynamo, *Geophys. Res. Lett.*, *29*(12), 1566, doi:10.1029/2001GL014649.

Buffett, B. A., H. E. Huppert, J. R. Lister, and A. W. Woods (1996), On the thermal evolution of the Earth's core, *J. Geophys. Res.*, *101*, 7989–8006.

Buffett, B. A., E. J. Garnero, and R. Jeanloz (2000), Sediments at the top of Earth's core, *Science*, *290*, 1338–1342.

Buffett, B. A., P. M. Mathews, and T. A. Herring (2002), Modeling of nutation and precession: Effects of electromagnetic coupling, *J. Geophys. Res.*, *107*(B4), 2070, doi:10.1029/2000JB000056.

Bullen, K. E. (1949), Compressibility-pressure hypothesis and the Earth's interior, *Geophys. J. R. Astron. Soc.*, *5*, 355–368.

Bullen, K. E. (1950), An Earth model based on a compressibility-pressure hypothesis Geophys, *J. R. Astron. Soc.*, *6*, 50–59.

Burke, K., W. S. F. Kidd, and J. T. Wilson (1973), Relative and latitudinal motion of Atlantic hotspots, *Nature*, *245*, 133–137.

Campbell, I. H., and R. W. Griffiths (1990), Implications of mantle plume structure for the evolution of flood basalts, *Earth Planet. Sci. Lett.*, *99*, 79–93.

Campbell, I. H., and R. W. Griffiths (1992), The changing nature of mantle hotspots through time: Implications for the chemical evolution of the mantle, *J. Geol.*, *92*, 497–523.

Campbell, I. H., and R. W. Griffiths (1993), Evolution of the mantle's chemical structure, *Lithos*, *30*, 389–399.

Castle, J. C., K. C. Creager, J. P. Winchester, and R. D. van der Hilst (2000), Shear wave speeds at the base of the mantle, *J. Geophys. Res.*, *105*, 21,543–21,557.

Chase, C. G. (1981), Oceanic island Pb: Two-stage histories and mantle evolution, *Earth Planet. Sci. Lett.*, *52*, 277–284.

Christensen, U. R. (1984a), Heat transport by variable viscosity convection, *Phys. Earth Planet. Inter.*, *35*, 264–282.

Christensen, U. R. (1984b), Instability in a hot boundary layer and initiation of thermo-chemical plumes, *Ann. Geophys.*, *2*, 311–320.

Christensen, U. R., and A. W. Hofmann (1994), Segregation of subducted oceanic crust in the convecting mantle, *J. Geophys. Res.*, *99*, 19,867–19,884.

Clement, B. M. (1991), Distribution of transitional VGPs—Evidence for non-zonal equatorial symmetry during the Matuyama-Brunhes geomagnetic reversal, *Earth Planet. Sci. Lett.*, *104*, 48–58.

Clouard, V., and A. Bonneville (2001), How many Pacific hotspots are fed by deep-mantle plumes?, *Geology*, *29*, 695–698.

Collerson, K. D., R. Schroenberg, and B. S. I. Kamber (2002), Unradiogenic W in kimberlites: Direct evidence for core-mantle interaction (abstract), *Geochim. Cosmochim. Acta*, *66*, 148.

Coltice, N., and Y. Ricard (1998), Geochemical observations and one layer mantle convection, *Earth Planet. Sci. Lett.*, *174*, 125–137.

Coltice, N., and Y. Ricard (2002), On the origin of noble gases in mantle plumes, *Philos. Trans. R. Soc. London, Ser. A*, *360*, 2633–2648.

Coltice, N., S. Ferrachat, and Y. Ricard (2000), Box modeling the chemical evolution of geophysical systems: Case study of the Earth's mantle, *Geophys. Res. Lett.*, *27*, 1579–1582.

Constable, C. (1992), Link between geomagnetic reversal paths and secular variation of the field over the last 4 Myr, *Nature*, *358*, 230–233.

Constable, C. G. (2003), Geomagnetic reversals: Rates, timescales, preferred paths, statistical models, and simulations, in *Earth's Core and Lower Mantle*, edited by C. A. Jones, A. M. Soward, and K. Zhang, pp. 77–99, Taylor and Francis, Philadelphia, Pa.

Cordery, M. J., G. F. Davies, and I. H. Campbell (1997), Genesis of flood basalts from eclogite-bearing mantle plumes, *J. Geophys. Res.*, *102*, 20,179–20,197.

Costin, S. O., and B. A. Buffett (2004), Preferred reversal paths caused by a heterogeneous conducting layer at the base of the mantle, *J. Geophys.*, *109*, B06101, doi:10.1029/2003JB002853.

Courtillot, V., C. Jaupart, I. Manighetti, P. Tapponnier, and J. Besse (1999), On causal links between flood basalts and continental breakup, *Earth Planet. Sci. Lett.*, *166*, 177–195.

Courtillot, V., A. Davaille, J. Besse, and J. Stock (2003), Three distinct types of hotspots in the Earth's mantle, *Earth Planet. Sci. Lett.*, *205*, 295–308.

Craig, H. (1990), Helium isotope distribution in mantle hot spots (abstract), *Eos Trans. AGU*, *71*(43), 1669.

Davaille, A. (1999a), Simultaneous generation of hot spots and superswells by convection in a heterogeneous planetary mantle, *Nature*, *402*, 756–760.

Davaille, A. (1999b), Two-layer thermal convection in miscible viscous fluids, *J. Fluid Mech.*, *379*, 223–253.

Davaille, A., and C. Jaupart (1993), Transient high Rayleigh number convection with large viscosity variations, *J. Fluid Mech.*, *253*, 141–166.

Davaille, A., F. Girard, and M. Le Bars (2002), How to anchor hot spots in a convecting mantle?, *Earth Planet. Sci. Lett.*, *203*, 621–634.

Davaille, A., M. Le Bars, and C. Carbonne (2003), Thermal convection in a heterogeneous mantle, *C. R. Geosci.*, *335*, 141–156.

Davies, G. F. (1988), Ocean bathymetry and mantle convection: 1. Large-scale flow and hotspots, *J. Geophys. Res.*, *93*, 10,467–10,480.

Davies, G. F. (1990), Mantle plumes, mantle stirring and hotspot chemistry, *Earth Planet. Sci. Lett.*, *99*, 94–109.

Davies, G. F. (1992), Temporal variations of the Hawaiian plume flux, *Earth Planet. Sci. Lett.*, *13*, 277–286.

Davies, G. F. (1993), Cooling of the core and mantle by plume and plate flows, *Geophys. J. Int.*, *115*, 132–146.
Davies, G. F., and M. Gurnis (1986), Interaction of mantle dregs with convection: Lateral heterogeneity at the core-mantle boundary, *Geophys. Res. Lett.*, *13*, 1517–1520.
Davies, G. F., and M. A. Richards (1992), Mantle convection, *J. Geol*, *100*, 151–206.
DePaolo, D. J., and M. Manga (2003), Deep origin of hotspots—The mantle plume model, *Science*, *300*, 920–921.
DePaolo, D. J., J. G. Bryce, A. Dodson, D. Shuster, and B. Kennedy (2001), Isotopic evolution of Mauna Loa and the chemical structure of the Hawaiian plume, *Geochem. Geophys. Geosyst.*, *2*, Paper number 2000GC000139.
Deschamps, F., and C. Sotin (2000), Inversion of two-dimensional numerical convection experiments for a fluid with a strongly temperature-dependent viscosity, *Geophys. J. Int.*, *143*, 204–218.
Dickinson, W. R., and W. C. Luth (1971), A model for the plate tectonic evolution of mantle layers, *Science*, *174*, 400–404.
Doornbos, D. J. (1978), On seismic wave scattering by a rough core-mantle boundary, *Geophys. J. R. Astron. Soc.*, *53*, 643–662.
Doornbos, D. J. (1988), Multiple scattering by topographic relief with application to the core-mantle boundary, *Geophys. J.*, *92*, 465–478.
Dubrovinsky, L., H. Annersten, N. Dubrovinskala, F. Westman, H. Harryson, O. Fabrichnaya, and S. Carlson (2001), Chemical interactions of Fe and Al_2O_3 as a source of heterogeneity at the Earth's core-mantle boundary, *Nature*, *412*, 527–529.
Duncan, R. A., and M. A. Richards (1991), Hotspots, mantle plumes, flood basalts, and true polar wander, *Rev. Geophys.*, *29*, 31–50.
Dziewonski, A. M. (1984), Mapping the lowermost mantle: Determination of lateral heterogeneity in *P* velocity up to degree and order 6, *J. Geophys. Res.*, *89*, 5929–5952.
Dziewonski, A., and J. H. Woodhouse (1987), Global images of Earth's interior, *Science*, *236*, 37–48.
Earle, P. S., and P. M. Schearer (1997), Observations of *PKKP* precursors used to estimate small-scale topography on the core-mantle boundary, *Science*, *277*, 667–670.
Ely, J. C., and C. R. Neal (2003), Using platinum-group elements to investigate the origin of the Ontong Java Plateau, SW Pacific, *Chem. Geol.*, *196*, 235–257.
Farley, K. A., and E. Neroda (1998), Noble gases in the Earth's mantle, *Annu. Rev. Earth Planet. Sci.*, *26*, 189–218.
Farley, K. A., J. H. Natland, and H. Craig (1992), Binary mixing of enriched and undegassed (primitive-questionable) mantle components (He, Sr, Nd, Pb) in Samoan lavas, *Earth Planet. Sci. Lett.*, *111*, 183–199.
Farnetani, C. G. (1997), Excess temperature of mantle plumes: The role of chemical stratification across D″, *Geophys. Res. Lett.*, *24*, 1583–1586.
Farnetani, C., and M. A. Richards (1994), Numerical investigation of the mantle plume initiation model for flood basalt events, *J. Geophys. Res.*, *99*, 13,813–13,883.
Farnetani, C. G., and M. A. Richards (1995), Thermal entrainment and melting in mantle plumes, *Earth Planet. Sci. Lett.*, *136*, 251–267.
Farnetani, C. G., M. A. Richards, and M. S. Ghiorso (1996), Petrological models of magma evolution and deep crustal structure beneath hotspots and flood basalt provinces, *Earth Planet. Sci. Lett.*, *143*, 81–94.
Farnetani, C. G., B. Legras, and P. J. Tackley (2002), Mixing and deformations in mantle plumes, *Earth Planet. Sci. Lett.*, *196*, 1–15.
Ferrachat, S., and Y. Ricard (2001), Mixing properties in the Earth's mantle: Effects of the viscosity stratification and of oceanic crust segregation, *Geochem. Geophys. Geosyst.*, *2*, Paper number 2000GC000092.
Forte, A. M., and J. X. Mitrovica (2001), Deep mantle high viscosity flow and thermochemical structure inferred from seismic and geodynamic data, *Nature*, *410*, 1881–1884.
Forte, A. M., R. L. Woodward, and A. M. Dziewonski (1994), Joint inversions of seismic and geodynamics data for models of three-dimensional mantle heterogeneity, *J. Geophys. Res.*, *99*, 21,857–21,877.
Forte, A. M., J. X. Mitrovica, and A. Espesset (2002), Geodynamic and seismic constraints on the thermochemical structure and dynamics of convection in the deep mantle, *Philos. Trans. R. Soc. London, Ser. A*, *360*, 2521–2543.
Fouch, M. J., K. M. Fisher, and M. E. Wysession (2001), Lowermost mantle anisotropy beneath the Pacific: Imaging the source of the Hawaiian plume, *Earth Planet. Sci. Lett.*, *190*, 167–180.
Foulger, G. R., and J. H. Natland (2003), Is "hotspot" volcanism a consequence of plate tectonics?, *Science*, *300*, 921–922.
Foulger, G. R., and D. G. Pearson (2001), Is Iceland underlain by a plume in the lower mantle? Seismology and helium isotopes, *Geophys. J. Int.*, *145*, F1–F5.
Fukao, Y., S. Widiyantori, and M. Obayashi (2001), Stagnant slabs in the upper and lower mantle transition region, *Rev. Geophys.*, *39*, 291–323.
Garnero, E. J. (2000), Heterogeneity of the lowermost mantle, *Annu. Rev. Earth Planet. Sci.*, *28*, 509–537.
Garnero, E. J., and D. V. Helmberger (1993), Travel times of *S* and *SKS*: Implications for three-dimensional lower mantle structure beneath the central Pacific, *J. Geophys. Res.*, *98*, 8225–8241.
Garnero, E. J., and D. V. Helmberger (1996), Seismic detection of a thin laterally varying boundary layer at the base of the mantle beneath the central Pacific, *Geophys. Res. Lett.*, *23*, 977–980.
Garnero, E. J., and R. Jeanloz (2000), Fuzzy patches on the Earth's core-mantle boundary, *Geophys. Res. Lett.*, *27*, 2777–2780.
Garnero, E., and M. Wysession (2000), What on Earth is D″?, *Eos Trans. AGU*, *81*(44), 501.
Garnero, E. J., J. Revenaugh, Q. Williams, T. Lay, and L. H. Kelloggn (1998), Ultralow velocity zone at the core-mantle boundary, in *The Core-Mantle Boundary Region*, *Geodyn. Ser.*, vol. 28, edited by M. Gurnis et al., pp. 319–334, AGU, Washington, D. C.
Giannandrea, E., and U. Christensen (1993), Variable viscosity convection experiments with a stress-free upper boundary and implications for the heat transport in the Earth's mantle, *Phys. Earth. Planet. Inter.*, *78*, 139–147.
Gibbons, S. J., and D. Gubbins (2000), Convection in the Earth's core driven by lateral variations in the core-mantle boundary heat flux, *Geophys. J. Int.*, *142*, 631–642.
Gill, J. B., and R. W. Williams (1990), Th isotope and U-series studies of subduction-related volcanic rocks, *Geochim. Cosmochim. Acta*, *54*, 1427–1442.
Goarant, F., F. Guyot, J. Peyronneau, and J.-P. Poirer (1992), High-pressure and high-temperature reactions between silicates and liquid iron alloys, in the diamond anvil cell, studied by analytical electron microscopy, *J. Geophys. Res.*, *97*, 4477–4487.
Gonnermann, H. M., M. Manga, and A. M. Jellinek (2002), Dynamics and longevity of an initially stratified mantle, *Geophys. Res. Lett.*, *29*(10), 1399, doi:10.1029/2002GL014851.
Gonnermann, H. M., A. M. Jellinek, M. A. Richards, and M. Manga (2004), Modulation of mantle plumes and heat flow at the core-mantle boundary by plate-scale flow: Results from laboratory experiments, *Earth Planet. Sci. Lett.*, in press.
Gordon, R. G., and C. D. Cape (1981), Cenozoic latitudinal shift of the Hawaiian hotspot and its implications for true polar wander, *Earth Planet. Sci Lett.*, *55*, 37–47.
Gordon, R. G., et al. (2004), Apparent polar wander of the Pacific plate and Pacific hotspots: Implications for true polar wander and hotspot fixity, *Eos Trans. AGU*, *85*(17), Jt. Assem. Suppl. Abstract U52A-04.
Grand, S. P. (1994), Mantle shear structure beneath the Americas and surrounding oceans, *J. Geophys. Res.*, *99*, 11,591–11,622.
Grand, S. P. (2002), Mantle shear-wave tomography and the fate of subducted slabs, *Philos. Trans. R. Soc. London, Ser. A*, *360*, 2475–2491.

Grand, S. P., R. D. van der Hilst, and S. Widiyantoro (1997), Global seismic tomography: A snapshot of convection in the Earth, *GSA Today*, *7*, 1–7.

Griffiths, R. W. (1986), Thermals in extremely viscous fluids, including the effects of temperature-dependent viscosity, *J. Fluid. Mech.*, *166*, 115–138.

Griffiths, R. W., and I. H. Campbell (1990), Stirring and structure in mantle starting plumes, *Earth Planet. Sci. Lett.*, *99*, 66–78.

Griffiths, R. W., and I. H. Campbell (1991), On the dynamics of long-lived plume conduits in the convecting mantle, *Earth Planet. Sci. Lett.*, *103*, 214–227.

Gubbins, D. (1977), Energetics of Earth's core, *J. Geophys.*, *43*, 453–464.

Gubbins, D. (1998), Interpreting the paleomagnetic field, in *The Core-Mantle Boundary Region*, *Geodyn. Ser.*, vol. 28, edited by M. Gurnis et al., pp. 167–183, AGU, Washington, D. C.

Gubbins, D. (2003), Thermal core-mantle interactions, in *Earth's Core: Dynamics*, *Structure, Rotation*, *Geodyn. Ser.*, vol. 31, edited by V. Dehant et al., pp. 163–180, AGU, Washington, D. C.

Gubbins, D., and R. S. Coe (1993), Longitudinally-confined geomagnetic reversal paths from non-dipolar transition fields, *Nature*, *362*, 51–53.

Gubbins, D., and P. Kelly (1993), Persistent patterns in the geomagnetic field over the last 2.5 Myr, *Nature*, *365*, 829–832.

Gurnis, M., M. E. Wysession, E. Knittle, and B. A. Buffett (Eds.) (1998), *The Core-Mantle Region*, *Geodyn. Ser.*, vol. 28, 334 pp., AGU, Washington, D. C.

Gurnis, M., J. X. Mitrovica, J. Ritsema, and H.-J. van Heijst (2000), Constraining mantle density structure using geological evidence of surface uplift rates: The case of the African superplume, *Geochem. Geophys. Geosyst.*, *1*, Paper number 1999GC000035.

Halliday, A. N. (2004), Mixing, volatile loss and compositional change during impact-driven accretion of the Earth, *Nature*, *427*, 505–509.

Hamblin, W. K., and E. H. Christiansen (1998), *Earth's Dynamic Systems*, 8th ed., 740 pp., Prentice-Hall, Old Tappan, N. J.

Hansen, U., and D. A. Yuen (1988), Numerical simulations of thermo-chemical instabilities at the core-mantle boundary, *Nature*, *334*, 237–240.

Hansen, U., and D. A. Yuen (1989), Dynamical influences from thermal-chemical instabilities at the core-mantle boundary, *Geophys. Res. Lett.*, *16*, 629–632.

Hansen, U., and D. A. Yuen (2000), Numerical simulations of thermo-chemical convection with moving heat sources and variable viscosity, *Earth Planet. Sci. Lett.*, *176*, 401–411.

Hart, S. R., E. H. Hauri, L. A. Oschmann, and J. A. Whitehead (1992), Mantle plumes and entrainment—Isotopic evidence, *Science*, *256*, 517–520.

Hauri, E. (2004), Earth science—Keeping score on the core, *Nature*, *427*, 207–208.

Hauri, E. H., and S. R. Hart (1993), Re-Os systematics of EMII and HIMU oceanic island basalts from the south Pacific Ocean, *Earth Planet. Sci. Lett.*, *114*, 353–371.

Hauri, E. H., J. C. Lassiter, and D. J. DePaolo (1996), Osmium isotope systematics of drilled lavas from Mauna Loa, Hawaii, *J. Geophys. Res.*, *101*, 11,793–11,806.

Hirth, G., and D. L. Kohlstedt (1995), Experimental constraints on the dynamics of the partially-molten upper mantle: Deformation in the diffusion creep regime, *J. Geophys. Res.*, *100*, 1981–2001.

Hofmann, A. W. (1997), Mantle chemistry: The message from oceanic volcanism, *Nature*, *385*, 219–229.

Hofmann, A. W., and W. M. White (1982), Mantle plumes from ancient oceanic crust, *Earth Planet. Sci. Lett.*, *57*, 421–436.

Holme, R. (1998), Electromagnetic core coupling II: Probing deep mantle conductance, in *The Core-Mantle Boundary Region*, *Geodyn. Ser.*, vol. 28, edited by M. Gurnis et al., pp. 139–151, AGU, Washington, D. C.

Houard, S., and H.-C. Nataf (1993), Laterally varying reflector at the top of D$''$ beneath northern Siberia, *Geophys. J. Int.*, *115*, 168–182.

Howard, L. N. (1964), Convection at high Rayleigh number, in *Proceedings of the 11th International Congress of Applied Mechanics*, edited by H. Gortler, pp. 1109–1115, Springer-Verlag, New York.

Humayun, M. (2003), Geochemical Constraints on Core-Mantle Interaction from Fe/Mn Ratios, *Eos Trans. AGU*, *84*(46), Fall Meet. Suppl., Abstract U41A-03.

Ihinger, P. D. (1995), Mantle flow beneath the Pacific plate: Evidence from seamount segments in the Hawaiian-Emperor chain, *Am. J. Sci.*, *295*, 1035–1057.

Inoue, H., Y. Fukao, K. Tanabe, and Y. Ogata (1990), Whole mantle *P* wave travel time tomography, *Phys. Earth Planet. Inter.*, *59*, 294–328.

Ishii, M., and J. Tromp (1999), Normal-mode and free-air gravity constraints on lateral variations in velocity and density, *Science*, *285*, 1231–1236.

Ito, G., J. Lin, and D. Graham (2003), Observational and theoretical studies of the dynamics of mantle plume–mid-ocean ridge interaction, *Rev. Geophys.*, *41*(4), 1017, doi:10.1029/2002RG000117.

Jeanloz, R. (1993), Chemical reactions at Earth's core-mantle boundary: Summary of evidence and geomagnetic implications, in *Relating Geophysical Structures and Processes: The Jeffreys Volume*, *Geophys. Monogr. Ser.*, vol. 76, edited by K. Aki and R. Dmowska, pp. 121–127, AGU, Washington, D. C.

Jellinek, A. M., and M. Manga (2002), The influence of a chemical boundary layer on the fixity, spacing and lifetime of mantle plumes, *Nature*, *418*, 760–763.

Jellinek, A. M., R. C. Kerr, and R. W. Griffiths (1999), Mixing and compositional stratification produced by natural convection: 1. The experiments and their application to Earth's core and mantle, *J. Geophys. Res.*, *104*, 7183–7202.

Jellinek, A. M., A. Lenardic, and M. Manga (2002), The influence of interior mantle temperature on the structure of plumes: Heads for Venus, tails for the Earth, *Geophys. Res. Lett.*, *29*(11), 1532, 10.1029/2001GL014624.

Jellinek, A. M., H. M. Gonnermann, and M. A. Richards (2003), Plume capture by divergent plate motions: Implications for the distribution of hotspots, geochemistry of mid-ocean ridge basalts, and estimates of the heat flux at the core-mantle boundary, *Earth Planet. Sci. Lett.*, *205*, 361–378.

Johnson, C. L., and C. G. Constable (1997), The time-averaged geomagnetic field: Global and regional biases for 0–5 Ma, *Geophys. J. Int.*, *131*, 643–666.

Johnson, C. L., and C. G. Constable (1998), Persistently anomalous Pacific geomagnetic fields, *Geophys. Res. Lett.*, *25*, 1011–1014.

Kellogg, L. H. (1997), Growing the Earth's D$''$ layer—Effect of density variations at the core-mantle boundary, *Geophys. Res. Lett.*, *24*, 2749–2752.

Kellogg, L. H., and S. King (1993), Effect of mantle plumes on the growth of D$''$ by reaction between the core and mantle, *Geophys. Res. Lett.*, *20*, 379–382.

Kellogg, L. H., and S. King (1997), The effect of temperature dependent viscosity on the structure of new plumes in the mantle: Results of a finite element model in a spherical, axisymmetric shell, *Earth Planet Sci, Lett.*, *148*, 13–26.

Kellogg, L. H., and G. J. Wasserburg (1990), The role of plumes in mantle helium fluxes, *Geochim. Cosmochim. Acta.*, *99*, 276–289.

Kellogg, L. H., B. H. Hager, and R. van der Hilst (1999), Compositional stratification in the deep mantle, *Science*, *283*, 1881–1884.

Kendall, J. M. (2000), Seismic anisotropy in the boundary layers of the mantle, in *Earth's Deep Interior: Mineral Physics and Tomography From the Atomic to the Global Scale*, *Geophys. Monogr. Ser.*, vol. 117, edited by S. Karato et al., pp. 133–159, AGU, Washington, D. C.

Kendall, J. M., and P. Silver (1998), Investigating causes of D″ anisotropy, in *The Core-Mantle Boundary Region*, *Geodyn. Ser.*, vol. 28, edited by M. Gurnis et al., pp. 97–118, AGU, Washington, D. C.

Kerr, R. A. (2003), Plumes from the core lost and found, *Science*, *299*, 35–36.

Kesson, S. E., J. D. F. Gerald, and J. M. Shelley (1998), Mineralogy and dynamics of a pyrolite lower mantle, *Nature*, *393*, 252–255.

Kincaid, C., D. W. Sparks, and R. Detrick (1996), The relative importance of plate-driven and buoyancy-driven flow at mid-ocean ridges, *J. Geophys. Res.*, *101*, 16,177–16,193.

King, S. D., and D. L. Anderson (1995), An alternative mechanism of flood basalt formation, *Earth Planet Sci. Lett.*, *136*, 269–279.

King, S. D., and J. Ritsema (2000), African hot spot volcanism: Small-scale convection in the upper mantle beneath cratons, *Science*, *290*, 1137–1140.

Knittle, E. (1998), The solid/liquid partitioning of major and radiogenic elements at lower mantle pressures: Implications for the core-mantle boundary region, in *The Core-Mantle Boundary Region*, *Geodyn. Ser.*, vol. 28, edited by M. Gurnis et al., pp. 97–118, AGU, Washington, D. C.

Knittle, E., and R. Jeanloz (1989), Simulating the core-mantle boundary: An experimental study of high-pressure reactions between silicates and liquid iron, *Geophys. Res. Lett.*, *16*, 609–612.

Knittle, E., and R. Jeanloz (1991), The Earth's core-mantle boundary: Results of experiments at high pressures and temperatures, *Science*, *251*, 1438–1453.

Koch, D. M., and D. L. Koch (1995), Numerical and theoretical solution for a drop spreading below a free fluid surface, *J. Fluid Mech.*, *287*, 251–278.

Korenaga, J. (2003), Energetics of mantle convection and the fate of fossil heat, *Geophys. Res. Lett.*, *30*(8), 1437, doi:10.1029/2003GL016982.

Korenaga, J., and T. H. Jordan (2003), Physics of multiscale convection in Earth's mantle: Onset of sublithospheric convection, *J. Geophys. Res.*, *108*(B7), 2333, doi:10.1029/2002JB001760.

Krishnamurti, R. (1970a), On the transition to turbulent convection. part 1. The transition from two- to three-dimensional flow, *J. Fluid Mech.*, *42*, 295–307.

Krishnamurti, R. (1970b), On the transition to turbulent convection. part 2. The transition to time-dependent flow, *J. Fluid Mech.*, *42*, 308–320.

Kuo, C., and B. Romanowicz (2002), On the resolution of density anomalies in the Earth's mantle using spectral fitting of normal-mode data, *Geophys. J. Int.*, *150*, 162–179.

Kuo, B. Y., E. J. Garnero, and T. Lay (2000), Tomographic inversion of *S-SKS* times for shear wave velocity heterogeneity in D″: Degree 12 and hybrid models, *J. Geophys. Res.*, *105*, 28,139–28,157.

Kurz, M. D., W. J. Jenkins, and S. R. Hart (1982), Helium isotope systematics of ocean islands and mantle heterogeneity, *Nature*, *297*, 43–46.

Kurz, M. D., W. J. Jenkins, S. R. Hart, and D. Clague (1983), Helium isotopic variations in volcanic rocks from Loihi seamount and the island of Hawaii, *Earth. Planet. Sci. Lett.*, *66*, 388–399.

Labrosse, S. (2002), Hotspots, mantle plumes and core heat loss, *Earth Planet. Sci. Lett.*, *61*, 1–10.

Labrosse, S., J.-P. Poirier, and J.-L. LeMouel (2001), The age of the inner core, *Earth Planet. Sci. Lett.*, *190*, 111–123.

Laj, C., A. Mazaud, R. Weeks, M. Fuller, and E. Herrero-Bervera (1991), Geomagnetic reversal paths, *Nature*, *351*, 447.

Langel, R. A., and R. H. Estes (1982), Comparison of candidate IGRF models, *J. Geomagn. Geoelectr.*, *34*, 365–381.

Langmuir, C. H., E. M. Klein, and T. Plank (1992), Petrological systematics of mid-ocean ridge basalts: Constraints on melt generation beneath ocean ridges, in *Mantle Flow and Melt Generation at Mid-Ocean Ridges*, *Geophys. Monogr. Ser.*, vol. 71, edited by J. Phipps Morgan, D. K. Blackman, and J. M. Sinton, pp. 183–280, AGU, Washington, D. C.

Lassiter, J. C., and E. H. Hauri (1998), Osmium-isotope variations in Hawaiian lavas: Evidence for recycled oceanic lithosphere in the Hawaiian plume, *Earth Planet. Sci. Lett.*, *164*, 483–496.

Lay, T., E. J. Garnero, C. J. Young, and J. B. Gaherty (1997), Scale lengths of shear velocity heterogeneity at the base of the mantle from *S* wave differential travel times, *J. Geophys. Res.*, *102*, 9887–9909.

Lay, T., Q. Williams, and E. J. Garnero (1998a), The core-mantle boundary layer and deep Earth dynamics, *Nature*, *392*, 461–468.

Lay, T., Q. Williams, E. J. Garnero, L. H. Kellogg, and M. E. Wysession (1998b), Seismic wave anisotropy in the D″region and its implications, in *The Core-Mantle Boundary Region*, *Geodyn. Ser.*, vol. 28, edited by M. Gurnis et al., pp. 299–318, AGU, Washington, D. C.

Lay, T., E. J. Garnero, and Q. Williams (2004), Partial melting in a thermo-chemical boundary layer at the base of the mantle, *Phys. Earth. Planet. Inter*, in press.

Lenardic, A., and W. M. Kaula (1994), Tectonic plates, D″ thermal structure, and the nature of mantle plumes, *J. Geophys. Res.*, *99*, 15,697–15,708.

Lister, J. R., and R. C. Kerr (1989), The effect of geometry on the gravitational instability of a buoyant region of viscous fluid, *J. Fluid Mech.*, *202*, 577–594.

Lithgow-Bertelloni, C., and P. G. Silver (1998), Dynamic topography, plate driving forces and the African superswell, *Nature*, *395*, 269–272.

Lithgow-Bertelloni, C., M. A. Richards, R. W. Griffiths, and C. Conrad (2001), Plume generation in natural thermal convection at high Rayleigh and Prandtl numbers, *J. Fluid Mech.*, *434*, 1–21.

Loper, D. E. (1984), Structure of the core and lower mantle, *Adv. Geophys.*, *26*, 1–34.

Loper, D. E. (1989), Dynamo energetics and the structure of the outer core, *Geophys. Astrophys. Fluid Dyn.*, *49*, 212–219.

Loper, D. E., and T. Lay (1995), The core-mantle boundary region, *J. Geophys. Res.*, *100*, 6397–6420.

Loper, D. E., and F. D. Stacey (1983), The dynamical and thermal structure of deep mantle plumes, *Phys. Earth Planet. Inter.*, *33*, 304–317.

Love, J. J. (1998), Paleomagnetic volcanic data and geometric regularity of reversals and excursions, *J. Geophys. Res.*, *103*, 12,435–12,452.

Love, J. J. (2000), Statistical assessment of preferred transitional VGP longitudes based on palaeomagnetic lava data, *Geophys. J. Int.*, *140*, 211–221.

Manga, M., and R. Jeanloz (1996), Implications of a metal-bearing chemical boundary layer in D″ for mantle dynamics, *Geophys. Res. Lett.*, *23*, 3091–3094.

Manga, M., and D. Weeraratne (1999), Experimental study of non-Boussinesq Rayleigh-Benard convection at high Rayleigh and Prandtl numbers, *Phys. Fluids*, *11*, 2969–2976.

Manga, M., D. Weeraratne, and S. J. S. Morris (2001), Boundary layer thickness and instabilities in Benard convection of a liquid with a temperature-dependent viscosity, *Phys. Fluids*, *13*, 802–805.

Marcantonio, F., A. Zindler, T. Elliott, and H. Staudigel (1995), Os isotope systematics of La Palma, Canary Islands: Evidence for recycled crust in the mantle source of HIMU ocean islands, *Earth Planet. Sci. Lett.*, *133*, 397–410.

Masters, G., G. Laske, H. Bolton, and A. M. Dziewonski (2000), The relative behavior of shear velocity, bulk sound speed, and compressional velocity in the mantle: Implications for chemical and thermal structure, in *Earth's Deep Interior: Mineral Physics and Tomography From the Atomic to the Global Scale*, *Geophys. Monogr. Ser.*, vol. 117, edited by S. Karato et al., pp. 63–87, AGU, Washington, D. C.

Mathews, P. M., and I. I. Shapiro (1992), Nutations of the Earth, *Annu. Rev. Earth Planet. Sci.*, *20*, 469–500.

Mathews, P. M., T. A. Herring, and B. A. Buffett (2002), Modeling of nutation and precession: New nutation series for nonrigid

Earth and insights into the Earth's interior, *J. Geophys. Res.*, *107*(B4), 2068, doi:10.1029/2001JB000390.

McCulloch, M. T., and J. A. Gamble (1991), Geochemical and geodynamical constraints on subduction zone magmatism, *Earth Planet. Sci. Lett.*, *102*, 358–374.

McNamara, A. K., and S. Zhong (2004a), The influence of thermochemical convection on the fixity of mantle plumes, *Earth Planet. Sci. Lett.*, *222*, 485–500.

McNamara, A. K., and S. Zhong (2004b), Thermochemical structures within a spherical mantle: Superplumes or piles?, *J. Geophys. Res.*, *109*, B07402, doi:10.1029/2003JB002847.

McNutt, M. K. (1998), Superswells, *Rev. Geophys*, *36*, 211–244.

Megnin, C., and B. Romanowicz (2000), The three-dimensional shear velocity structure of the mantle from the inversion of body, surface and higher-mode waveforms, *Geophys. J. Int.*, *143*, 709–728.

Menke, W. (1986), Few 2–50 km corrugations on the core-mantle boundary, *Geophys. Res. Lett.*, *13*, 1501–1504.

Molnar, P., and T. Atwater (1973), Relative motion of hotspots in the mantle, *Nature*, *246*, 288–291.

Molnar, P., and J. Stock (1987), Relative motions of hotspots in the Pacific, Atlantic and Indian oceans since late Cretaceous time, *Nature*, *327*, 587–591.

Montague, N. L., and L. H. Kellogg (2000), Numerical models of a dense layer at the base of the mantle and implications for the geodynamics of D″, *J. Geophys. Res.*, *105*, 11,101–11,114.

Montague, N. L., L. H. Kellogg, and M. Manga (1998), High Rayleigh number thermo-chemical models of a dense boundary layer in D″, *Geophys. Res. Lett.*, *25*, 2345–2348.

Montelli, R., G. Nolet, F. A. Dahlen, G. Masters, E. R. Engdahl, and S. Hung (2004), Finite-frequency tomography reveals a variety of plumes in the mantle, *Science*, *303*, 338–343.

Moore, M. M., E. J. Garnero, T. Lay, and Q. Williams (2004), Shear wave splitting and waveform complexity for lowermost mantle structures with low-velocity lamellae and transverse isotropy, *J. Geophys. Res.*, *109*, B02319, doi:10.1029/2003JB002546.

Moresi, L.-N., and V. S. Solomatov (1995), Numerical investigation of 2D convection with extremely large viscosity variations, *Phys. Fluids*, *7*, 2154–2162.

Moresi, L.-N., and V. S. Solomatov (1998), Mantle convection with a brittle lithosphere: Thoughts on the global tectonic style of the Earth and Venus, *Geophys. J.*, *133*, 669–682.

Morgan, W. J. (1971), Convection plumes in the lower mantle, *Nature*, *230*, 42–43.

Morgan, W. J. (1972), Plate motions and deep mantle convection, *Mem. Geol. Soc. Am.*, *132*, 7–22.

Morgan, W. J. (1974), Hotspot tracks and the breakup of Gondwana-Laurasia (abstract), *Eos, Trans. AGU*, *55*(12), 1186.

Morgan, W. J. (1981), Hotspot tracks and the opening of the Atlantic and Indian oceans, in *The Seas*, vol. 7, *The Oceanic Lithosphere*, edited by C. Emiliani, pp. 443–489, John Wiley, Hoboken, N. J.

Morgan, J. P., E. M. Parmentier, and J. Lin (1987), Mechanisms for the origin of mid-ocean ridge axial topography—Implications for the thermal and mechanical structure of accreting plate boundaries, *J. Geophys. Res.*, *92*, 12,823–12,836.

Morgan, J. W., M. F. Horan, R. J. Walker, and J. N. Grossman (1995), Rhenium-osmium concentration and isotope systematics in group IIAB iron meteorites, *Geochim. Cosmochim. Acta*, *59*, 2331–2344.

Mori, J., and D. V. Helmberger (1995), Localized boundary layer below the mid-Pacific velocity anomaly identified from a *PcP* precursor, *J. Geophys. Res.*, *100*, 20,359–20,365.

Morris, S. (1982), The effect of a strongly temperature-dependent viscosity on slow flow past a hot sphere, *J. Fluid Mech.*, *124*, 1–26.

Morris, S., and D. Canright (1984), A boundary-layer analysis of Bernard convection in a fluid of strongly temperature-dependent viscosity, *Phys. Earth. Planet. Inter.*, *36*, 355–373.

Muller, R. D., J.-Y. Royer, and L. A. Lawyer (1993), Revised plate motions relative to the hotspots from combined Atlantic and Indian Ocean hotspot tracks, *Geology*, *16*, 275–278.

Namiki, A. (2003), Can the mantle entrain D″?, *J. Geophys. Res.*, *108*(B10), 2487, doi:10.1029/2002JB002315.

Namiki, A., and K. Kurita (1999), The influence of boundary heterogeneity in experimental models of mantle convection, *Geophys. Res. Lett.*, *26*, 1929–1932.

Namiki, A., and K. Kurita (2003), Heat transfer and interfacial temperature of two-layered convection: Implications for D″-mantle coupling, *Geophys. Res. Lett.*, *30*(1), 1023, doi:10.1029/2002GL015809.

Nataf, H.-C. (1991), Mantle convection, plates, and hotspots, *Tectonophysics*, *187*, 361–377.

Nataf, H.-C., and S. Houard (1993), Seismic discontinuity at the top of D″—A world-wide feature?, *Geophys. Res. Lett.*, *20*, 2371–2374.

Ni, S., and D. Helmberger (2001a), Horizontal transition from fast to slow structures at the core-mantle boundary, South Atlantic, *Earth Planet. Sci. Lett.*, *187*, 301–310.

Ni, S., and D. Helmberger (2001b), Probing an ultra-low velocity zone at the core mantle boundary with *P* and *S* waves, *Geophys. Res. Lett.*, *28*, 2345–2348.

Ni, S., E. Tan, M. Gurnis, and D. Helmberger (2002), Sharp sides to the African superplume, *Science*, *296*, 1850–1852.

Niemela, J. J., L. Skrbek, K. R. Sreenivasan, and R. J. Donnelly (2000), Turbulent convection at very high Rayleigh numbers, *Nature*, *404*, 837–840.

Norman, M. D., and M. O. Garcia (1999), Primitive magmas and source characteristics of the Hawaiian plume petrology and geochemistry of shield picrites, *Earth Planet. Sci. Lett.*, *168*, 27–44.

Norton, I. O. (2000), Global hotspot reference frames and plate motion, in *The History and Dynamics of Global Plate Motions*, *Geophys. Monogr. Ser.*, vol. 121, edited by M. A. Richards, R. G. Gordon, and R. D. van der Hilst, pp. 339–358, AGU, Washington, D. C.

Ogawa, M., G. Schubert, and A. Zebib (1991), Numerical simulation of three-dimensional thermal convection in a fluid with strongly temperature-dependent viscosity, *J. Fluid Mech.*, *233*, 299–328.

Ohtani, E., and M. Maeda (2001), Density of basaltic melt at high pressure and stability of the melt at the base of the lower mantle, *Earth Planet. Sci. Lett.*, *193*, 69–75.

Olson, P., and G. A. Glatzmaier (1996), Magnetoconvection and thermal coupling of the Earth's core and mantle, *Philos. Trans. R. Soc. London, Ser. A*, *354*, 1413–1424.

Olson, P., and C. Kincaid (1991), Experiments on the interaction of thermal convection and compositional layering at the base of the mantle, *J. Geophys. Res.*, *96*, 4347–4354.

Olson, P., and H. Singer (1985), Creeping plumes, *J. Fluid Mech*, *158*, 511–535.

Olson, P., G. Schubert, and C. Anderson (1993), Structure of axisymmetric mantle plumes, *J. Geophys. Res.*, *98*, 6829–6844.

O'Nions, R. K., and L. N. Tolstikhin (1996), Limits on the mass flux between lower and upper mantle and the stability of layering, *Earth Planet. Sci. Lett.*, *139*, 213–222.

Panning, M., and B. Romanowicz (2004), Inferences on flow at the base of Earth's mantle based on seismic anisotropy, *Science*, *303*, 351–353.

Parmentier, E. M., and J. P. Morgan (1990), Spreading rate dependence of 3-dimensional structure in oceanic spreading centers, *Nature*, *348*, 325–328.

Pegram, W. J., and C. J. Allegre (1992), Osmium isotopic compositions from basalts, *Earth Planet. Sci. Lett.*, *111*, 59–68.

Pernicka, E., and J. T. Wasson (1987), Ruthenium, rhenium, osmium, platinum, and gold in iron meteorites, *Geochim. Cosmochim. Acta.*, *51*, 1717–1726.

Plummer, C. C., D. McGeary, and D. H. Carlson (1999), *Physical Geology*, 8th ed., 577 pp., McGraw-Hill, New York.

Poirer, J.-P. (1993), Core-infiltrated mantle and the nature of the D″ layer, *J. Geomagn. Geoelectr.*, *45*, 1221–1227.

Poirer, J.-P., V. Malavergne, and J. L. Le Mouel (1998), Is there a thin electrically conducting layer at the base of the mantle?, in *The Core-Mantle Boundary Region*, *Geodyn. Ser.*, vol. 28, edited by M. Gurnis et al., pp. 131–138, AGU, Washington, D. C.

Porcelli, D., and G. J. Wasserberg (1993), Mass transfer of helium, neon, argon, and xenon through a steady-state upper mantle, *Geochim. Cosmochim. Acta.*, *59*, 4921–4937.

Puchtel, I. S., and M. Humayun (2000), Platinum group elements in Kostomuksha komatiites and basalts: Implications for oceanic crust recycling and core-mantle interactions, *Geochim. Cosmochim. Acta*, *64*, 4227–4242.

Puchtel, I. S., G. E. Brugmann, and A. W. Hofmann (1999), Precise Re-Os mineral isochron and Pb-Nd-Os isotope systematics of a mafic-ultramafic sill in the 2.0 Ga Onega plateau (Baltic Shield), *Earth Planet. Sci. Lett.*, *170*, 447–461.

Raymond, C. A., J. M. Stock, and S. C. Cande (2000), Fast Paleocene motions of the Pacific hotspots from revised global plate circuit constraints, in *The History and Dynamics of Global Plate Motions*, *Geophys. Monogr. Ser.*, vol. 121, edited by M. A. Richards, R. G. Gordon, and R. van der Hilst, pp. 359–375.

Ravizza, G., J. Blusztajn, and H. M. Pritchard (2001), Re-Os systematics of platinum-group element distribution in metalliferous sediments from the Troodos ophiolite, *Earth Planet. Sci. Lett.*, *188*, 369–381.

Revenaugh, J., and R. Meyer (1997), Seismic evidence of partial melt within a possibly ubiquitous low-velocity layer at the base of the mantle, *Science*, *277*, 670–673.

Ribe, N. M., and U. R. Christensen (1999), The dynamical origin of Hawaiian volcanism, *Earth Planet. Sci., Lett.*, *171*, 517–531.

Richards, M. A., and D. C. Engebretsen (1992), Large-scale mantle convection and the history of subduction, *Nature*, *355*, 437–440.

Richards, M. A., and R. W. Griffiths (1988), Deflection of plumes by mantle shear-flow: Experimental results and a simple theory, *Geophys. J. Int.*, *94*, 367–376.

Richards, M. A., B. H. Hager, and N. H. Sleep (1988), Dynamically supported geoid highs over hotspots—Observation and theory, *J. Geophys. Res.*, *93*, 7690–7708.

Richards, M. A., R. A. Duncan, and V. E. Courtillot (1989), Flood basalts and hot-spot tracks: Plume heads and tails, *Science*, *246*, 103–107.

Richards, M. A., R. G. Gordon, and R. van der Hilst (Eds.) (2000), *The History and Dynamics of Global Plate Motions*, *Geophys. Monogr. Ser.*, vol. 121, 398 pp., AGU, Washington, D. C.

Richter, F. M., H. C. Nataf, and S. F. Daly (1983), Heat transfer and horizontally-averaged temperature of convection with large viscosity variations, *J. Fluid Mech.*, *129*, 173–192.

Rigden, S. M., T. J. Ahrens, and E. M. Stolper (1984), Densities of liquid silicates at high pressures, *Science*, *226*, 1071–1074.

Rigden, S. M., T. J. Ahrens, and E. M. Stolper (1989), High-pressure equation of state of molten anorthite and diopside, *J. Geophys. Res.*, *94*, 9508–9522.

Ringwood, A. E. (1975), *Composition and Petrology of the Earth's Mantle*, 618 pp., McGraw-Hill, New York.

Ringwood, A. E. (1982), Phase transformations and differentiation in subducted lithosphere: Implications for mantle dynamics, basalt petrogenesis, and crustal evolution, *J. Geol.*, *90*, 611–643.

Ritsema, J., and R. Allen (2003), The elusive mantle plume, *Earth Planet. Sci. Lett.*, *207*, 1–12.

Ritsema, J., J. J. van Heijst, and J. H. Woodhouse (1999), Complex shear wave velocity structure imaged beneath Africa and Iceland, *Science*, *286*, 125–128.

Romanowicz, B. (2001), Can we resolve 3D density heterogeneity in the lower mantle?, *Geophys. Res. Lett.*, *28*, 1107–1110.

Romanowicz, B., and Y. Gung (2002), Superplumes from the core-mantle boundary to the lithosphere: Implications for heat flux, *Science*, *296*, 513–516.

Rost, S., and J. Revenaugh (2001), Seismic detection of rigid zones at the top of the core, *Science*, *294*, 1911–1914.

Roy-Barman, M., and C. J. Allegre (1995), $^{187}Os/^{186}Os$ in oceanic island basalts: Tracing oceanic crust recycling in the mantle, *Earth Planet. Sci. Lett.*, *129*, 145–161.

Runcorn, S. K. (1992), Polar path in geomagnetic reversals, *Nature*, *356*, 654–656.

Russell, S. A., T. Lay, and E. J. Garnero (1998), Seismic evidence for small-scale dynamics in the lowermost mantle at the root of the Hawaiian hotspot, *Nature*, *369*, 255–257.

Saltzer, R. L., R. D. van der Hilst, and H. Karason (2001), Comparing *P* and *S* wave heterogeneity in the mantle, *Geophys. Res. Lett.*, *28*, 2281–2284.

Samuel, H., and C. G. Farnetani (2003), Thermochemical convection and helium concentrations in mantle plumes, *Earth Planet. Sci. Lett.*, *207*, 39–56.

Schaefer, B. F., S. Turner, I. Parkinson, N. Rogers, and C. Hawkesworth (2002), Evidence of recycled Archean oceanic mantle lithosphere in the Azores plume, *Nature*, *420*, 304–307.

Schaeffer, N., and M. Manga (2001), Interactions between rising and sinking mantle plumes, *Geophys. Res. Lett.*, *28*, 455–458.

Schersten, A., T. Elliott, C. Hawkesworth, and M. Norman (2004), Tungsten isotope evidence that mantle plumes contain no contribution from the Earth's core, *Nature*, *427*, 234–237.

Schilling, J.-G. (1973), Iceland mantle plume geochemical study of the Reykjanes ridge, *Nature*, *242*, 565–571.

Schilling, J.-G. (1986), Geochemical and isotopic variation along the Mid-Atlantic ridge axis from 79°N to 0°N, in *The Geology of North America*, vol. M, *The Western North Atlantic Region*, edited by P. R. Vogt and B. E. Tucholke, pp. 137–156, Geol. Soc. of Am., Boulder, Colo.

Schilling, J.-G. (1991), Fuxes and excess temperatures of mantle plumes inferred from their interaction with migrating midocean ridges, *Nature*, *352*, 397–403.

Schilling, J.-G., M. Zajac, R. Evans, T. Johnston, W. White, J. D. Devine, and R. Kingsley (1983), Petrologic and geochemical variations along the Mid-Atlantic Ridge from 29-degrees-N to 73-degrees-N, *Am. J. Sci.*, *28*, 510–586.

Schearer, P. M., M. A. H. Hedlin, and P. S. Earle (1998), *PKP* and *PKKP* precursor observations: Implications for small-scale structure of the deep mantle and core, in *The Core-Mantle Boundary Region*, *Geodyn. Ser.*, vol. 28, edited by M. Gurnis et al., pp. 37–55, AGU, Washington, D. C.

Schubert, G., P. Olson, G. Masters, and P. Tackley (2004), Superplumes or plume clusters?, *Phys. Earth Planet. Inter*, *146*, 147–162.

Selig, F. (1965), A theoretical prediction of salt dome patterns, *Geophysics*, *30*, 633–643.

Shirey, S. B., and R. J. Walker (1998), The Re-Os isotope system in cosmochemistry and high temperature geochemistry, *Annu. Rev. Earth Planet. Sci.*, *26*, 423–500.

Sidorin, I., and M. Gurnis (1998), Geodynamically consistent seismic velocity predictions at the base of the mantle, in *The Core-Mantle Boundary Region*, *Geodyn. Ser.*, vol. 28, edited by M. Gurnis et al., pp. 209–230, AGU, Washington, D. C.

Silver, P. G., R. M. Russo, and C. Lithgow-Bertelloni (1998), Coupling of South American and African plate motion and plate deformation, *Science*, *279*, 60–63.

Simmons, N. A., and S. P. Grand (2002), Partial melting in the deepest mantle, *Geophys. Res. Lett.*, *29*(11), 1552, doi:10.1029/2001GL013716.

Skilbeck, J. N., and J. A. Whitehead (1978), Formation of discrete islands in a linear chain of islands, *Nature*, *272*, 499–501.

Skinner, B. J., and S. C. Porter (2000), *The Dynamic Earth: An Introduction to Physical Geology*, 4th ed., John Wiley, Hoboken, N. J.

Sleep, N. H. (1988), Gradual entrainment of a chemical layer at the base of the mantle by overlying convection, *Geophys. J.*, *95*, 437–447.

Sleep, N. H. (1990), Hotspots and mantle plumes: Some phenomenology, *J. Geophys. Res.*, *95*, 6715–6736.

Sleep, N. H., M. A. Richards, and B. H. Hager (1988), Onset of mantle plumes in the presence of preexisting convection, *J. Geophys. Res.*, *93*, 7672–7689.

Small, C. (1995), Observations of ridge-hotspot interactions in the Southern Ocean, *J. Geophys. Res.*, *100*, 17,931–17,946.

Smoliar, M., R. J. Walker, and J. W. Morgan (1996), Re-Os ages of Group IIA, IIIA, IVA, and IVB iron meteorites, *Science*, *271*, 1099–1102.

Solomatov, V. S. (1995), Scaling of temperature- and stress-dependent viscosity convection, *Phys. Fluids*, *7*, 266–274.

Solomatov, V. S., and L.-N. Moresi (1996), Stagnant lid convection on Venus, *J. Geophys. Res.*, *101*, 4737–4753.

Solomatov, V. S., and L.-N. Moresi (2000), Scaling of time-dependent stagnant lid convection: Application to small-scale convection on Earth and other terrestrial planets, *J. Geophys. Res.*, *105*, 21,795–21,817.

Solomatov, V. S., and L.-N. Moresi (2002), Small-scale convection in the D$''$ layer, *J. Geophys. Res.*, *107*(B1), 2016, doi:10.1029/2000JB000063.

Song, X., and T. J. Ahrens (1994), Pressure-temperature range of reactions between liquid iron in the outer core and mantle silicates, *Geophys. Res. Lett.*, *21*, 153–156.

Sparrow, E. M., R. B. Husar, and R. J. Goldstein (1970), Observations and other characteristics of thermals, *J. Fluid Mech.*, *41*, 793–800.

Stacey, F. D., and D. E. Loper (1983), The thermal boundary layer interpretation of D$''$ and its role as a plume source, *Phys. Earth Planet. Inter.*, *33*, 45–55.

Stacey, F. D., and D. E. Loper (1984), Thermal histories of the core and mantle, *Phys. Earth Planet. Inter.*, *36*, 99–115.

Steinberger, B. (2000), Plumes in a convecting mantle: Models and observations for individual hotspots, *J. Geophys. Res.*, *105*, 11,127–11,152.

Steinberger, B., and R. J. O'Connell (1998), Advection of plumes in mantle flow: Implications for hotspot motion, mantle viscosity, and plume distribution, *Geophys. J. Int.*, *132*, 412–434.

Steinberger, B., and R. J. O'Connell (2000), Effects of mantle flow on hotspot motion, in *The History and Dynamics of Global Plate Motions*, *Geophys. Monogr. Ser.*, vol. 121, edited by M. A. Richards et al., pp. 377–398. AGU, Washington, D. C.

Steinberger, B., R. Sutherland, and R. J. O'Connell (2004), Prediction of Emperor-Hawaii seamount locations from a revised model of global plate motion and mantle flow, *Nature*, *430*, 167–173.

Stengel, K. C., D. S. Oliver, and J. R. Booker (1982), Onset of convection in a variable-viscosity fluid, *J. Fluid Mech.*, *120*, 411–431.

Stevenson, D. J. (1981), Models of the Earth's core, *Science*, *214*, 611–619.

Stevenson, D. J. (2003), Planetary magnetic fields, *Earth Planet. Sci. Lett.*, *208*, 1–11.

Stevenson, D. J., T. Spohn, and G. Schubert (1983), Magnetism and thermal evolution of the terrestrial planets, *Icarus*, *54*, 466–489.

Su, W.-J., and A. M. Dziewonski (1991), Predominance of long-wavelength heterogeneity in the mantle, *Nature*, *352*, 121–126.

Su, W.-J., R. L. Woodward, and A. M. Dziewonski (1994), Degree-12 model of shear velocity heterogeneity in the mantle, *J. Geophys. Res.*, *99*, 6945–6980.

Sylvander, M., and A. Souriau (1996), Mapping *S*-velocity heterogeneities in the D$''$ region, from *SmKS* differential travel times, *Phys. Earth Planet. Inter.*, *94*, 1–21.

Tackley, P. J. (1998a), Self-consistent generation of tectonic plates in three-dimensional mantle convection, *Earth Planet. Sci. Lett.*, *157*, 9–22.

Tackley, P. J. (1998b), Three-dimensional simulations of mantle convection with a thermochemical CMB boundary layer: D$''$?, in *The Core-Mantle Boundary Region*, *Geodyn. Ser.*, vol. 28, edited by Gurnis et al., pp. 231–253, AGU, Washington, D. C.

Tackley, P. J. (2000), Mantle convection and plate tectonics: Toward an integrated physical and chemical theory, *Science*, *288*, 2002–2007.

Tackley, P. J. (2002), Strong heterogeneity caused by deep mantle layering, *Geochem. Geophys. Geosyst.*, *3*(4), 1024, doi:10.1029/2001GC000167.

Tackley, P. J., and S. D. King (2003), Testing the tracer ratio method for modeling active compositional fields in mantle convection simulations, *Geochem. Geophys. Geosyst.*, *4*(4), 8302, doi:10.1029/2001GC000214.

Tackley, P. J., and S. Xie (2002), The thermochemical structure and evolution of Earth's mantle: Constraints and numerical models, *Philos. Trans R. Soc. London, Ser. A*, *360*, 2593–2609.

Tan, E., M. Gurnis, and L. Han (2002), Slabs in the lower mantle and their modulation of plume formation, *Geochem. Geophys. Geosyst.*, *3*(11), 1067, doi:10.1029/2001GC000238.

Tanimoto, T. (1990), Long wavelength *S* velocity structure throughout the mantle, *Geophys. J. Int.*, *100*, 327–336.

Tarbuck, E. J., and F. K. Lutgens (1999), *Earth: An Introduction to Physical Geology*, 6th ed., 638 pp., Prentice-Hall, Old Tappan, N. J.

Tarduno, J. A., et al. (2003), Emperor Seamounts: Southward motion of the Hawaiian hotspot plume in the Earth's mantle, *Science*, *301*, 1064–1069.

Tatsumi, Y., and S. Eggins (1995), *Subduction Zone Magmatism*, 211 pp., Blackwell Sci., Malden, Mass.

Tatsumi, Y., D. L. Hamilton, and R. W. Nesbitt (1986), Chemical characteristics of fluid phase released from a subducted lithosphere and origin of arc magmas—Evidence from high-pressure experiments and natural rocks, *J. Volcanol. Geotherm. Res.*, *29*, 293–309.

Thomas, C., M. Weber, C. W. Wicks, and F. Scherbaum (1999), Small scatterers in the lower mantle observed at German broadband arrays, *J. Geophys. Res.*, *104*, 15,073–15,088.

Trompert, R. A., and U. Hansen (1998), On the Rayleigh number dependence of convection with a strongly temperature-dependent viscosity, *Phys. Fluids*, *10*, 351–360.

Turcotte, D. L., and L. H. Kellogg (1986), Isotopic modeling of the evolution of the mantle and crust, *Rev. Geophys.*, *24*, 311–328.

Turner, J. S. (1973), *Buoyancy Effects in Fluids*, 367 pp., Cambridge Univ. Press, New York.

van der Hilst, R. D., and H. Karason (1999), Compositional heterogeneity in the bottom 1000 kilometers of Earth's mantle: Toward a hybrid convection model, *Science*, *283*, 1885–1888.

van der Hilst, R. D., S. Widiyantoro, and E. R. Engdahl (1997), Evidence for deep mantle circulation from global tomography, *Nature*, *386*, 578–584.

van Keken, P. E. (1997), Evolution of starting mantle plumes–A comparison between numerical and laboratory models, *Earth Planet. Sci. Lett.*, *148*, 1–11.

van Keken, P. E., and C. J. Ballentine (1999), Dynamical models of mantle volatile evolution and the role of phase transitions and temperature-dependent rheology, *J. Geophys. Res.*, *104*, 7137–7151.

van Keken, P. E., et al. (1997), A comparison of methods for the modeling of thermochemical convection, *J. Geophys. Res.*, *102*, 22,477–22,495.

Vasco, D. W., and L. R. Johnson (1998), Whole Earth structure estimated from seismic arrival times, *J. Geophys. Res.*, *103*, 2633–2671.

Verhoogen, J. (1961), Heat balance of the Earth's core, *Geophys. J. R. Astron. Soc.*, *4*, 276–281.

Vidal, V., and A. Bonneville (2004), Variations of the Hawaiian hot spot activity revealed by variations in the magma production rate, *J. Geophys.*, *109*, B03104, doi:10.1029/2003JB002559.

Vidale, J. E., and M. Benz (1993), Seismological mapping of fine structure near the base of Earth's mantle, *Nature*, *361*, 529–532.

Vidale, J. E., and M. A. H. Hedlin (1998), Evidence for partial melt at the core-mantle boundary north of Tonga from the strong scattering of seismic waves, *Nature*, *391*, 682–684.

Walker, R. J. (2000), Core participation in mantle geochemistry, *Geochim. Cosmochim. Acta*, *64*, 2897–2911.
Walker, R. J., J. W. Morgan, and M. F. Horan (1995), ^{187}Os enrichment in some mantle plume sources: Evidence for core-mantle interaction?, *Science*, *269*, 819–822.
Walker, R. J., J. W. Morgan, E. Beary, M. I. Smoliar, G. K. Czamanske, and M. F. Horan (1997), Applications of the ^{190}Pt-^{186}Os isotope system to geochemistry and cosmochemistry, *Geochim. Cosmochim. Acta.*, *61*, 4799–4808.
Weeraratne, D., and M. Manga (1998), Transitions in the style of mantle convection at high Rayleigh numbers, *Earth Planet. Sci., Lett.*, *160*, 563–568.
Weinstein, S. A., and U. Christensen (1991), Convection planforms in a fluid with a temperature-dependent viscosity beneath a stress-free upper boundary, *Geophys. Res. Lett.*, *18*, 2035–2038.
Weinstein, S. A., and P. Olson (1989), The proximity of hotspots to convergent and divergent plate, *Geophys. Res. Lett.*, *16*, 433–436.
Wen, L. X., and D. V. Helmberger (1998), Ultra-low velocity zones near the core-mantle boundary from broadband *PKP* precursors, *Science*, *279*, 1701–1703.
Wen, L. X., P. Silver, D. James, and R. Kuehnel (2001), Seismic evidence for a thermo-chemical boundary at the base of the Earth's mantle, *Earth Planet. Sci. Lett.*, *189*, 141–153.
Wenzel, M. J., M. Manga, and A. M. Jellinek (2004), Tharsis as a consequence of Mars' dichotomy and layered mantle, *Geophys. Res. Lett.*, *31*, L04702, doi:10.1029/2003GL019306.
White, W., and D. McKenzie (1989), Magmatism at rift zones: The generation of volcanic continental margins and flood basalts, *J. Geophys. Res.*, *94*, 7685–7729.
Whitehead, J. A., and D. S. Luther (1975), Dynamics of laboratory diapir and plume models, *J. Geophys. Res.*, *80*, 705–717.
Widom, E., et al. (1997), Th-Sr-Nd-Pb isotope and trace element evidence for the origin of the Sao Miguel, Azores, enriched mantle source, *Chem. Geol.*, *140*, 49–68.
Williams, Q. (1998), The temperature contrast across D″, in *The Core-Mantle Boundary Region*, *Geodyn. Ser.*, vol. 28, edited by M. Gurnis et al., pp. 73–82, AGU, Washington, D. C.
Williams, Q., and E. J. Garnero (1996), Seismic evidence for partial melt at the base of the mantle, *Science*, *273*, 1528–1530.
Williams, Q., J. Revenaugh, and E. Garnero (1998), A correlation between ultra-low basal velocities in the mantle and hot spots, *Science*, *281*, 546–549.
Wilson, J. T. (1963), Evidence from islands on the spreading of the ocean floor, *Can. J. Phys.*, *41*, 863–868.
Wysession, M. E. (1996), Large-scale structure at the core-mantle boundary from diffracted waves, *Nature*, *382*, 244–248.
Wysession, M. E., T. Lay, J. Revenaugh, Q. Williams, and E. J. Garnero (1998), The D″ discontinuity and its implications, in *The Core-Mantle Boundary Region*, *Geodyn. Ser.*, vol. 28, edited by M. Gurnis et al., pp. 273–298, AGU, Washington, D. C.
Yin, Q. Z., S. B. Jacobsen, K. Yamashita, J. Blichert-Toft, P. Telouk, and F. Albarede (2002), A short timescale for terrestrial planet formation from Hf-W chronometry of meteorites, *Nature*, *418*, 949–952.
Young, C. J., and T. Lay (1987), The core mantle boundary, *Annu. Rev. Earth Planet. Sci.*, *15*, 25–46.
Yuen, D. A., and G. Schubert (1976), Mantle plumes: A boundary layer approach for Newtonian and non-Newtonian temperature-dependent rheologies, *J. Geophys. Res.*, *81*, 2499–2510.
Zerr, A., A. Diegler, and R. Boehler (1998), Solidus of the Earth's deep mantle, *Science*, *281*, 243–245.
Zhao, D. (2001), Structure and origin of hotspots and mantle plumes, *Earth Planet. Sci. Lett.*, *192*, 251–265.
Zhong, S. J., and B. H. Hager (2003), Entrainment of a dense layer by thermal plumes, *Geophys. J. Int.*, *154*, 666–676.
Zhong, S. J., and A. B. Watts (2002), Constraints on the dynamics of mantle plumes from uplift of the Hawaiian Islands, *Earth Planet. Sci. Lett.*, *203*, 105–116.
Zhong, S. J., M. T. Zuber, and L.-N. Moresi (2000), Role of temperature-dependent viscosity and surface plates in spherical shell models of mantle convection, *J. Geophys. Res.*, *105*, 11,063–11,082.
Zindler, A. E., and S. Hart (1986), Chemical geodynamics, *Annu. Rev. Earth Planet. Sci.*, *14*, 493–571.
Zindler, A., E. Jagoutz, and S. Goldstein (1982), Nd, Sr and Pb isotopic systematics in a three component mantle: A new perspective, *Nature*, *298*, 519–523.

A. M. Jellinek, Geophysical Laboratories, Department of Physics, University of Toronto, Toronto, Ontario, Canada M5S 1A7. (markj@physics.utoronto.ca)
M. Manga, Department of Earth and Planetary Science, University of California, Berkeley, Berkeley, CA 94720-4767, USA. (manga@seismo.berkeley.edu)